ENVIRONMENTAL IMPLICATIONS OF *FRANCISELLA TULARENSIS* BIOFILMS

A DISSERTATION

SUBMITTED TO

THE DEPARTMENT OF MICROBIOLOGY AND IMMUNOLOGY

AND THE COMMITTEE ON GRADUATE STUDIES

OF STANFORD UNIVERSITY

IN PARTIAL FULFILLMENT OF THE REQUIREMENTS

FOR THE DEGREE OF

DOCTOR OF PHILOSOPHY

Jeffrey J. Margolis

November 2009

I certify that I have read this dissertation and that, in my opinion, it is fully adequate in scope and quality as a dissertation for the degree of Doctor of Philosophy.

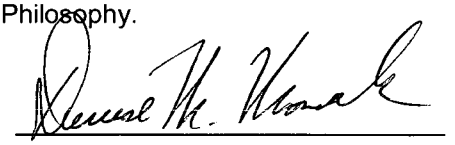

Denise Monack

I certify that I have read this dissertation and that, in my opinion, it is fully adequate in scope and quality as a dissertation for the degree of Doctor of Philosophy.

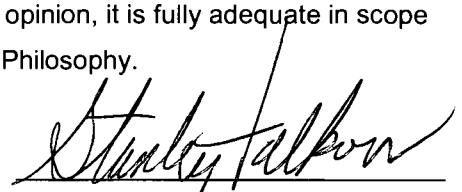

Stanley Falkow

I certify that I have read this dissertation and that, in my opinion, it is fully adequate in scope and quality as a dissertation for the degree of Doctor of Philosophy.

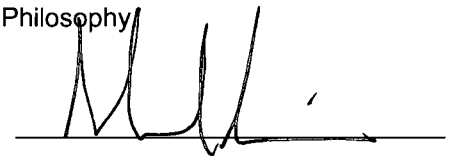

Manuel Amieva

I certify that I have read this dissertation and that, in my opinion, it is fully adequate in scope and quality as a dissertation for the degree of Doctor of Philosophy.

Gary Schoolnik

I certify that I have read this dissertation and that, in my opinion, it is fully adequate in scope and quality as a dissertation for the degree of Doctor of Philosophy.

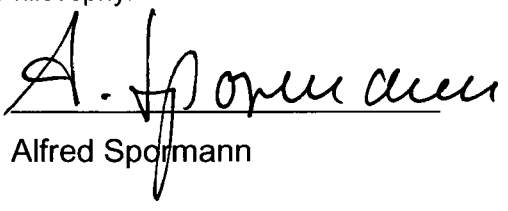

Alfred Spormann

Approved for the Stanford University Committee on Graduate Studies.

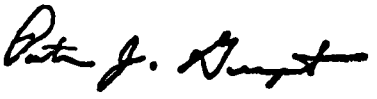

Abstract

Francisella tularensis survives in one of the widest environmental ranges of any pathogen. Numerous mammals and arthropod vectors are infected by this highly virulent organism. How this zoonotic pathogen persists outside of its many hosts remains unexplored. We aimed to examine how *F. tularensis* interacts with environmental surfaces, and hypothesized that biofilm formation may enable survival of this organism in nature. By understanding the role these surface-attached bacterial communities play in *F. tularensis* ecology, we hope to gain insight into the mechanisms of environmental persistence and transmission of this pathogen.

We identify chitin as a potential non-host niche for *F. tularensis* in nature using genetic, microscopic, and biochemical techniques. This abundant polysaccharide supported *F. tularensis* biofilm formation in the absence of an exogenous carbon source. This interaction was dependent on putative chitinase enzymes which hydrolyze the glycosidic bonds that connect GlcNAc monomers. Using a genetic screen, we identified adherence factors, including FTN_0308 and FTN_0714 that promote attachment to chitin and colonization of chitin surfaces. We propose that biofilm formation on chitin surfaces in nature enables nutrient scavenging in oligotrophic environments allowing this pathogen to replicate and seed disease transmission.

We found that the effect of nutrient limitation on *F. tularensis* biofilm formation extended beyond chitin utilization. Genetic studies indicated that

nutrient starvation triggers a biofilm stress response. We identified static growth and nutrient deprivation as cues for enhanced biofilm formation. Microarray expression studies identified genes highly expressed under these conditions, including *F. tularensis* biofilm determinants. Expression of nutrient transporters further indicated that biofilm formation promotes environmental persistence.

We finally examined statically grown *F. tularensis* microscopically to determine if altered morphology explained the enhanced biofilm phenotype of these cultures. We discovered a novel *F. tularensis* appendage conserved between subspecies and structurally homologous to the *Caulobacter crescentus* stalk. These structures were observed in association with surfaces during both biofilm formation and during intracellular infection. A genetic screen for mutants in stalk formation revealed that stalk biosynthetic components are essential. We predict this structure aids in environmental persistence by facilitating surface attachment and nutrient uptake. Through this collective work we define evidence that surface association via biofilm formation promotes survival during nutrient limitation.

Acknowledgements

I would like to thank Ed Goebel for sparking my interest in microbiology when I was in high school. As an undergrad, this fascination was nurtured by Matthew Parsek and Mary Jo Kirisits. Holly Falk-Krzesinski guided me to graduate school and continues to serve as an adviser and mentor.

At Stanford, Denise Monack has been a wonderful boss. I really appreciate her continued support of my interests wherever they take me. Stan Falkow, Lucy Tompkins, and Manuel Amieva have also been phenomenal mentors. Alfred Spormann and Gary Schoolnik were also intregal to my scientific development. Having access to such a breadth and depth of knowledge has been invaluable. I would also like to thank all past and present members of the Monack, Amieva, and Falkow labs. The Bug Dungeon has been a fun and educational place to work. Jon Jones has been a great friend and compatriot in graduate school. Jon, David Weiss, Annie Brotcke, Laura McLoughlin and Thomas Henry were the best Monack lab version 1.0 I could have hoped for. Kaitian Peng, Smita Gopinath, Kamila Belhocine, Tom Ruby, Petr Broz, and Hanza Matthew have also been great labmates and friends.

Last, but certainly not least, I need to thank my family. My parents and sister have always supported my interests and helped me in so many ways. I also must express my unending gratitude to my wife, Lacey. Not only is she a wonderful friend, she has always supported my scientific endeavors from the beginning. She deserves her own PhD's in psychology and baking!

Table of Contents

Table of Figures

List of Tables

Chapter 1: General Introduction

Tularemia

Francisella tularensis is a Gram-negative bacterium that causes the systemic disease, tularemia (55). Initially characterized as Rabbit Fever by Edward Francis, tularemia is acquired via numerous routes from contaminated water and infected vectors and mammals (20, 47). *F. tularensis* is a facultative intracellular pathogen that can infect most eukaryotic cell types. Macrophages are thought to be the main replicative niche for the bacterium within a mammalian host, but bacteria have also been recovered from hepatocytes and dendritic cells, amongst others (4, 19, 46). The majority of *F. tularensis* research has focused on virulence mechanisms within host cells and methods of immune modulation that facilitate systemic infection.

Disease manifestation and severity depends on the route of infection. Pneumonic tularemia, the most severe form of the disease, stems from inhalation of the bacterium. As few as ten organisms can cause a lethal infection via this route (146). Introduction of *F. tularensis* through the skin by insect bite or contamination of wounded skin is the most common means of acquisition (20, 35). Tularemia can also be contracted through the conjuctiva or by ingestion of contaminated food or water. In all cases, severe morbidity and mortality is associated with trafficking of the local site of infection to systemic sites within the lymphatic and vascular systems (177). While the routes of infection are well defined, how *F. tularensis* survives outside of mammalian hosts and seeds infection is unclear.

Francisella tularensis subspecies

Four highly related *F. tularensis* subspecies have been differentiated based on genome sequence homology, geographic distribution, and infectivity to mammals. The subspecies are approximately 99% identical in sequence and all have conserved the *Francisella* pathogenecity island (FPI), the major virulence determinant of pathogenic strains (192). While the infective dose varies between strains, all four *F. tularensis* subspecies cause similar systemic disease in mammals including the mouse model of infection (5, 146).

Two *F. tularensis* subspecies cause the majority of tularemia cases worldwide. *F. tularensis* subspecies *tularensis* (Type A) is the most virulent strain classification for this pathogen. Type A strains, including SchuS4 which is used as a model strain, can cause lethal infection with less than 10 organisms (26). This subspecies is isolated exclusively in North America. Subspecies *holartica* (Type B) is found throughout the Northern Hemisphere, primarily in Europe. Although less virulent than Type A strains, Type B strains can cause disease with an LD_{50} of a few hundred bacteria (183). In addition to these mammalian pathogens, numerous aquatic *Francisella* species have been identified. These strains include *F. philomiragia* which infects both fresh water and marine fish, but is avirulent in mammals (134).

To study *F. tularensis* virulence and ecology under laboratory conditions, strains with lower infectivity are utilized. These strains are larger similar to virulent Type A and Type B strains genetically and cause a tularemia-like

disease in mice. These strains are essentially avirulent to immunocompetent humans. The live vaccine strain (LVS) is utilized as an attenuated Type B strain that can be worked with under BSL-2 laboratory conditions (49). In the Monack lab, we work primarily with *F. tularensis* subsp. *novicida* (*F. novicida*). This subspecies is genetically tractable and numerous genetic and molecular tools have been developed to study this organism (22, 38).

Francisella tularensis epidemiology and ecology

Each *F. tularensis* strain is confined to both a specific geographic location and subsequent environmental niche. Historically, virulent Type A strains were associated with warm, arid climates and are transmitted by arthropod vectors (55, 90). *F. tularensis* subsp. *tularensis* strains have been further subdivided into Type A1 (Eastern United States) and Type A2 (Western United States) strains (27). Type A1 strains are found in moist climates, while Type A2 strains inhabit the more prototypical dry environments associated with early cases of tularemia. While both subtypes are highly virulent, Type A1 strains were connected to 100% of lethal tularemia cases in a recent epidemiological study (27). Sequence comparisons between the two Type A subtypes have not explained this difference in lethality. Type B strains cause severe but less lethal cases of tularemia and are closely associated with fresh water (2, 7, 17, 44). Numerous outbreaks have been tracked to wells and natural springs (10, 31, 53). In Northern Europe where Type B strains are endemic, transmission of tularemia is closely connected to mosquitoes.

Outbreaks in Sweden peak in the summer when mosquito numbers are highest and the number of cases correlates with (54).

Overall, *F. tularensis* inhabits a wide variety of environments. This pathogen can infect hundreds of mammals and arthropods (146, 153). In addition, this organism has been isolated from fresh water sources and can survive within environmental amoeba (1, 16, 34, 42). Given the severity of disease manifestations caused by *F. tularensis,* identifying which of these environments serves as a reservoir for disease transmission remains an important question. Tularemia is typically classified as a vector-borne disease, but the disease state within arthropod vectors is unknown. Experimentally, *Drosophila melanogaster* succumbs to systemic *F. tularensis* infection (51), suggesting that vectors are not a true reservoir of disease. Fresh water is believed to be the other major site of *F. tularensis* persistence in nature (2, 10, 31, 42, 49). For this pathogen to persist in such an environment, it must have a means to grow in these oligotrophic environments; a question we address in this work. Chitin is a common component of both vector- and water-borne *F. tularensis* and we hypothesized that this abundant polysaccharide may be the key to persistence in both environments.

The lack of tropism is unique among bacterial pathogens. How *F. tularensis* inhabits this breadth of temperatures, nutritional availabilities, and environmental stress remains an unaddressed question. Does one colonization method allow survival in multiple locations or has *F. tularensis* evolved separate means of surviving in each habitat? By studying how this

pathogen senses each environment and the mechanisms of colonization for each niche, we can better understand the ecology of this organism

Stress responses in *F. tularensis*

Bacteria have evolved numerous mechanisms to interpret and respond to various environmental stresses. These responses mediate proteins that promote bacterial survival and include two-component systems, secondary messenger production and alternate sigma factors that regulate gene expression in stationary phase. The stringent response to starvation and the SOS response to DNA damage by antibiotics and reactive oxygen are examples of specialized stress responses (62).

Stress responses and gene regulation have been minimally explored in *F. tularensis.* The majority of information available pertains to the regulation of virulence determinants. Given the large number of signals *F. tularensis* must interpret and respond to in order to survive in its large number of hosts and environments, stress responses must control more than adaptation to a mammalian host. A striking lack of two-component systems, a basic means of environmental response, are present in the *F. tularensis* genome. In fact, a single complete histidine kinase-response regulator pairs is annotated based on sequence homology to other systems in other bacteria (*kdpDE*) (108). This two-component system regulates the response to potassium availability in other Gram negative bacteria. KdpD and QseC histidine kinases, along with the PmrA response regulator have been shown to impact *F. tularensis*

virulence (208). Mohapatra *et al.* reported that PmrA regulates the *Francisella* pathogenecity island which is required for intracellular replication. Recently, *qseC* and *pmrA* mutations were reported to confer a defect in *F. tularensis* biofilm formation, suggesting these genes regulate more than virulence factors (48). Which environmental cues activate these two-component proteins and how these systems switch between infection and biofilm formation is unknown.

Starvation, particularly, amino acid starvation is one well characterized trigger of bacterial stress responses. The stringent response in particular responds to this cue by generating a secondary messenger. Uncharged tRNAs are detected at the ribosome by RelA and SpoT which synthesized the guanosine tetraphosphate (ppGpp) alarmone (166). Production of ppGpp leads to specific expression response that mediates environmental and host-associated survival for bacteria including *Campylobacter jejuni* (67), *Escherichia coli* (11), and *Streptococcus mutans* (113). Recently, a deletion in *relA* was shown to confer decreased intracellular replication and increased biofilm formation (43). The stringent response may therefore mediate the transition between environmental colonization and mammalian infection.

The Dove lab at Harvard has found that the stringent response facilitates *F. tularensis* virulence through interaction with the MglA signaling pathway (personal communication). MglA is a homolog of the general stress response regulator SspA in *E. coli* and is the best studied *F. tularensis* regulatory protein due to its requirement for virulence (6, 9, 24, 30). Anna Brotcke, a former graduate student in the Monack lab, determined the 102

gene MglA-regulon by microarray analysis (21) and identified other genes in the regulatory pathway (*fevR, caiC,* and *cphA*) (20). While many MglA-regulated genes, including the entire FPI, function in *F. tularensis* virulence, at least one gene does not impact virulence. MglA may therefore function as a general stress response regulator, like SspA, and regulated genes may promote environmental and mammalian colonization. Work by Guina *et al.* (79) on the post-transcriptional roles of MglA supports this idea. Numerous general stress response regulators and chaperones were altered at the protein level in a *mglA* mutant strain. Additionally, deletions in specific MglA-regulated genes conferred decreased survival in stationary phase and resistance to reactive oxygen. By investigating the role of MglA and other *F. tularensis* stress response pathways it may be possible to understand the cues that influence environmental colonization and the mechanisms persistence.

Bacterial biofilms

Bacteria survive in numerous environments in structured communities termed, biofilms. These surface-attached bacterial populations are encapsulated within an extrapolymeric substance (EPS) matrix that can consist of polysaccharides, protein, and/or DNA (37). Bacterial physiology within a biofilm population is heterogenous given varying microenvironments within the community structure (155). Biofilms are ubiquitous in natural, industrial, and medical settings, usual in or near aqueous environments. These bacterial communities promote resistance to environmental stresses,

antibiotic treatment, and host immune clearance. EPS barrier function and an alternate sigma factor-regulated response that includes decreased metabolism mediate this persistence (37).

The first stage in biofilm formation is surface attachment. Planktonic bacteria respond to various environmental and intercellular signals by switching to a sessile form. Initial association is normally weak and facilitated by van der Waals interactions (37). Surface proteins then strengthen surface attachment and connect neighboring cells. Molecular mechanisms of surface attachment vary widely between biofilm-forming organisms. Type-IV pili are the best characterized attachment factors (36, 41). Beyond connecting bacteria to a surface, pili mediate twitching motility, which enables microcolony formation and biofilm maturation. Non-motile bacteria can also form biofilms, however. *Staphylococcal* biofilms initiate by Bap-mediated surface attachment (151). Once bacteria attach to abiotic and biotic surfaces, cell division and EPS production yield three-dimensional biofilms. Biofilm architecture varies from thin matts to elaborate mushroom shapes based on species and nutrient environment.

Given the multiple stresses that biofilms respond to and the diverse responses that are required for survival, these bacterial populations have become a model for understanding inter- and intracellular signaling. The paradigm shift that bacteria can communicate and coordinate gene expression was discovered in the context of biofilms. Cell-cell communication, termed quorum sensing, allows a biofilm to sense population density and express

biofilm and virulence genes only when sufficient bacterial numbers are present (158). More recently, 3′,5′-cyclic diguanylic acid (c-di-GMP) has emerged as an essential regulator of biofilm function (38, 191, 215). This secondary messenger, which is produced by diguanylate cyclase and degraded by phosphodiesterase A (38). These GGDEF and EAL domain-containing enzymes mediate the transition between an infectious, planktonic state and biofilm formation for bacterial pathogens by controlling c-di-GMP levels (38). Environmental cues and other regulatory systems determine GGDEF and EAL domain protein levels and activities, forming complex regulatory networks. These signaling pathways allow bacteria to sense and successfully respond to starvation, oxygen availability, oxidative stress and other detractors of survival.

By integrating multiple signals to express biofilm genes, bacteria are able to withstand nutrient and other environmental stresses to persist in the environment. Biofilm formation is an essential survival and transmission mechanism for many bacterial pathogens. *Legionella pneumophila*, one of the closest relatives to *F. tularensis*, survives in aquatic environments in biofilms (109, 186). Biofilm formation by this pathogen enables persistence in cooling towers and drinking water sources, seeding numerous Legionnaire's disease outbreaks (109). *Vibrio cholerae* is another human pathogen that lives in the environment in aquatic environments. *V. cholerae* biofilms formed on copepod molts promote environmental replication of this organism. Cell division in this marine environment requires carbon scavenging from the copepod, itself (14). The copepod exoskeleton is predominately chitin, a polymer of *N*-acetyl-D-

glucosamine. Numerous bacteria have evolved chitinase enzymes to hydrolyze chitin into useable metabolites (50). Seeding of Cholera outbreaks in the developing world requires the establishment of this environmental niche (167).

Tularemia is characterized as both vector-borne and water-borne disease (55, 138, 146, 164). Chitin is a common surface present in both transmissive environments: chitinous exoskeletons of arthropod vectors and chitin-containing crustaceans in fresh water. We hypothesized that *F. tularensis* utilizes chitin in nature to persist outside of its wide host range. Biofilm formation by this zoonotic pathogen would promote interaction with and retention of chitin and chitin-derivatives. We found that *F. tularensis* responds to carbon limitation and other environment stresses by prominent biofilm formation. Biofilm formation on chitin surfaces required Sec-secreted attachment factors and two chitinase enzymes. Static growth strongly promoted *F. tularensis* biofilm formation and upregulated numerous persistence genes. A novel polar appendage similar to the *Caulobacter crescentus* stalk may further facilitate environmental persistence with biofilms. Further study of the molecular mechanisms of *F. tularensis* chitin colonization will provide insight into how biofilm formation on this nutritive surface establishes the first described non-host niche for this highly virulent pathogen.

Chapter 2: *Francisella tularensis* subspecies *novicida* chitinases mediate biofilm formation on chitin surfaces

Jeffrey J. Margolis[1], Sahar El-Etr[2], Lydia-Marie Joubert[3], Emily Moore[4], Richard Robison[4], Amy Rasley[2], Alfred M. Spormann[5], and Denise M. Monack[1]

[1] Department of Microbiology and Immunology, Stanford University School of Medicine, Stanford, CA 94305, USA.
[2] Bioscience and Biotechnology Division, Lawrence Livermore National Laboratory, Livermore, CA 94550, USA.
[3] Cell Sciences Imaging Facility, Stanford University School of Medicine, Stanford, CA 94305.
[4] Department of Microbiology and Molecular Biology, Brigham Young University, Provo, UT 84602, USA.
[5] Department of Civil and Environmental Engineering, Stanford University, Stanford, CA 94304, USA.

This chapter has been accepted for publication in *Applied Environmental Microbiology.*

2.1 CHAPTER 2 SUMMARY

Francisella tularensis, the zoonotic cause of tularemia, can infect numerous mammals and other eukaryotes. Although studying *F. tularensis* pathogenesis is essential to comprehending disease, mammalian infection is just one step in the ecology of *Francisella* species. Many pathogenic bacteria possess the ability to persist in the environment outside of a host. The potential mechanisms of *F. tularensis* nutrient scavenging in nature and environmental replication have not been addressed in the literature. *F. tularensis* has been isolated from aquatic environments and arthropod vectors, environments in which chitin could serve as a potential carbon source and surface for attachment and growth. We show by scanning electron microscopy that *F. tularensis* subsp. *novicida* forms biofilms during colonization of chitin surfaces. Importantly, the bacterial communities proliferated in the absence of exogenous sugar suggesting that *Francisella* species can utilize chitin as a carbon source for growth. Growth curves in minimal media supplemented with different sugar sources confirmed this hypothesis. Further, the ability of *F. tularensis* to persist using chitin as a sole carbon source is dependent on chitinases, since mutants lacking *chiA* or *chiB* are attenuated for chitin colonization and biofilm formation in the absence of exogenous sugar. Our results suggest that chitin surfaces may provide a viable environmental niche for *F. tularensis* in nature by providing a substrate for growth.

2.2 INTRODUCTION

F. tularensis inhabits one of the widest environmental ranges of any known pathogens. Indeed, *F. tularensis* has been isolated from a variety of sources including lagomorphs, arthropods, amoeba and fresh water (5, 146, 153, 154). The high mortality rate in infected mammalian hosts (177) suggests that mammals are not the natural reservoir for this pathogen. Understanding the environmental lifestyle of *F. tularensis* will help elucidate the survival mechanisms of this pathogen outside of a host and identify risks for human exposure.

Recently, outbreaks of tularemia were associated with fresh water, particularly outbreaks of *F. tularensis* subspecies *holarctica* (Type B) in Eurasia (25, 214). While the most virulent subspecies, *F. tularensis* subsp. *tularensis* (Type A), was historically linked with the arid climates of North America, a recent epidemiological study found that 100% of tularemia mortality was associated with Type A1 strains found in moist climates of the United States (103), suggesting that water may serve as an environmental reservoir for *F. tularensis*.

The survival of some bacteria in an aquatic environment is associated with their ability to utilize chitin as a carbon source. Chitin is the second most abundant biopolymer in nature and provides structure to many organisms, including the cell wall of fungi (13) and the exoskeleton of arthropods and insects (132). This oligomer of *N*-acetyl-D-glucosamine (GlcNAc) is hydrolyzed by a family of enzymes, termed chitinases (14). These enzymes serve a

variety of roles and are conserved from bacteria to mammals. Bacterial chitinases provide environmental organisms the ability to acquire carbon in otherwise nutrient-limiting conditions (99). For example, *Vibrio cholerae*, the etiological agent of cholera, utilizes chitinases to persist in marine environments on copepod molts (139). The interaction of *V. cholerae* with chitin influences various metabolic and physiologic responses in this microorganism. For example, Meibom *et al.* demonstrated that association with chitin and chitin-derivatives led to a specific expression profile in *V. cholerae* that included two chitinase genes and the pili genes required for colonization and subsequent biofilm formation on nutritive and non-nutritive surfaces (129). Environmental studies have clearly shown that attachment to chitin surfaces is an integral part of the aquatic lifestyle of *V. cholerae*, and biofilm formation constitutes a successful survival mechanism (167). Outbreaks of tularemia in Europe have now been specifically attributed to crustaceans (4, 45), suggesting a similar means of persistence and transmission may exist for *F. tularensis*.

Survival of microbes in aquatic environments is promoted by the ability to form biofilms on various surfaces (41). Biofilms are surface-attached bacterial populations encased in an extracellular matrix found mainly in aquatic environments (36). Distinct stages of biofilm formation have been described (193). The initial stage involves the attachment of planktonic bacteria to a substrate. After attachment, the bacteria replicate on the surface and then mature into three-dimensional, matrix-encapsulated communities

(120, 193). Formation of these biofilm communities is associated with enhanced survival during environmental stress (2) and increased resistance to antibiotics (37).

Biofilms formed by pathogenic bacteria play an important role in colonizing a variety of environmental and medically-relevant surfaces. *Pseudomonas aeruginosa* biofilms promote colonization of in-dwelling catheters in hospital patients and a biofilm-like physiology occurs during cystic fibrosis lung infection (35, 180). *Yersinia pestis* biofilms are reported to function in transmission of plague bacteria via colonization of the proventriculus of fleas and the mouth of nematodes (40, 95). Formation of biofilms by these microorganisms is believed to facilitate environmental survival and provide a potential mechanism of transmission (83).

A review by Hassett *et al.* (87) indicated that the *F. tularensis* subsp. *holartica* live vaccine strain (LVS) can form biofilms on glass coverslips (87). However, the environmental relevance and molecular mechanisms of *F. tularensis* biofilm formation were not characterized. *F. tularensis* subspecies encode for 2 conserved putative chitinases, *chiA* and *chiB* (http://www.biohealthbase.org). Various *F. tularensis* subspecies have been isolated from chitin-exoskeletoned arthropods (146) and from fresh water, where outbreaks have been associated with chitinous crustaceans (4, 45). We, therefore, investigated the interaction of *F. tularensis* subsp. *novicida* (*F. novicida*) with chitin. We show that *F. novicida* forms biofilms on natural and synthetic chitin surfaces. Formation of these bacterial communities was

dependent on two chitinase genes when exogenous sugar was not present. From the published epidemiology data (4, 29, 45) and our discovery of *F. novicida* utilization of chitin during biofilm growth, we propose that chitin may represent a replicative niche for non-host associated *F. tularensis* strains in nature.

2.3 RESULTS

2.3.1 *F. novicida* forms a biofilm on chitin surfaces.

We hypothesized that chitin may be an environmentally relevant surface for the persistence of *F. tularensis* in nature based on the presence of two well-conserved chitinase genes in the sequenced *F. tularensis* genomes (Table 1). Homology to glycosyl hydrolase family 18 chitinases was determined using the SMART bioinformatics algorithm (114, 173). Maintenance of the *chiA* and *chiB* genes in *F. tularensis* subspecies and the related but divergent fish pathogen, *Francisella philomiragia*, suggested that chitinases provide a selective advantage for *Francisella* species in nature. We, therefore, reasoned that these enzymes may confer the ability of this non-motile pathogen to acquire carbon from the local microenvironment. *F. tularensis* subsp. *novicida* (*F. novicida*) is a close relative of the highly virulent Type A *F. tularensis* subsp. *tularensis* and encodes for both chitinase enzymes. Because *F. novicida* is genetically tractable, we used this subspecies as a model to study the molecular aspects of *F. tularensis* ecology.

Table 1 – *Francisella* species chitinase genes

Strain	*chiA* homolog (E-value)*	*chiB* homolog (E-value)*
F. tularensis subsp. *tularensis* SchuS4	FTT0715 (9e-66)	FTT_1768c (2e-15)
F. tularensis subsp. *tularensis* FSC198	FTF0715 (3e-70)	FTF_1768c (2e-15)
F. tularensis subsp. *holarctica* LVS	FTL_1521 (9e-66)	FTL_0093 (1e-15)
F. tularensis subsp. *holarctica* OSU18	FTH_1471 (2e-68)	FTH_0088 (1e-15)
F. tularensis subsp. *novicida* U112	FTN_0627 (4e-69)	FTN_1744 (4e-14)
Francisella philomiragia	Fphi_0215 (1e-66)	Fphi_0864 (1e-15)

* E-value based on comparison to glycosyl hydrolase 18 family chitinases

To test the ability of *F. tularensis* species to adhere to a chitin-containing surface, we incubated *F. novicida* with crab shell pieces. Crab shells are rich in chitin, a constituent of various surfaces *Francisella* species may encounter and subsequently colonize in their natural habitats. These surfaces include copepod and zooplankton shells in fresh water environments and the exoskeletons of arthropod vectors.

We first compared the ability of *F. novicida* to colonize crab shell pieces to known chitin colonizer, *Vibrio cholerae* (92, 129, 167), the causative agent of cholera. Meibom *et al.* established that significant *V. cholerae* El Tor colonization is observed on crab shells and chitin beads when logarithmic phase bacteria grown in rich LB are allowed to colonize for 24 h at 30° C and then subsequently incubated for an additional 24-48 h in minimal Defined Artificial Salt Water medium (129). We tested *F. novicida* in parallel with wild-type *V. cholerae* El Tor and the Δ*mshA V. cholerae* pili mutant strain negative control in this crab shell colonization assay. *F. novicida* was grown in rich modified Mueller Hinton (MH) broth and inoculated onto approximately 1 cm^2 pieces of sterile crab shell for 24 h. Both wild-type *V. cholerae* and *F. novicida*

were recovered at higher levels than the Δ*mshA V. cholerae* pili mutant (Figure 1A). Parallel samples were washed and incubated for an additional 24 h in minimal Chamberlain's defined medium (CDM). After 48 h, *F. novicida* was recovered at statistically equivalent numbers from the crab shell pieces as wild-type *V. cholerae* (Figure 1B). The Δ*mshA* mutant strain had a siginificant defect in chitin colonization compared to both wild-type *V. cholerae* and *F. novicida* ($P<0.002$). For all strains, approximately two-logs replication were observed between the 24 h and 48 h time point indicating replication of the initially adhered bacteria, potentially on the crab shell surface.

(A)

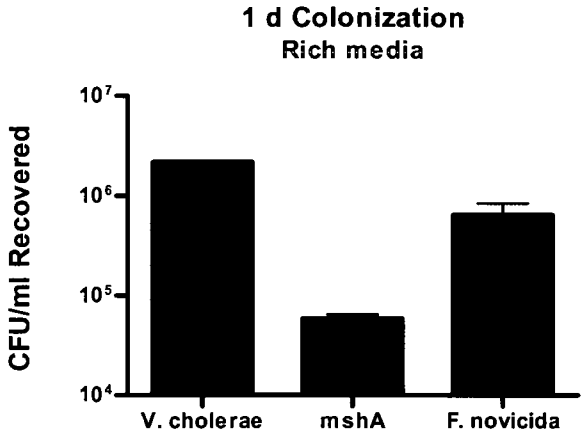

(B)

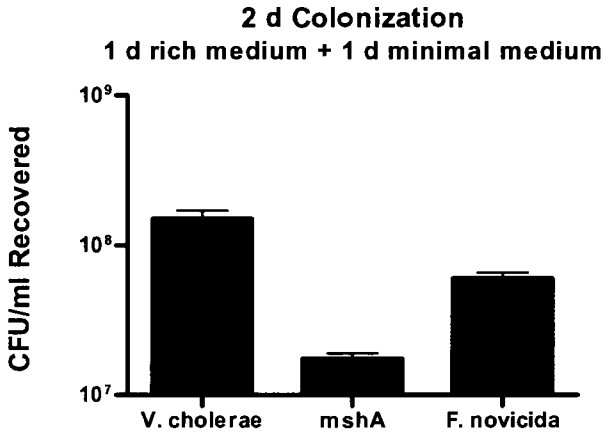

Figure 1 - *F. novicida* colonizes chitin-based crab shells equivalently to *V. cholerae*. Wild-type *F. novicida* chitin colonization was compared to the wild-type *V. cholerae* El Tor and the Δ*mshA* pili deletion mutant strains. All strains were grown to mid-logarithmic phase in rich medium and then inoculated onto sterile crab shell pieces and allowed to associate with the surface for 24 h (A). Parallel samples were washed and incubated for an additional 24 h in minimal medium (B). The graphs above represent the mean of three independent samples. Both wild-type *F. novicida* and *V. cholerae* were recovered at statistically equivalent higher CFU than the Δ*mshA* mutant strain at both time points ($P \leq 0.002$).

After establishing that *F. novicida* colonizes crab shells to a similar extent to *V. cholerae,* we sought to differentiate between bacteria settling on the crab shell surface over time and actual proliferation on the chitin surface. We visualized *F. novicida* chitin colonization by scanning electron microscopy (SEM) to address this question. To establish if *F. novicida* could replicate on the crab shell surface, we shortened the time allotted for bacterial attachment to 1 h. At this point, the shells were washed and the rich medium was replaced with CDM lacking a sugar source. After 1 h attachment at 30°C, individual and small groups of adhered bacteria were present on the shell surface as visualized by SEM (Figure 2A,B). Three-dimensional bacterial communities were present on the chitin-based surface for the parallel samples that were washed after 1 h and incubated for an additional one week in CDM (Figure 2C). At higher magnification (Figure 2D), we observed microcolonies consisting of individual bacteria surrounded by an extracellular polymeric substance (EPS) matrix. This experiment clearly demonstrated an increase in adhered biomass between 1 h and one week, indicating that *F. novicida* can replicate on this surface. Additionally, the observed community structure at one week suggests *F. novicida* can proliferate as biofilms on the environmentally relevant surface, chitin.

Although crab shells consist mainly of chitin, they contain additional components, such as other carbohydrates and protein (143). To test if chitin is sufficient to support *F. novicida* colonization and proliferation, we visualized bacterial attachment and biofilm formation on synthetic chitin films provided

generously by Melanie Blokesch and Gary Schoolnik (217). The 1 h attachment and one week proliferation experiments were performed as above on the crab shell experiment. At 1 h post-inoculation, single bacteria were attached to the chitin films (Figure 2E,F). One week after shift to minimal medium, the surface of the chitin films contained *F. novicida* microcolonies and EPS extensions (Figure 2G,H), and were similar in architecture to the biofilms that we observed on crab shell pieces (Figure 2A-D).

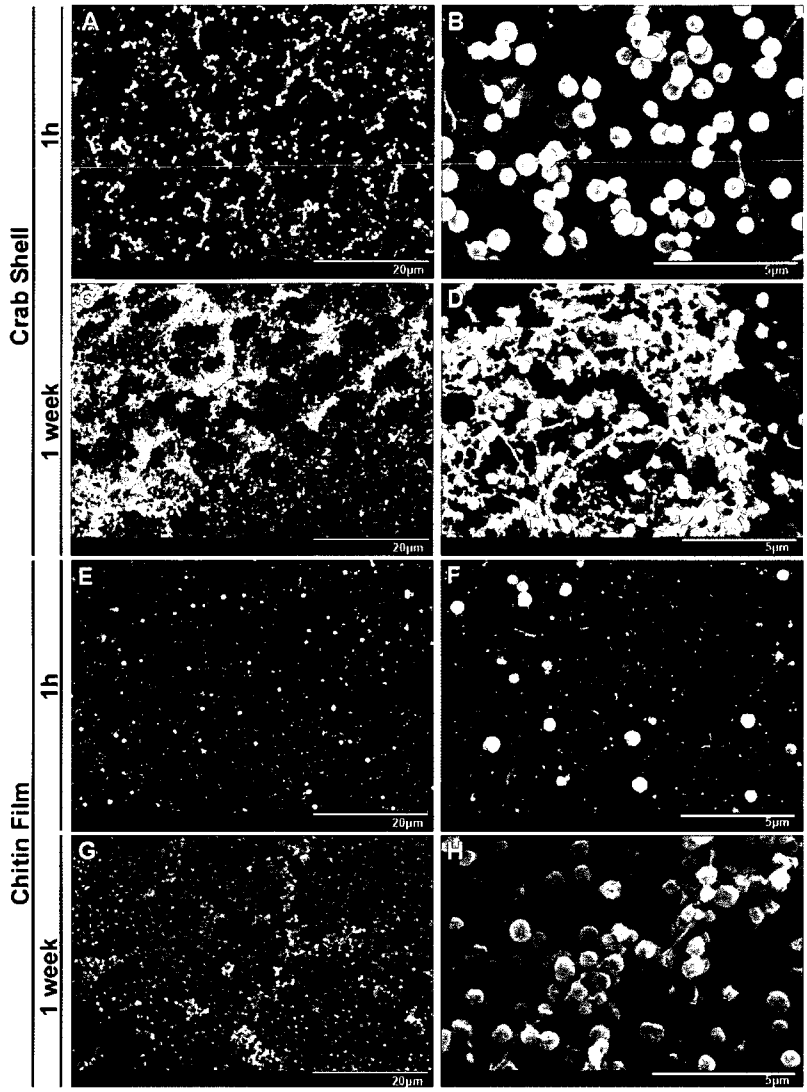

Figure 2 - *F. novicida* biofilm formation on chitin surfaces.

Images display SEM visualization of F. novicida colonization of crab shell pieces (A-D) and synthetic chitin films (E-H). Individual attached bacteria and small attached microcolonies were observed on the crab shell pieces at one hour (A,B). After one week, typical 3D biofilm architecture was observed, consisting of bacteria surrounded by an EPS matrix (C,D). Similar results were obtained after one hour (E,F) and one week (G,H) on synthetic chitin. Scale bar is 20µm for lower magnification images (left column) and 5µm for higher magnification images (right column).

2.3.2 *F. novicida* can utilize *N*-acetyl-D-glucosamine as a carbon source for growth.

F. novicida persistence and proliferation on chitin surfaces in the absence of exogenous sugar suggested that this pathogen was able to utilize the chitin component of the surface as a nutrient source. To test this, we grew *F. novicida* in CDM either without added sugar, supplemented with 10mM glucose (a known metabolic substrate for *Francisella* species (116)), or with 10mM GlcNAc (the monosaccharide end product of chitin hydrolysis (50)) in aerated batch culture. We grew cultures overnight in CDM with glucose and subcultured into the appropriate medium. Optical density at 600 nm (OD_{600}) and colony forming units (CFU) were tracked over time. *F. novicida* growth was negligible in CDM in the absence of an added sugar (doubling time 11.25 h; Figure 3). In contrast, *F. novicida* grew in CDM supplemented with 10mM glucose with a doubling time of 63 minutes (Figure 3). Similarly, *F. novicida* grew in CDM supplemented with 10mM GlcNAc (doubling time of 76 minutes). The high proliferation of *F. novicida* on chitin surfaces (Figure 2) may, therefore, be explained by the ~11-fold increase in growth rate between *F. novicida* grown in CDM with GlcNAc compared to CDM without sugar. We conclude that *F. novicida* can metabolize GlcNAc, suggesting that hydrolysis of chitin by chitinases to generate GlcNAc (99) may provide a local nutrient source for persistence and growth.

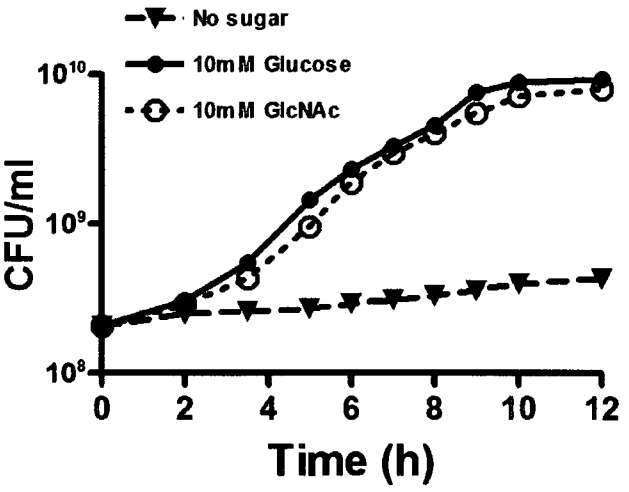

Figure 3 - *F. novicida* can utilize GlcNAc as a carbon source for growth.
Graph indicates growth of Wild-type *F. novicida* in CDM with glucose was diluted into CDM with 10mM glucose, 10mM GlcNAc, or CDM with no sugar added. Wild-type bacteria were grown overnight to stationary phase in CDM with 10mM glucose and then diluted into the appropriate medium. Growth in broth was measured over time in terms of CFU/ml culture.

2.3.3 Chitinase genes facilitate *F. novicida* growth on chitin surfaces.

To further address the importance of chitin as a non-host niche for *Francisella* species in nature, we constructed *F. novicida* mutants lacking either of the chitinase genes, *ΔchiA* (FTN_0627) and *ΔchiB* (FTN_1744), and a mutant strain lacking both chitinases. Hager *et al.* demonstrated that the *F. novicida* homologs of these enzymes that contain chitin-binding domains are secreted and bind to chitin beads (82). Deletion mutants were constructed using the

splicing of overlap extension (SOE) PCR technique (121) to generate constructs with an antibiotic resistance cassette flanked by regions of homology to the approximately 500 bp immediately upstream and downstream of the targeted gene. These PCR constructs were introduced into wild-type *F. novicida* via chemical transformation (23). The single chitinase mutants were complemented using the SOE technique, as well. We complemented the Δ*chiA* deletion mutant in *cis* and the Δ*chiB* strain in *trans* by recombining the SOE construct into pFNLTP6 (123). This plasmid expresses genes under control of the *groEL* promoter in *Francisella* species. We expected the chitinase deletion mutant strains to be attenuated for persistence and biofilm formation on chitin surfaces if *F. tularensis* species have evolved to form biofilms on chitin surfaces to scavenge carbon.

We tested the ability of the chitinase mutant strains to adhere and proliferate on chitin surfaces compared to wild-type *F. novicida.* Indeed, the *ΔchiA* and *ΔchiB* deletion mutants were attenuated for colonization when incubated on chitin-containing crab shells in the presence of CDM without sugar. The chitinase mutant bacteria attached to crab shells to the same extent as wild-type *F. novicida* based on the 1 h attachment assay described above (Figure 4). Therefore, these hydrolytic enzymes do not appear to function in the initial association with a chitin surface. Despite an equivalent adhered starting population as wild-type *F. novicida*, we recovered 16- and 15-fold fewer *ΔchiA* and *ΔchiB* mutant bacteria compared to wild-type *F. novicida* ($P<0.001$), respectively, after 2 days colonization on crab shells in CDM

without sugar (Figure 5A). Furthermore, we recovered equivalent *ΔchiAΔchiB* double chitinase mutant bacteria compared to the *ΔchiA* or *ΔchiB* single chitinase mutant strains (Figure 5A), suggesting that the two chitinase genes act in the same metabolic pathway, as predicted by KEGG pathway analysis (97). Mutant *ΔchiA* and *ΔchiB* strains growth on chitin was restored by the re-introduction of wild-type copies of each chitinase gene into the coinciding mutant strain as measured by increased crab shell colonization to near wild-type *F. novicida* levels (Figure 5A).

We postulated that the inability of chitinase mutant bacteria to convert chitin to the useable metabolite, GlcNAc, explains the attenuated colonization of these mutants on chitin. Indeed, the inability of the chitinase mutants to colonize crab shells was alleviated by the addition of 10mM GlcNAc to the exogenous medium (Figure 5B), indicating that the chitinase mutant bacteria possess the determinants required to colonize a chitin surface, but lack the ability to generate a useable carbon source in order to proliferate. The 13-fold decrease in recovered wild-type *F. novicida* when GlcNAc was added (Figure 5) is consistent with microarray data published for *V. cholerae* demonstrating that when this pathogen was grown in the presence of excess GlcNAc, the pili and chitinases required to colonize this surface were repressed (129).

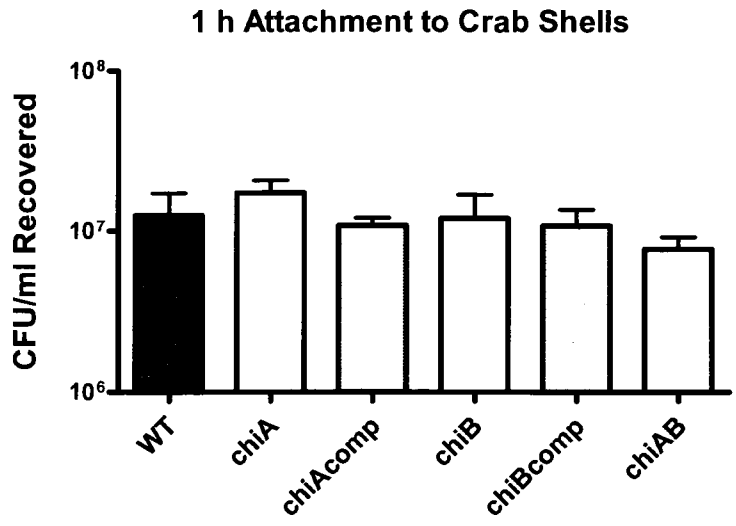

Figure 4 – *F. novicida* chitinase attach to crab shells equivalent to wild-type bacteria. Wild-type (black), chitinase mutant (white), and complemented mutant strains (grey) were grown in MH medium overnight at 30° C and then inoculated for 1 h onto sterile crab shell pieces. The average CFU/ml recovered after 1 h for triplicate samples is displayed above. Both the individual Δ*chiA* and Δ*chiB* deletion mutant strains, as well as the double Δ*chiA* Δ*chiB* mutant were recovered at equivalent levels to wild-type *F. novicida*. Complemented chitinase mutant strains were recovered at approximately $1x10^7$ CFU/ml, as well.

□

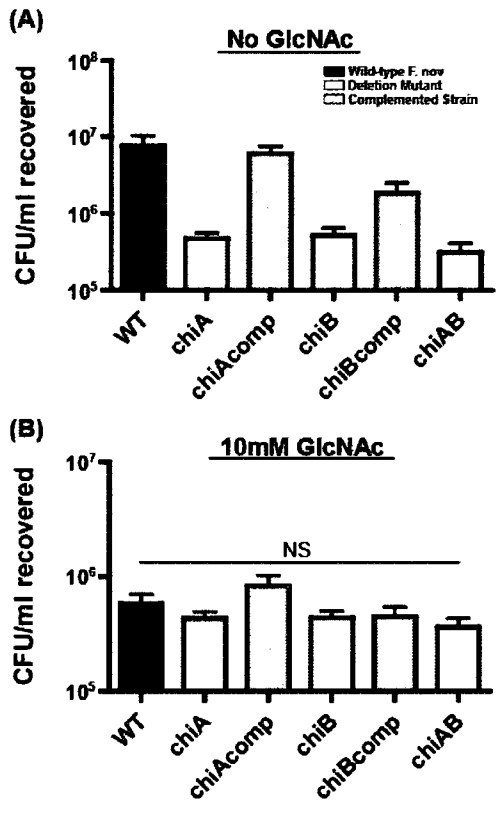

Figure 5 - Chitinase mutants are attenuated for chitin colonization in the absence of exogenous sugar.

Stationary phase wild-type and chitinase mutant bacteria were allowed to adhere for 1 h to crab shell pieces. Equivalently adhered strains were allowed to colonize these chitin surfaces in CDM with or without GlcNAc at 30°C. Triplicate samples were harvested 2 d post-inoculation and enumerated for CFU. Chitinase mutant *F. novicida* (white) were recovered at statistically lower levels than wild-type bacteria (black), ($P<0.001$) when incubated in CDM (A), but in equivalent numbers in CDM with GlcNAc (B). Addition of wild-type chiA and chiB genes to deletion mutant strains (grey) complemented the chitin colonization defects observed during colonization in CDM without GlcNAc (A).

We next compared the architecture of the communities formed by the chitinase mutants on crab shells or chitin films in the absence of exogenous sugar for one week by SEM. In contrast to wild-type *F. novicida*, the chitinase mutants were present as single bacteria or small, mostly monolayer, clusters of bacteria (Figure 6). This level of colonization resembled that observed at 1 h (Figure 2). Since we demonstrated that chitinase mutants strains adhere equal to wild-type (Figure 4), the differences in accumulated biomass at one week is indicative of a defect in replication. We concluded that *F. novicida* biofilm formation on chitin in the absence of exogenous sugar requires functional chitinase enzymes.

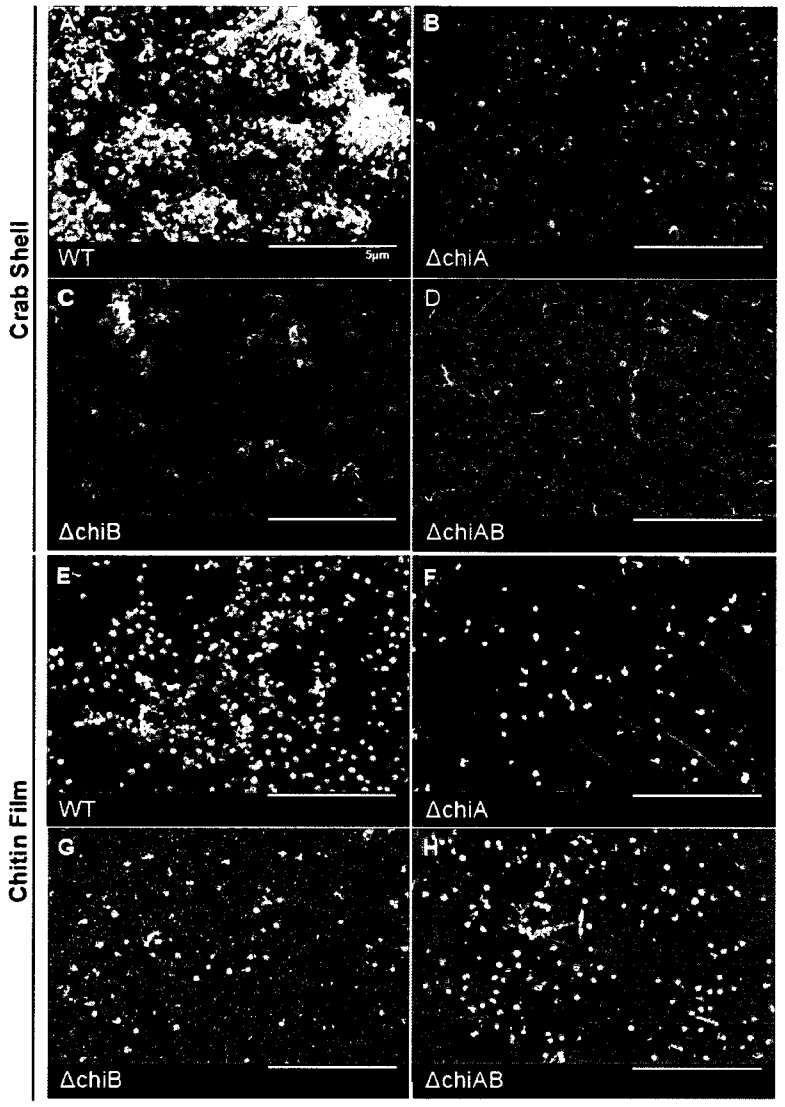

Figure 6 - Chitinase genes are required for biofilm architecture on chitin surfaces during nutrient stress.

Images show representative colonization by wild-type and chitinase mutant strains on crab shells (A-D) or synthetic chitin films (E-H). Bacteria were allowed to attach for 1 h and then incubated for one week at 30°C before being processed for SEM. In contrast to extensive 3D biofilm development in wild-type *F. novicida*, the chitinase mutants were present as single bacteria or small clusters of bacteria on both natural and synthetic chitin. Scale bar is 10μm.

2.4 DISCUSSION

In this chapter we describe the first characterization of *F. tularensis* biofilms on an environmentally relevant surface. One limitation in biofilm studies has been the reliance on glass and polystyrene to characterize the formation of these surface-associated bacterial communities. In a review, Hasset *et al.* reported unpublished data stating that the *F. tularensis* LVS strain formed biofilms under static conditions (87). While the authors claimed that biofilm formation by *F. tularensis* species promotes interaction with amoeba, the single figure provided merely shows fluorescence imaging of GFP-labeled LVS overlaid over a phase image of *Acanthamoeba castellanii.* Two additional publications have recently discussed *F. tularensis* biofilms (43, 48), but neither offered relevance for these communities or provided structural characterization. Both publications relied solely on crystal violet staining of polystyrene-attached bacteria to establish biofilm formation.

Our microscopy studies revealed that *F. novicida* forms biofilms on chitin surfaces (Figure 2), providing potential insight into where biofilm formation by this pathogen may be relevant in nature. These surfaces include fresh water crustaceans and arthropod vectors. The lower attachment of *F. novicida* to the smooth chitin films compared to the topographically varied crab shells after one hour (Figure 2A,E) may explain the decreased biofilm growth on the pure chitin surface compared to crab shells (Figure 2C,G). Alternatively, additional components in the crab shell, like protein, may allow for more rapid expansion of the adhered population.

During the chitin colonization experiments, biofilms formed in the absence of exogenous sugar. Growth in CDM without sugar enhanced chitin surface growth approximately 13-fold compared to *F. novicida* grown on crab shell pieces in the presence of GlcNAc (Figure 5). We hypothesized that *F. novicida* could utilize the chitin surface, itself, as a substrate for growth and that carbon limitation was a cue for chitin colonization. The ability to grow with chitin as a carbon source is conserved amongst many environmental microorganisms, including *Shewanella oneidensis, Serratia marcescens, Streptomyces coelicolor,* and a number of marine *Vibrio* species (34, 47, 92, 194). Hydrolysis of chitin to GlcNAc monomers is catalyzed by chitinase enzymes. These enzymes cleave the β1→4 linkages that connect these monosaccharides (14). GlcNAc liberated by chitinase hydrolysis of chitin can be converted to the glycolytic intermediate, fructose-6-phosphate (99). By comparing *F. novicida* growth in minimal medium with no exogenous sugar, glucose, or GlcNAc, we demonstrated that this organism can grow with GlcNAc as a carbon source (Figure 3). To understand the full array of chitin derivatives that *F. tularensis* species can metabolize, growth on different GlcNAc polysaccharides including chitobiose, chitosan, and $(GlcNAc)_6$ should be explored in the future.

We further illustrated that *F. novicida* biofilm formation on crab shell pieces requires chitin utilization by characterizing the biofilm phenotype of deletion mutants in two well-conserved chitinase genes (Table 1). Although we have not been able to express these proteins to confirm chitinase activity

biochemically, Hager *et al.* did show that ChiA and ChiB have chitin-binding domains and bind to chitin beads in vitro (82). Chitinases are divided into two functional classes, with distinct substrate specificities. Exochitinases demonstrate specific activity for the non-reducing end of the chitin polymer, while endochitinases hydrolyze the β1→4 linkages that connect GlcNAc monomers (14). The *chiA* gene is annotated by KEGG pathway analysis as the *F. tularensis* endochitinase and *chiB* the exochitinase (97). Single deletions in *chiA* and *chiB*, as well as a double deletion strain, attached equivalently to wild-type *F. novicida* (Figure 4), but colonized to a lesser extent (Figure 5) and showed little biofilm formation when grown on chitin surfaces in the absence of exogenous sugar (Figure 6). While equal CFU were recovered for the Δ*chiA* and Δ*chiB* deletion mutants after 2 d crab shell colonization in CDM lacking sugar (Figure 5), visually larger microcolonies were consistently observed for the Δ*chiB* mutant strain in our SEM images of crab shell colonization at one week (Figure 6). The putative exochitinase activity of this gene product may explain this intermediate phenotype. A mutant lacking the ChiB enzyme would not be able to cleave the ends of chitin strands, but would still have the ability to hydrolyze β1→4 linkages generating short chain GlcNAc polymers. The equivalent phenotype of the single deletion mutants as the Δ*chiA*Δ*chiB* double mutant strain in these assays furthers the idea that these gene products function in the same metabolic pathway.

The ability of the chitinase mutant strains to persist at low levels could be due to the utilization of the amino acids present in the CDM medium.

Although severely retarded compared to growth in CDM with glucose or GlcNAc added, *F. novicida* did grow in CDM with no sugar (Figure 3). Alternatively, natural degradation of the crab shell during the experiment could liberate enough free GlcNAc to enable the bacteria to persist, but not replicate. Regardless, the highly significant difference between wild-type and chitinase mutant bacteria suggests that chitinases strongly contributes to *F. novicida* persistence on chitin in otherwise carbon-limiting conditions. From these results we conclude that functional ChiA and ChiB gene products are required for *F. novicida* biofilm formation during nutrient-limited growth. Chitinases, therefore, may provide a nutrient source for *F. tularensis* in fresh water, allowing for environmental persistence of this pathogen. Biofilms formed on chitin surfaces may then sequester freed GlcNAc in the local microenvironment enabling *F. tularensis* replication.

Survival of *F. tularensis* outside of a mammalian or arthropod host has only been limitedly investigated. Mironchuck *et al.* found that shrimp, mullosks, diatoms, or zooplankton increased the persistence of this pathogen for an additional week to one month in nutrient-poor water (135). Each of these organisms presented a chitin source for *F. tularensis* to utilize in this environmental modeling study.

The observed biofilm phenotype on crab shells and synthetic chitin is similar to what is observed with *V. cholerae* (14, 129). Cholera, which affects millions in seasonal outbreaks of diarrheal disease in the developing world (60), relies on chitinous copepods to replicate and seed infection. *V. cholerae*

has evolved a well controlled means to sense the combination of starvation and chitin availability to regulate expression of genes that promote survival on this complex polysaccharide (129). While only a few thousand cases of tularemia are reported annually (177), the emergence of disease in Europe where tularemia is now endemic (146) and the threat of weaponization (153) make understanding how *F. tularensis* survives in nature crucial. Our observation that *F. novicida* forms biofilms similar to *V. cholerae* on chitin provides a first indication of the *F. tularensis* environmental persistence mechanisms. Unlike *V. cholerae, F. tularensis* is non-flagellated and non-motile and cannot chemotax towards higher nutrient gradients (39). Therefore, attachment to and utilization of chitin surfaces may be one of few means of nutrient acquisition in nature. With the experimental model system we developed in completing this work, we can now address the genetic determinants and molecular mechanisms of this interaction.

Chapter 3: Sec-secreted factors mediate *Francisella tularensis* subspecies *novicida* attachment during biofilm formation

Jeffrey J. Margolis[1], Sahar El-Etr[2], Lydia-Marie Joubert[3], Emily Moore[4], Richard Robison[4], Amy Rasley[2], Alfred M. Spormann[5], and Denise M. Monack[1]

[1] Department of Microbiology and Immunology, Stanford University School of Medicine, Stanford, CA 94305, USA.
[2] Bioscience and Biotechnology Division, Lawrence Livermore National Laboratory, Livermore, CA 94550, USA.
[3] Cell Sciences Imaging Facility, Stanford University School of Medicine, Stanford, CA 94305.
[4] Department of Microbiology and Molecular Biology, Brigham Young University, Provo, UT 84602, USA.
[5] Department of Civil and Environmental Engineering, Stanford University, Stanford, CA 94304, USA.

This chapter has been accepted for publication in *Applied Environmental Microbiology.*

3.1 CHAPTER 3 SUMMARY

The discovery of *F. novicida* biofilm formation on chitin surfaces provided us an opportunity to explore the establishment of these communities by non-motile pathogenic bacteria. If biofilms, indeed, promote survival of *F. tularensis* outside of a host, it is imperative to understand how these populations form and grow for the control of disease transmission. To further characterize *F. tularensis* biofilm formation and identify factors that promote biofilm attachment and growth we used established biofilm models: flow cells and crystal violet staining of static biofilm growth. Investigation of in vitro biofilms on abiotic surfaces provided a model system to characterize and genetically dissect *F. novicida* biofilm formation and test the ability of other pathogenic *F. tularensis* strains to similarly attach and proliferate on a surface.

To determine the genetic determinants of *F. tularensis* biofilm formation, we screened a "Two Allele" transposon-insertion mutant library for mutations that conferred altered biofilm formation. Biofilm formation was assayed by crystal violet staining. This forward genetic screen for biofilm mutants that exhibited both reduced and enhanced biofilm formation. In this chapter, the 88 genes required for wild-type levels of *F. novicida* biofilm formation are highlighted. Fifty-eight of these genes were attenuated for initial attachment to polystyrene based on a secondary screen for adhesion mutants. This gene list included the Sec translocon apparatus, as well as 14 putative secreted proteins. We mutated two chaperone genes (*secB1* and *secB2*) involved in Sec-dependent secretion and 4 genes that encode for putative

secreted proteins. All mutants were deficient for attachment to both polystyrene and chitin surfaces and for biofilm formation compared to wild-type *F. novicida*. These biofilm-deficient deletion mutants were also attenuated for systemic colonization of *Drosophila melanogaster*. Conversely, these mutants were virulent in macrophages and mice. We hypothesize that these Sec-secreted factors, particularly the FTN_0308 and FTN_0714 gene products that contain putative chitin-binding domains, allow for specific adherence to non-mammalian surfaces and enable *F. tularensis* to utilize chitin surfaces as a non-host niche in nature.

3.2 INTRODUCTION

In Chapter 1 we describe the potential environmental relevance of *F. tularensis* biofilm formation on chitin surfaces. The missing piece to this model was the genetic determinants that facilitate the initial association with the chitin surface that initiates this process. Identifying the bacterial factors that enable *F. tularensis* to attach to chitin will lead to a better understanding of how this zoonotic pathogen colonizes environmental surfaces and may eventually allow for blocking environmental persistence and transmission to the chitinous arthropod vectors that transmit tularemia. To further characterize *F. tularensis* biofilm formation and identify factors that promote biofilm attachment and growth we used established biofilm models: flow cells (161) and crystal violet staining of static biofilm growth (148).

Genetic screens have been used to identify the genetic factors required for biofilm formation in a variety of both Gram-negative and Gram-positive bacteria, including *Pseudomonas aeruginosa, Shewanella oneidensis*, *Caulobacter crecentus, Vibrio* species, and *Staphylococcus auerus* (56, 57, 148, 190, 196). These studies revealed that although many steps in biofilm formation are conserved among various biofilm-forming bacteria, the molecular mechanisms utilized by bacteria during biofilm growth can be species-specific. For example, Type-IV pili are required for adherence and biofilm formation for *S. oneidensis*, *Vibrio* and *Pseudomonas* species (147, 190, 216), but not for *Caulobacter crescentus* and *Staphylococcus aureus,* which form microcolonies via other means (57, 196).

Biofilm determinants for pathogenic bacteria often have a second role in virulence, including Type-IV pili, which are also required for attachment to epithelial surfaces and systemic colonization of mammalian hosts (210). It is unknown if such functional redundancy occurs in *F. tularensis.* Therefore, our screen for *F. tularensis* attachment and biofilm genes was particularly informative because very little is known about the adherence mechanisms of this bacterium to host or non-host surfaces.

As mentioned above, Type-IV pili are a common component of Gram-negative surface association. LVS Type-IV pili mutants are attenuated for systemic infection during intradermal infection, but surprisingly adhere and replicate within macrophages at wild-type levels (26). Although piliated, *F. tularensis* strains are not motile under laboratory conditions (39) which further

suggested that this pathogen utilizes novel molecular mechanisms to form biofilms.

The only factor directly attributed to *F. tularensis* adhesion in any context is *fpaP* (FTN_1596), a membrane protein that when expressed in non-adherent *Escherichia coli* confers the ability to attach to L549 lung epithelial cells (130). Nothing to date has been published on *F. tularensis* attachment factors for non-mammalian surfaces. Recently, Durham-Colleran *et al.* tested specific *F. novicida* transposon-insertion mutants for biofilm formation and identified *pmrA* as the first biofilm-attenuated mutant for *Francisella* species (48). The role of this virulence factor in biofilm formation remains unclear. Given the variety of environments and surfaces that *Francisella* species inhabit and the general lack of homology to known adhesins in other Gram-negative bacteria, we postulated that screening for *F. tularensis* biofilm formation would identify novel mechanisms of attachment that may be conserved among non-motile organisms.

We utilized a "Two Allele" transposon-insertion mutant library made available by Larry Gallagher and Colin Manoil at the University of Washington (66) to screen for genes that contribute to biofilm formation and initial attachment based on crystal violet staining (148). The Two Allele library consists of two or more independent transposon-insertion mutants in all non-essential *F. novicida* genes. At the time of screening, Plate 15 of the library was unavailable due to quality control issues, resulting in a library size of 2,954 mutants. We identified 98 mutants, representing 88 genes, that were

deficient for biofilm formation and here we describe the role of Sec-secreted proteins in initial attachment to abiotic and biotic surfaces.

3.3 RESULTS

3.3.1 Characterization of biofilm development by *Francisella* species.

High throughput testing of thousands of transposon-insertion mutants for biofilm formation on chitin was technically challenging. We, therefore, turned to in vitro biofilm formation on abiotic surfaces as a model system. Before we could screen for genetic determinants of *Francisella* species biofilm formation, we first needed to validate that these organisms formed biofilms in established in vitro biofilm models. We incubated GFP-labeled *F. novicida* in the flow cell system (31) to confirm in vitro formation of biofilm communities under flow conditions. Mid-logarithmic phase *F. novicida* were inoculated into flow cell chambers in triplicate and allowed to adhere for 1 h. Once flow of MH broth was initiated, we analyzed bacterial attachment and surface growth at ambient temperature (20-22°C) and a flow rate of 0.1 ml/min by confocal laser scanning microscopy (CLSM) at various timepoints (24h, 48h, 72h, 96h and 120h) (Figure7). At 24 h, we found only single cells and small clumps of bacteria, similar to the 1 h attachment SEM images of *F. novicida* attaching to chitin surfaces. This result suggested that the bacteria were not replicating or were replicating but becoming dissociated from the surface in the presence of laminar flow. At 48 h, however, we noted proliferation at the glass surface,

and over five days we observed the formation of a matt-like biofilm with an average depth of approximately 15 μm. Given an average width of 1 μm for a single bacterium, flow cell biofilms were about 15 cells high. This architecture of flow-cell-grown *F. novicida* biofilms was similar to that reported for other Gram-negative species, including the related γ-proteobacterium *S. oneidensis* (190) and α-proteobacterium *C. crescentus* (57). Our results indicate that *F. novicida* is able to form biofilms on an abiotic surface, such as glass, with similar architecture to that observed on chitin (Figure 2). These results are consistent with the report by Hassett *et al.* indicating that LVS can form biofilms on glass coverslips in the absence of flowing media (87).

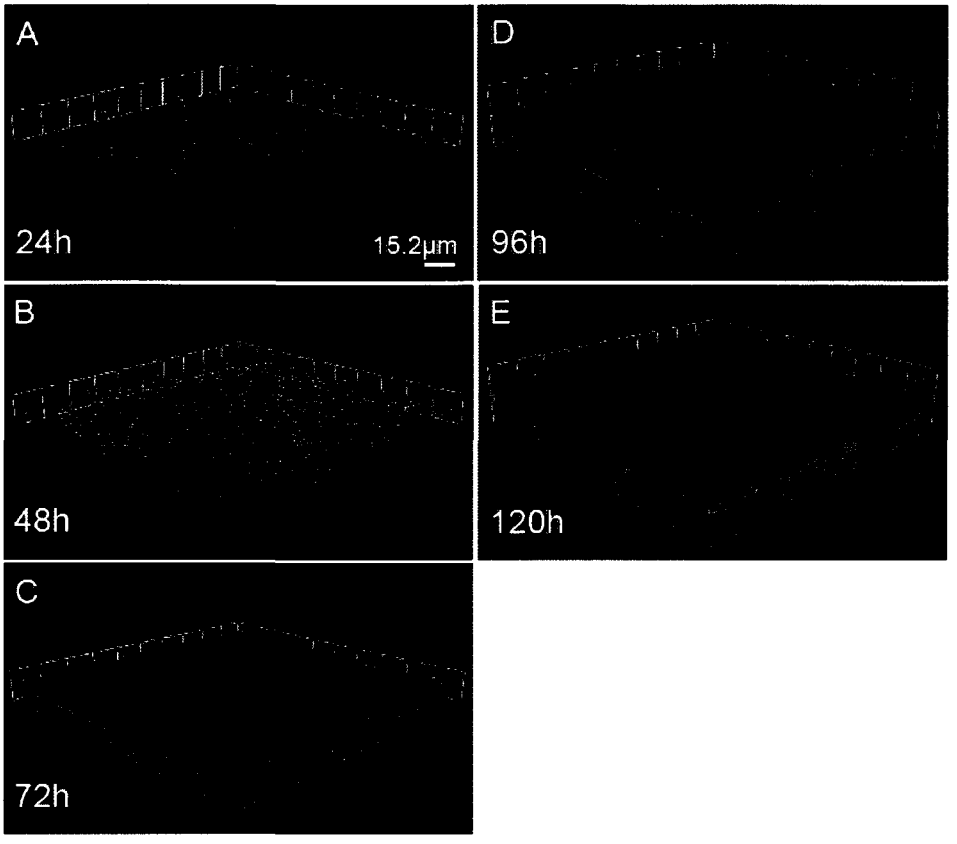

Figure 7 - *Francisella* forms a matt-like biofilm under flow conditions.
GFP expressing *F. novicida* grown at room temperature (20-22°C) were imaged daily in flow cells run at 0.1ml/min using confocal laser scanning microscopy. Representative images from triplicate experiments are shown. At 24h (A), small groups of bacteria are present. Over the next 48h (B,C), a uniform monolayer of bacteria is observed on the surface. By 96h (D), depth in the biofilm is observed and at 120h (E) the biofilm reached an average thickness of 15µm. Scale bar is 15.2µm.

We next utilized a modified O'Toole and Kolter microtiter assay (148) to establish a high throughput model for *F. tularensis* biofilm formation. This assay measures adhered biomass under static conditions by crystal violet stain. *F. novicida* and *F. tularensis* subsp. *holarctica* live-vaccine (LVS) strains

were grown at 26°C and 37°C in 96-well microtiter plates. Recent work by Horzempa *et al.* found that the LVS strain demonstrated different expression profiles at these two temperatures (91). The OD_{570} (Figure 8A,B) and crystal violet staining (CV_{570}), (Figure 8C,D) were measured over 152 h. The kinetics of static growth by *Francisella* species have not been previously reported. Consistent with the kinetics of aerated growth (88), LVS replicated slower than *F. novicida* at both temperatures (Figure 8A,B). At 26° C, *F. novicida* entered stationary phase at 54 h, while LVS did so at 112 h. A similar result was obtained at 37° C, where *F. novicida* and LVS entered stationary phase at 24 h and 54 h, respectively.

Both *F. novicida* and LVS strains showed increased crystal violet staining over time when grown at 26°C and 37°C, indicating increased accumulation of adhered biomass (biofilm formation). This result was consistent with our finding that *F. novicida* forms biofilms when adherent to an abiotic surface (Figure 7). Despite significant differences in growth kinetic between the two strains tested, similar crystal violet staining was observed at each time point at 37° C (Figure 8D). At both temperatures assayed we observed a decrease in crystal violet staining (Figure 8C,D) concurrent with *F. novicida* and LVS entering stationary phase (Figure 8A,B). This result suggested that the biofilms were undergoing dispersion (189), a process of biofilm dissolution and re-seeding occurring during decreased oxygen tension and nutrient deprivation. Similar dispersal did not occur in the flow cell system grown *F. novicida* biofilms (Figure 7), presumably because the population was

constantly provided an undepleted carbon and oxygen source under flow conditions.

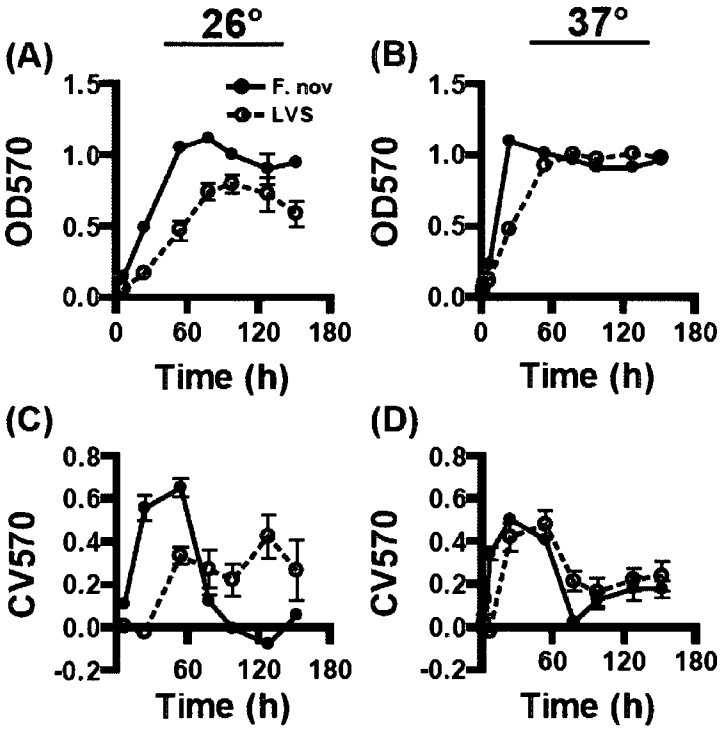

Figure 8 - Kinetics of *F. tularensis* biofilm formation under static conditions.
A modified O'Toole and Kolter assay was performed to compare the kinetics and relative levels of biofilm formation for *F. novicida* (solid circles) and LVS (open circles). Bacterial growth (A,B) and crystal violet staining (C,D) were determined over time at 26°C (A,C) and 37°C (B,D) by OD_{570} readings. Both *F. tularensis* strains were found to acquire crystal violet stain at both temperatures. Growth and crystal violet staining were faster at 37°C for both strains.

3.3.2 Type A *Francisella* strains form biofilms in the microtiter plate assay.

A high percentage of tularemia morbidity and mortality in humans is caused by infection with *F. tularensis* subsp. *tularensis* (Type A) strains (59). These strains have a very low infectious dose, and as few as ten organisms can cause a lethal infection in humans (55). Molecular subtyping of Type A strains has identified two distinct subtypes (A1 and A2) with specific geographic distributions (103). Type A1 strains are primarily found in the Eastern United States, while Type A2 strains are almost exclusively isolated in the West.

Work with Type A strains was performed by Sahar El-Etr, Amy Rasley, and Emily Moore at the BSL-3 facility of Richard Robison at Brigham Young University. The O'Toole and Kolter microtiter assay demonstrated that the Type A1 and Type A2 highly virulent strains were able to form biofilms to similar levels as *F. novicida* and LVS strains at 37° C (Figure 9). We used mammalian temperature to increase growth kinetics, due to time considerations for the BSL-3 facility at BYU. Although this temperature was not necessarily indicative of ambient temperature for *F. tularensis* biofilm formation in nature, our work comparing biofilm formation at 26° C and 37° C (Figure 8) suggested that biofilms could form at either temperature by *Francisella* species. Because we wanted to confirm the ability of virulent Type A strains to form the bacterial communities, we did not consider the temperature to be critical. SchuS4 (Type A1) and FT-10 (Type A2) *F. tularensis* subsp. *tularensis* strains reached similar optical densities as LVS

(Type B) when grown under static conditions (Figure 9), while SchuS4 and FT-10 exhibited higher crystal violet staining at 24 h ($P<0.05$), implying increased biofilm formation of Type A strains compared to LVS (Figure 9). *F. novicida* CV_{600} staining was approximately two-fold higher than the other strains tested ($P<0.001$). However, the optical density of the *F. novicida* culture was 2.5-fold higher than the other strains at 24h. Similar crystal violet staining by Type A1 and Type A2 strains compared to the Type B LVS strain suggests that biofilm formation may be pertinent to the survival of pathogenic *F. tularensis* strains in the environment.

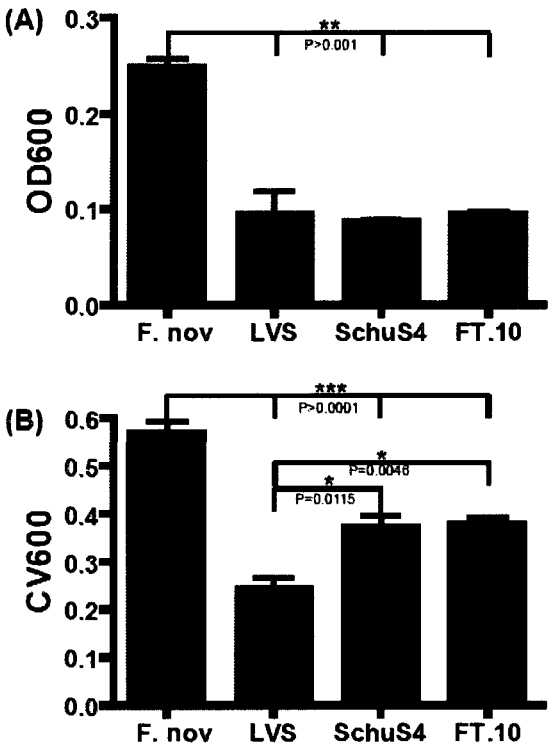

Figure 9 – Virulent Type A *F. tularensis* strains form biofilms under static conditions. Static growth (A) and 8 h biofilm formation (B) were determined for two Type A *F. tularensis* strains, SchuS4 and FT.10, compared to *F. novicida* and LVS (Type B). Quadruplicate samples of the Type A strains grew equivalent to LVS and had statistically higher crystal violet staining at 8 h ($P<0.05$).

3.3.3 Screen for biofilm-deficient mutants identifies novel genes important for *F. novicida* biofilm formation.

We utilized the established crystal violet staining method of biofilm enumeration to search for *F. novicida* attachment factors. Identification of novel adhesins may shed light on how this pathogen colonizes chitin and other nutritive surfaces in nature. We screened a two-allele transposon library (BEI Resources, Manassas, VA) that represented two or more transposon-insertion

mutants per non-essential gene in the *F. novicida* genome to elucidate the genetic determinants of *F. novicida* interaction with abiotic and biotic surfaces. To facilitate high-throughput screening, individual insertion mutants were assayed for biofilm formation in the microtiter assay established above rather than on chitin. We defined biofilm-deficient mutants as strains where crystal violet staining was two standard deviations below the mean of the plate at 8 h post-inoculation. We eliminated mutant strains that exhibited a significant growth defect from further characterization.

In total, we identified 98 *F. novicida* transposon-insertion mutants, representing 88 genes that were attenuated for biofilm formation (Table 2). Although only ten genes were identified by multiple transposon-insertion mutants, this result was consistent with other screens performed in our lab (personal communication with Jonathan Jones). Gene Ontology Classifications (www.biohealthbase.org) were used to elucidate pathways important for *F. novicida* surface attachment and growth (Figure 10). Roles for the 64 annotated genes included protein secretion, various metabolic pathways, signal transduction, protein transport, and cell envelope biogenesis. Despite bioinformatic inference to the function of these annotated genes, the role of the majority of these genes in biofilm formation was not evident. Of note, over 25% of genes identified by our screen had no known function.

Because we were particularly interested in identifying factors required for chitin attachment, biofilm-deficient mutants were subjected to a secondary screen for attachment competency. Stationary phase strains were incubated

for 1 h in microtiter wells and then tested for attachment by crystal violet assay. Stationary phase cultures were used to limit differences in growth phase and bacterial number between strains. Of the 88 genes that contribute to *F. novicida* biofilm formation, 58 were found to function during attachment (Table 2). The high percentage of attachment-deficient mutants was consistent with published crystal violet-based biofilm screens (16, 175, 196).

Table 2 - Genetic determinants of *F. novicida* biofilm formation

FTN	Well Id[a]	Gene	Gene Product	Biological Process	Attachment[b]
FTN_0014	9A06		conserved hypothetical protein	hypothetical - conserved	-
FTN_0031	23B08		transcriptional regulator, LysR family	signal transduction and regulation	-
FTN_0071	32C04		LPS fatty acid acyltransferase	cell wall / LPS / capsule	+
FTN_0090	4F07	acpA	acid phosphatase	fatty acids and lipids metabolism	-
FTN_0100	20C12		hypothetical membrane protein	hypothetical - novel	-
FTN_0107	18G03	lepA	GTP-binding protein LepA	cell wall / LPS / capsule	+
FTN_0107	6F05	lepA	GTP-binding protein LepA	cell wall / LPS / capsule	+
FTN_0109	14G06		protein of unknown function	unknown function - novel	-
FTN_0114	27C08	ribD	pyrimidine reductase/ pyrimidine deaminase	cofactors, prosthetic groups, electron carriers metabolism	-
FTN_0121	26G09	secB1	preprotein translocase, subunit B	motility, attachment and secretion structure	-
FTN_0121	4F06	secB1	preprotein translocase, subunit B	motility, attachment and secretion structure	-
FTN_0143	6G07		monovalent cation:proton antiporter	transport	-
FTN_0178	3A05	purA	adenylosuccinate synthetase	nucleotides and nucleosides metabolism	-
FTN_0191	19 E06		polar amino acid uptake transporter	transport - amino-acid	-
FTN_0197	22C11	cyoC	cytochrome bo terminal oxidase subunit III	energy metabolism	+
FTN_0292	10 E05		protein of unknown function	unknown function - novel	+
FTN_0304	20C11		pilus assembly protein	motility, attachment and secretion structure	-
FTN_0308	19H06		membrane protein of unknown function	unknown function - novel	-
FTN_0332	14C06	rpmG	50S ribosomal protein L33	translation, ribosomal structure and biogenesis	-
FTN_0337	11D06	fumA	fumarate hydratase, class I	energy metabolism	+
FTN_0354	12 E08	tolA	group A colicin translocation; tolA protein	transport - drugs / antibacterial compounds	+
FTN_0354	17H06	tolA	group A colicin translocation; tolA	transport - drugs / antibacterial	-

			protein	compounds	
FTN_0355	20F07	tolB	group A colicin translocation; tolB protein	transport - drugs / antibacterial compounds	-
FTN_0356	8G04		glutathione peroxidase	post-translational modification, protein turnover, chaperones - protein modification	-
FTN_0357	21B08	pal	peptidoglycan-associated lipoprotein, OmpA family	transport - drugs / antibacterial compounds	-
FTN_0358	11G10		tRNA-methylthiotransferase MiaB protein	translation, ribosomal structure and biogenesis	-
FTN_0429	14G12		conserved protein of unknown function	unknown function - conserved	-
FTN_0431	26H05		hypothetical membrane protein	hypothetical - novel	-
FTN_0454	4 E04		conserved protein of unknown function	unknown function - conserved	-
FTN_0456	4F05		EAL and a GGDEF domain	signal transduction and regulation	+
FTN_0516	1D09	glgA	glycogen synthasecarbohydrate	metabolism - biosynthesis	+
FTN_0516	31F07	glgA	glycogen synthasecarbohydrate	metabolism - biosynthesis	+
FTN_0527	6F12	thrC	threonine synthaseamino acid	metabolism - biosynthesis	-
FTN_0565	14D01		conserved protein of unknown function	unknown function - conserved	+
FTN_0582	9G12	gph	phosphoglycolate phosphatase	putative enzymes	+
FTN_0593	23H02	sucD	succinyl-CoA synthetase, alpha subunit	energy metabolism	+
FTN_0594	23 E02	sucC	succinyl-CoA synthetase, beta chain	energy metabolism	+
FTN_0617	23 E04		ROK family protein	putative enzymes	-
FTN_0624	20A08	sdaC1	serine permease	transport - amino-acid	-
FTN_0649	23D01		4Fe-4S ferredoxin, FAD dependent	energy metabolism	-
FTN_0672	12G03	secA	preprotein translocase, subunit A (ATPase, RNA helicase)	motility, attachment and secretion structure	-
FTN_0678	10A11		drug:H+ antiporter-1 (DHA1) family protein	transport - drugs / antibacterial compounds	+
FTN_0697	10G03		conserved protein	unknown function -	+

			of unknown function	conserved	
FTN_0713	14C04	ostA2	organic solvent tolerance protein OstA	cell wall / LPS / capsule	-
FTN_0713	21H10	ostA2	organic solvent tolerance protein OstA	cell wall / LPS / capsule	-
FTN_0713	26 E07	ostA2	organic solvent tolerance protein OstA	cell wall / LPS / capsule	-
FTN_0714	12G01		protein of unknown function	unknown function - novel	-
FTN_0714	27C09		protein of unknown function	unknown function - novel	-
FTN_0737	22A12	potI	ATP-binding cassette putrescine uptake system, membrane protein, subunit I	transport	+
FTN_0785	5B06		isochorismatase family protein	putative enzymes	-
FTN_0798	10D11		conserved protein of unknown function	unknown function - conserved	-
FTN_0907	20G04	dacD	D-alanyl-D-alanine carboxypeptidase	cell wall / LPS / capsule	-
FTN_0910	9H11		sugar:cation symporter family protein	transport - carbohydrates (sugars, polysaccharides)	+
FTN_0927	21B11	cysN	sulfate adenylate transferase, subunit 1	other metabolism - degradation, utilization, assimilation	-
FTN_0931	27C02		conserved protein of unknown function	unknown function - conserved	-
FTN_0994	10A05		hypothetical membrane protein	hypothetical - novel	-
FTN_1006	8G06		hypothetical membrane protein	hypothetical - novel	+
FTN_1057	10 E02	clpP	ATP-dependent Clp protease subunit P	post translational modification, protein turnover, chaperones - protein degradation	-
FTN_1067	14A09		apolipoprotein N-acyltransferase	cell wall / LPS / capsule	-
FTN_1067	23F12		apolipoprotein N-acyltransferase	cell wall / LPS / capsule	-
FTN_1071	26B08		protein of unknown function	unknown function - novel	-
FTN_1093	18A05		protein of unknown function	unknown function - novel	-
FTN_1164	2G08	smpB	SsrA (tmRNA)-binding protein	translation, ribosomal structure and biogenesis	-
FTN_1208	30D03	asn	asparaginase	amino acid metabolism - degradation,	+

				utilization, assimilation	
FTN_1231	16G09	gloA	lactoylglutathione lyase	other metabolism - degradation, utilization, assimilation	+
FTN_1290	24 E04	mglA	macrophage growth locus, protein A	signal transduction and regulation	-
FTN_1309	5F04	pdpA	protein of unknown function	unknown function - novel	-
FTN_1330	20F06	pyk	pyruvate kinase; carbohydrate	metabolism - degradation, utilization, assimilation	-
FTN_1333	11 E01	tktA	transketolase Icarbohydrate	metabolism - degradation, utilization, assimilation	-
FTN_1346	18D09		inositol monophosphatase family protein	putative enzymes	+
FTN_1384	11 E06	nusB	transcription termination factor	transcription	+
FTN_1387	21 E11		conserved protein of unknown function	unknown function - conserved	-
FTN_1387	21D11		conserved protein of unknown function	unknown function - conserved	-
FTN_1419	12H05		pseudogene: dTDP-D-glucose 4,6-dehydratase	pseudogene	-
FTN_1476	26A03		protein of unknown function	unknown function - novel	-
FTN_1501	23H12		monovalent cation:proton antiporter-1	transport	+
FTN_1503	26A08		protein of unknown function	unknown function - novel	-
FTN_1510	1 E01	secB2	preprotein translocase, subunit B	motility, attachment and secretion structure	-
FTN_1512	10C03		hydroxy/aromatic amino acid permease (HAAAP) family protein	transport - amino-acid	-
FTN_1519	22 E03		protein of unknown function	unknown function - novel	+
FTN_1535	4F02		short chain dehydrogena	seputative enzymes	-
FTN_1549	14C03		drug:H+ antiporter-1 (DHA1) family protein	transport - drugs / antibacterial compounds	-
FTN_1609	23C01		membrane fusion protein	transport	-
FTN_1610	20B03		RND efflux transporter,	transport	+

			AcrB/AcrD/AcrF family		
FTN_1630	13C11	secG	preprotein translocase, subunit G, membrane protein	motility, attachment and secretion structure	-
FTN_1688	1A01		protein of unknown function	unknown function - novel	+
FTN_1704	20B04	pcm	protein-L-isoaspartate O-methyltransferase	post-translational modification, protein turnover, chaperones - protein modification	-
FTN_1727	10D02	dapD	tetrahydrodipicolinate succinylase subunit	amino acid metabolism - biosynthesis	+
FTN_1738	11D09		metallocarboxypeptidase	post-translational modification, protein turnover, chaperones - protein degradation	+
FTN_1750	19H02		acyltransferase	fatty acids and lipids metabolism	-
FTN_1750	23D04		acyltransferase	fatty acids and lipids metabolism	-
FTN_1754	7A05		cytochrome b561 family protein	cofactors, prosthetic groups, electron carriers metabolism	+
FTN_1776	9A03		anthranilate phosphoribosyltransferase	amino acid metabolism - biosynthesis	+
FTN_1782	6B11	rng	ribonuclease G translation	ribosomal structure and biogenesis	+
isftu2	12 E02	isftu2	isftu2 IS element		-
intergenic	25H12		INTERGENIC		-
intergenic	32H01		INTERGENIC		-
intergenic	4D04		INTERGENIC		-

[a] Well ID annotation from BEI Resources *F. novicida* Two-Allele Transposon Library

[b] Results of secondary attachment screen. (+) indicates ability and (–) indicates inability of biofilm-mutant to adhere to polystyrene based on 1h attachment assay.

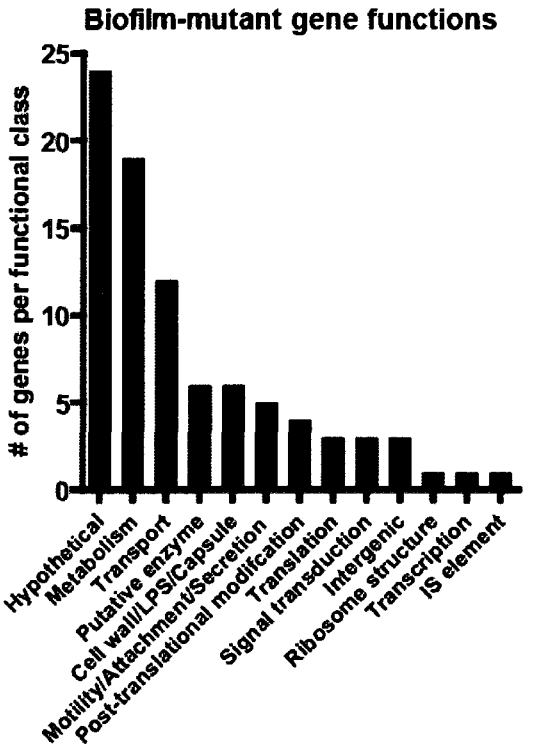

Figure 10 - Biological processes of biofilm-deficient transposon mutants.
F. novicida biofilm mutants were determined by absence of crystal violet staining. The BEI Resources two-allele *F. novicida* transposon mutant library was tested by microtiter assay after 8h of static growth at 37°C. Mutants in crystal violet uptake were identified by wells exhibiting staining two standard deviations below the plate mean. Mutant functional classes are displayed along with the number of genes identified in each category.

Although the majority of genes identified in this screen were either annotated as encoding hypothetical proteins or not previously associated with biofilm formation in other Gram-negative bacteria, a few genes have been previously described in the literature (16, 148). This includes *clpP*, a protease, that was first identified in a screen for biofilm-deficient mutants of *Pseudomonas fluorescens* (148), and a GGDEF and EAL domain gene

involved in the production of the known biofilm modulator 3',5'-cyclic diguanylic acid (c-di-GMP) (84, 215). Surprisingly, Type-II secretion and Type-IV pili, which are known to contribute to biofilm formation by other Gram negative organisms (101, 147, 206), were not identified in our biofilm screen. To confirm this result, all library transposon mutants in these two related systems were tested in the microtiter plate assay. We confirmed that these mutants were not attenuated for biofilm formation (Figure 11). Based on the results of our screen for *F. novicida* biofilm mutants, we concluded that this bacterium forms biofilms by novel means. Future study of other non-motile bacteria will discern whether the biofilm mechanisms of *F. novicida* are conserved.

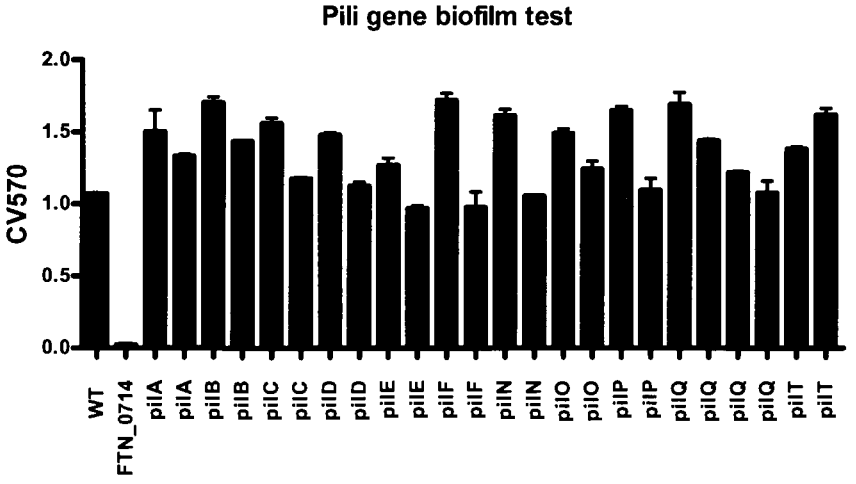

Figure 11 – Pili genes do not contribute to *F. novicida* biofilm formation.
All transposon-insertions in pili genes from the Two Allele library were tested for 8 h biofilm formation. None of the *pil* genes demonstrated statistically lower crystal violet staining than wild-type *F. novicida*. A deletion mutant in FTN_0714 was included as a positive control for biofilm attenuation.

F. tularensis species genomes contain an annotated chitin-binding protein, *cbpA*, that was not identified by our biofilm screen. This gene product may specifically mediate association with chitin. Additionally, we did not identify *chiA* and *chiB* in our screen, which is consistent with our results indicating that these chitinases do not mediate biofilm formation on polystyrene. This result was confirmed using clean deletion mutant stains (Figure 12).

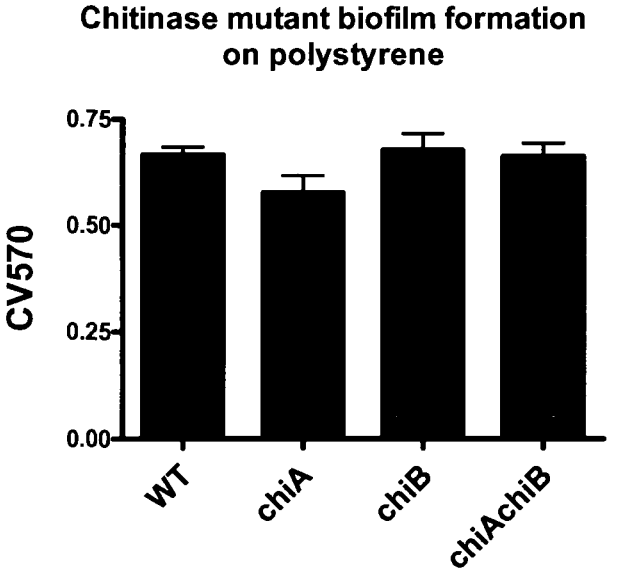

Figure 12 – *F. novicida* chitinase mutants form wild-type level biofilms on polystyrene. Crystal violet staining of microtiter well-grown *F. novicida* strains was utilized to test chitinase mutant biofilm formation on an abiotic surface. No significant differences were observed between the Δ*chiA*, Δ*chiB*,or Δ*chiA*Δ*chiB* strains and wild-type *F. novicida* in this assay. Graph displays the average of four independent samples.

3.3.4 Sec-dependent secretion functions in initial attachment during *F. novicida* biofilm formation on abiotic and biotic surfaces.

We were particularly interested in the four transposon-insertion mutants we identified in the Sec translocon complex involved in protein export from the cytoplasm (72). The core components of the Sec translocon in *Escherichia coli* are the SecYEG protein channel and the SecA ATPase motor protein (22). Due to the pleiotropic roles of general protein secretion in bacteria, components in this apparatus are considered essential in other Gram-negative organisms (72, 118). The Sec translocon in *F. novicida* is comprised of 13 proteins. Our screen identified the only four genes in this complex that were represented in the two-allele library: the *secA* motor ATPase and *secG* pore genes, as well as the *secB1* and *secB2* genes that encode for chaperones that specifically target pre-proteins to SecA (198). Additionally, we identified 18 transposon biofilm mutant clones, representing 14 genes that are predicted to encode for proteins with secretion signals based on the signal sequence detection algorithm, SignalP (15), (Table 3).

We hypothesized from the results of our genetic biofilm screen and a secondary attachment assay that proteins secreted by the Sec translocon may represent novel mediators of *F. novicida* adhesion, a process that has not been characterized. We confirmed that transposon mutants in the secretion apparatus were deficient for biofilm formation (Figure 13A) and attachment (Figure 13B). Deletion mutants in *secB1* and *secB2* were constructed while deletions in *secA* and *secG* could not be generated; suggesting that these

genes are essential and the transposon-insertion mutations present in the library represent an incomplete loss of gene function. Further analysis of the insertion sites for the transposon mutants identified in the screen found that in both cases only the very C-terminus of the *secA* and *secG* genes was disrupted suggesting an incomplete loss of function. Attempts to construct a double deletion of *secB1* and *secB2* did not yield viable colonies, inferring a redundant function for these genes as well. Both the *ΔsecB1* and *ΔsecB2* mutants were deficient in biofilm formation (Fig 13C) and attachment (Fig 13D) when grown in MMH. The *ΔsecB1* and *ΔsecB2* mutant phenotypes were restored to wild-type attachment and biofilm formation levels when wild-type copies of *secB1* and *secB2* were added back to the deletion mutants (Figure 13C,D). These experiments were also performed in CDM to confirm that the role of Sec-dependent secreted factors in biofilm formation was not limited to growth in a nutrient-rich environment (Figure 13E,F). Our data indicate that Sec-dependent secretion is important for *F. novicida* attachment to abiotic surfaces and biofilm formation. We, therefore, postulated that Sec-secreted proteins represent novel mediators of *F. novicida* adherence.

The 18 Sec-dependent transposon-insertion mutants (Table 3) were all defective for biofilm formation (Figure 13A) and initial attachment (Figure 13B) based on crystal violet staining, confirming our screen results. We focused on four of the secreted factors with homologs in all *F. tularensis* subspecies and were highly attenuated for biofilm formation when deleted; FTN_0308, FTN_0713, FTN_0714 and FTN_1750. FTN_0713 (*ostA2*), FTN_0714 and

FTN_1750 were all identified at least twice in the biofilm screen. We selected FTN_0308 due to the strong biofilm phenotype of the one transposon-insertion mutant that was identified in the genetic screen (Figure 13A,B).

FTN_0308 and FTN_0714 encode for hypothetical proteins that may function as *F. novicida* adhesins (66). Homologs of *ostA2* modify lipopolysaccharide in the bacterial periplasm (8) and FTN_1750 is a putative acyltransferase (66). We constructed deletion mutants in each of these genes and tested for attachment and biofilm formation. All four mutants were defective in initial attachment and biofilm formation in both rich and defined media (Figure 13C-F). The Δ*ostA2*, Δ*FTN_1750* and Δ*FTN*_0308 mutants were complemented for attachment and biofilm attenuation by re-introduction of the deleted genes in *cis* into the chromosome or in *trans* by expressing the gene in pFNLTP6 using the constitutive *gro* promoter. The Δ*FTN_0714* mutant could not be complemented for technical reasons, likely due to the length of the complementation PCR product (~8kb). Taken together, our data indicate that initial attachment during *Francisella* biofilm formation is facilitated by proteins secreted by the Sec-dependent secretion system.

Table 3- Sec translocon and Sec-dependent secreted proteins involved in biofilm formation

FTN	Well ID	Gene	Gene Product	Biological Process	Secretion
FTN_0090	4F07	acpA	acid phosphatase	fatty acids and lipids metabolism	Secreted
FTN_0100	20C12		hypothetical membrane protein	hypothetical - novel	Secreted
FTN_0109	14G06		protein of unknown function	unknown function - novel	Secreted
FTN_0121	26G09	secB1	preprotein translocase, subunit B	motility, attachment and secretion structure	Translocon
FTN_0121	4F06	secB1	preprotein translocase, subunit B	motility, attachment and secretion structure	Translocon
FTN_0191	19E06		polar amino acid uptake transporter	transport - amino-acid	Secreted
FTN_0304	20C11		pilus assembly protein	motility, attachment and secretion structure	Secreted
FTN_0308	19H06		membrane protein of unknown function	unknown function - novel	Secreted
FTN_0357	21B08	pal	peptidoglycan-associated lipoprotein, OmpA family	transport - drugs / antibacterial compounds	Secreted
FTN_0429	14G12		conserved protein of unknown function	unknown function - conserved	Secreted
FTN_0635	25C04		serine-type D-Ala-D-Ala carboxypeptidase	cell wall / LPS / capsule	Secreted
FTN_0672	12G03	secA	preprotein translocase, subunit A (ATPase, RNA helicase)	motility, attachment and secretion structure	Translocon
FTN_0713	14C04	ostA2	organic solvent tolerance protein OstA	cell wall / LPS / capsule	Secreted
FTN_0713	21H10	ostA2	organic solvent tolerance protein OstA	cell wall / LPS / capsule	Secreted
FTN_0713	26E07	ostA2	organic solvent tolerance protein	cell wall / LPS /	Secreted

			OstA	capsule	
FTN_0714	12G01		protein of unknown function	unknown function - novel	Secreted
FTN_0714	27C09		protein of unknown function	unknown function - novel	Secreted
FTN_1093	18A05		protein of unknown function	unknown function - novel	Secreted
FTN_1476	26A03		protein of unknown function	unknown function - novel	Secreted
FTN_1503	26A08		protein of unknown function	unknown function - novel	Secreted
FTN_1510	1E01	secB2	preprotein translocase, subunit B	motility, attachment and secretion structure	Translocon
FTN_1630	13C11	secG	preprotein translocase, subunit G, membrane protein	motility, attachment and secretion structure	Translocon
FTN_1750	19H02		acyltransferase	fatty acids and lipids metabolism	Secreted
FTN_1750	23D04		acyltransferase	fatty acids and lipids metabolism	Secreted

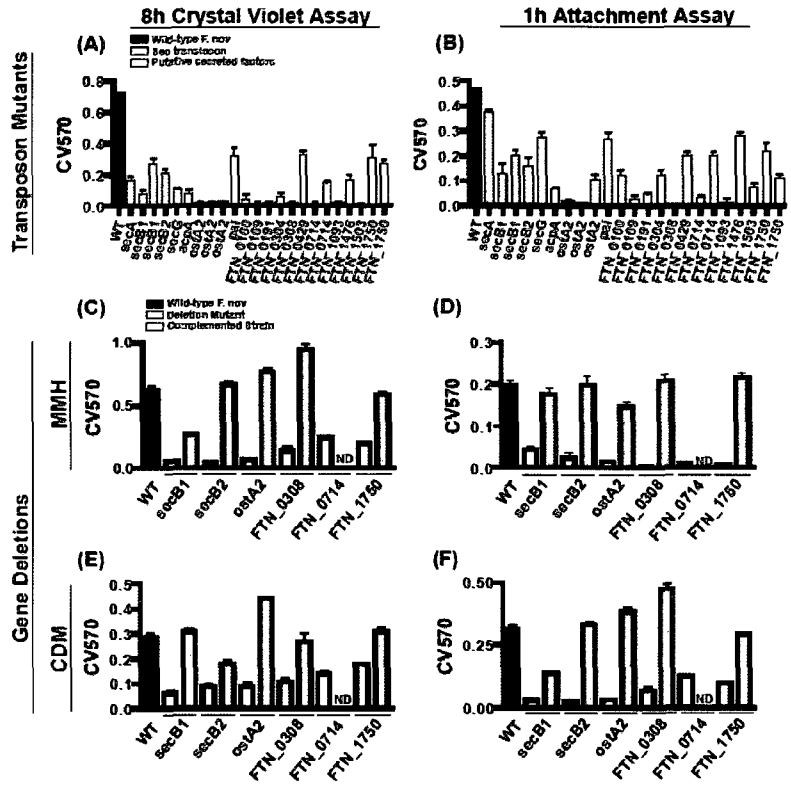

Figure 13 - Sec-secreted factors mediate initial attachment during biofilm formation. Five transposon-insertions representing mutants in 4 genes in the Sec translocon (grey) and 18 transposon-insertions representing mutants in 14 genes in putative secreted factors (white) identified in the forward genetic screen were tested in triplicate compared to wild-type *F. novicida* (black) for 8h biomass accumulation (A) and 1 h initial attachment (B). Multiple transposon-mutants were tested for genes identified more than once in the screen. Adherence of biomass at 8h was used as a measurement for biofilm formation. Attachment was assessed by crystal violet stain 1 h post-inoculation of stationary phase cultures. Targeted mutants in selected representative genes (white) showed similar defects in biofilm formation (C, E) and attachment (D, F) compared to wild-type *F. novicida* (black) when grown in MMH and CDM, respectively, based on crystal violet staining. Complementation of deleted genes (grey) restored mutants to wild-type levels in all cases. Bars represent the mean and the lines indicate standard deviation calculated from triplicate samples of a representative experiment. Each experiment was repeated in triplicate. No data (ND) was obtained for FTN_0714 complementation due to technical difficulties.

3.3.5 Sec secretion mutants are not attenuated in murine models of infection.

Functional overlap often exists for attachment mechanisms to environmental surfaces and mammalian cells (157, 169, 175). To test the potential role of the attachment factors identified in our biofilm screen in mammalian virulence, we compared each of the deletion mutants to wild-type bacteria in in vitro and in vivo infection models. *F. tularensis* species are primarily found within macrophages in a mammalian host (75). Therefore, RAW264.7 macrophage-like cells were infected at a multiplicity of infection of 20:1 with wild-type *F. novicida* or the Sec-dependent secretion mutants. At 0.5 h post-infection, non-cell associated *F. novicida* were washed away and the remaining bacteria were recovered and enumerated. No statistical differences in CFU counts were observed (Figure 14A), suggesting that the mutants that are defective for attachment to polystyrene and chitin were still able to efficiently associate with eukaryotic cells. Intracellular replication was monitored in the presence of extracellular gentamicin for 8- and 24h (Figure 14B). Wild-type *F. novicida* and all mutants showed approximately 100–fold replication at 24h compared to the initial 0.5 h counts. Thus, the mutants successfully entered and replicated within macrophages, demonstrating that the Sec secretion biofilm mutants that we characterized are not deficient for attachment to, or replication within macrophages.

To test the potential role of *secB1, secB2, ostA2, FTN_0308, FTN_0714* and *FTN_1750* during local or systemic mouse infections, we

infected C57BL/6J mice with a 1:1 mixture of $5x10^3$ colony forming units of wild-type and deletion mutant bacteria. Competitive indices (CIs) for each wild-type/mutant combination were obtained for both intradermal (ID) and intraperitoneal (IP) routes of infection. Mutants that are not attenuated in mice should have a CI of one, *i.e.,* equal numbers of wild-type and mutant bacteria are recovered in the tissue at the time of harvest, as is observed for the previously described Δ*hspX* strain (208). As a positive control, we included a *F. novicida* FPI mutant that lacks the entire *Francisella* pathogenecity island (208). As expected, this mutant was severely attenuated in mice (Figure 14C,D). However, none of the Sec secretion biofilm mutants demonstrated a CI value statistically different from one via either route of infection (Figure 14C,D). Our data indicate that these genes that are crucial for association to non-mammalian surfaces do not contribute to local or systemic colonization of mammalian hosts.

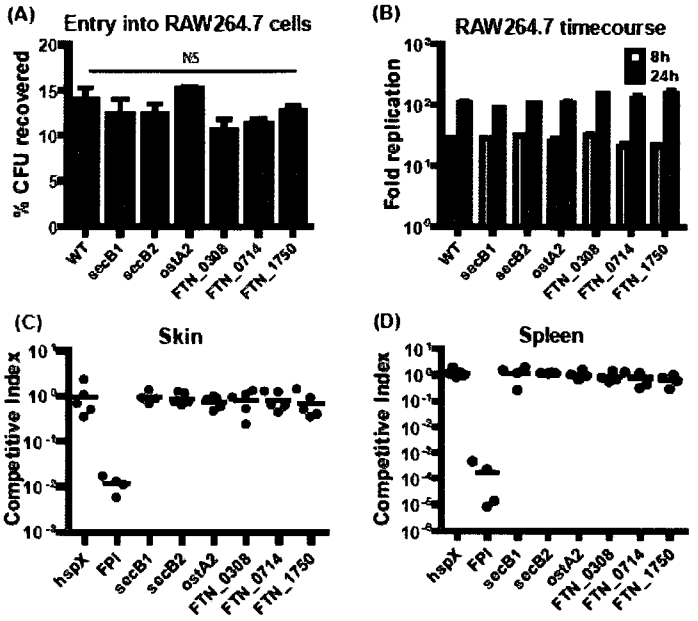

Figure 14 - The Sec translocon and secreted factors do not influence *F. novicida* virulence.

Sec secretion targeted deletion mutants were assessed in *in vitro* and *in vivo* models for *F. tularensis* virulence. Entry efficiency of *F. novicida* strains into RAW264.7 macrophage-like cells was measured as the percent of inocula recovered from inside the cells 30min post-infection (A). Intracellular replication of wild-type and mutant bacteria was assessed as fold-replication compared to 30 min counts at 8 h and 24 h post-infection (B). The ability of mutants to colonize the skin after intradermal (C) and the spleen after intraperitoneal (D) routes of inoculation was determined by competitive indices in C57BL/6J mice 2 d post-infection. For all virulence assays, no difference was observed between the Sec secretion biofilm mutants and wild-type *F. novicida*.

3.3.6 *F. novicida* biofilm determinants also play a role in attachment to chitin-based surfaces.

Given *Francisella* species induce biofilm formation on both abiotic and chitin surfaces, we hypothesized that the attachment determinants we identified for association with polystyrene may also facilitate attachment to chitin. After a 1 h incubation at 30°C, an average of 3.33×10^7 CFU/ml wild-type *F. novicida* were attached to the crab shell pieces (Figure 15). Sec secretion mutants were 5.6- to 16.2-fold attenuated for attachment to this chitin-based surface compared to wild-type bacteria ($P<0.01$), confirming that Sec-secreted proteins contribute to attachment to chitin-based surfaces. The specificity of these adherence factors for non-mammalian surfaces further supports our suggestion that *F. tularensis* biofilm formation in nature has evolved to promote this pathogen's survival outside of a host, potentially by facilitating chitin utilization.

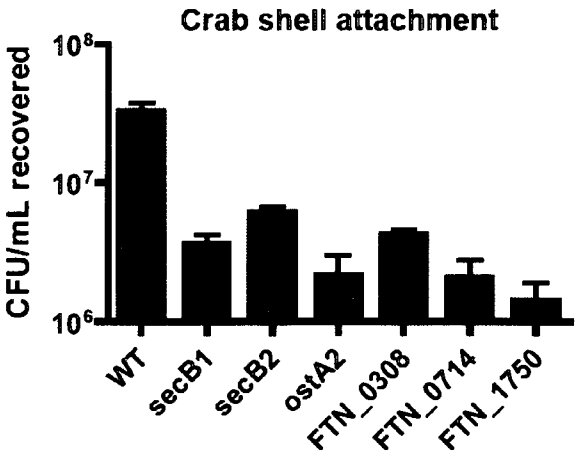

Figure 15 - Biofilm mutants are attenuated for attachment to chitin-based crab shell pieces.

Stationary phase cultures of *secB1, secB2, ostA2,* FTN_0308, FTN_0714, and FTN_1750 deletion mutants were allowed to attach for 1 h to sterile crab shell pieces. Attached bacteria were enumerated for CFU in triplicate samples. Sec secretion biofilm mutants were found to attach statistically lower (P>0.01) than wild-type *F. novicida* by unpaired *t*-test.

3.3.7 Sec-secretion biofilm mutants are attenuated for systemic colonization of *Drosophila melanogaster.*

The decreased attachment of the Sec translocon chaperone and Sec-secreted factors mutants to chitin suggested that these proteins may contribute to infection of chitin-exoskeletoned arthropod vectors. Only a systemic model of vector infection has been characterized. Vonkavaara *et al.* published that *Drosophila melanogaster* develop a systemic infection after injection of *F. tularensis* into the abdomen of the fly (201). With the assistance of Madeleine Moule from David Schneider's lab, we performed a competitive index experiment by injecting $5x10^3$ CFU each of wild-type *F. novicida* and Sec

secretion biofilm mutant per fly. As in the mouse CI experiment described above, defective mutants are defined by a CI value less than one. All mutants tested had a CI value statistically less than the *hspX* negative control ($P<0.0001$) (Figure 16). All biofilm mutants tested were approximately 10-fold attenuated for systemic colonization of *D. melanogaster*, while the complete FPI deletion strain was over 1,000-fold attenuated consistent with the published literature (201). The decreased fitness for Sec secretion biofilm mutants suggests that these attachment factors may be required for association with some site within the fly.

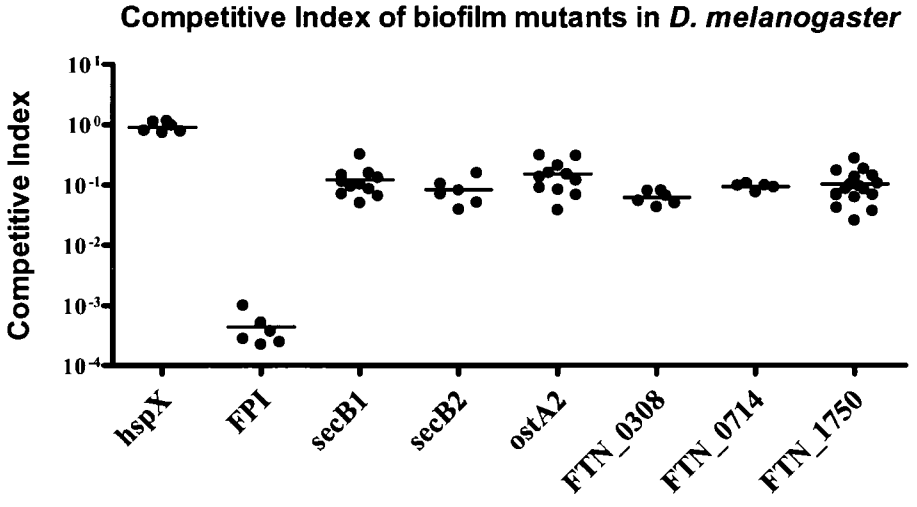

Figure 16 – Sec secretion biofilm mutants have a competitive index defect during systemic *D. melanogaster* infection.

The biofilm mutant strains characterized for association to abiotic and biotic surfaces were tested for their ability to colonize *D. melanogaster*. Each data point represents the CI value of a single fly. The Δ*hspX* and Δ*FPI* strains were included as negative and positive controls, respectively. All biofilm mutant strains tested were significantly attenuated for systemic colonization ($P<0.0001$).

3.4 DISCUSSION

One of the greatest dogmas in the biofilm field is that one biofilm is equivalent to another. Examining the literature on mechanisms of biofilm formation, however, we find that there are many genetic and molecular paths to reach the same result. Although many Gram-negative and Gram-positive bacteria can form biofilms, the bacterial mechanisms utilized to facilitate these communities are decidedly varied (10, 122, 140, 148, 199). For example, the role of Type-IV pili and flagella in surface attachment and microcolony formation is well documented (147, 157). However, little is known about attachment and surface growth during biofilm maturation of non-motile bacteria such as *F. tularensis*. By characterizing the roles of the genes we identified in this study, including the approximately 25% with no annotated function, we aimed to elucidate alternate methods of environmental persistence by non-motile bacteria.

Comparing biofilm mutant screens we found little overlap with the biofilm determinants of non-motile *S. aureus.* Only two genes FTN_0456 (EAL and GGDEF domain gene) and FTN_1093 (annotated as hypothetical for *F. novicida* but transcription-repair coupling factor in *S. aureus*) overlapped between the two non-motile bacteria (196). *S. aureus* predominantly forms biofilms on host tissues and indwelling hospital devices (151), while we found that *Francisella* species form strong biofilms on chitin (Figures 1-2), but have a slow biofilm kinetic on an abiotic surface, such as glass (Figure 7). This

difference in substrate preference may explain the lack of conserved colonization genes.

Identification of all Sec translocon genes present in the Two Allele library (Table 2) pointed us to look at Sec-secreted factors as novel mediators of surface adhesion. The presence of these transposon-insertion mutants in the library was serendipitous given the many roles that Sec-dependent secretion plays in bacteria. Sec-secreted factors involved in *F. novicida* biofilm formation serve a variety of putative functions, including the four adherence factors we further characterize. The protein encoded by FTN_0713 (*ostA2*) has significant homology to organic solvent tolerance proteins involved in lipopolysaccharide (LPS) modification (18). Although *ostA2* homologs have not been implicated in biofilm formation, LPS chemistry has been shown to influence attachment during biofilm formation in other bacteria (10, 42, 63). The unique structure of *Francisella* species LPS (81) could contribute to adhesion of *F. tularensis* to non-mammalian surfaces.

FTN_1750 is a putative acyltransferase with strong homology (E-value $4e^{-27}$) to acylhomoserine-lactone biosynthesis enzyme, HdtS, suggesting that this protein may function in quorum sensing, a cell-cell communications process that regulates biofilm formation under certain conditions (100). Our biofilm screen also identified the GGDEF and EAL domain-containing gene, FTN_0456 (Table 2), suggesting c-di-GMP as an additional regulator of *F. novicida* biofilm formation as is observed for other biofilm-forming bacteria (189, 215, 216). Quorum sensing has not been experimentally demonstrated

for *Francisella* species, although homologs to quorum sensing genes *qseC* and an annotated homolog to *hdtS* are found in these genomes. These processes of bacterial communication have been shown under certain environmental conditions to regulate biofilm formation genes (158).

While *F. novicida* biofilm genes were identified by screening for mutants defective for adherence and biofilm formation on polystyrene, we identified two novel putative chitin-binding proteins, FTN_0308 and FTN_0714. The protein encoded by FTN_0714 is annotated as a hypothetical lipoprotein (www.biohealthbase.org). The SMART domain prediction algorithm (114, 173) indicates that FTN_0714 contains repeating polycystic kidney disease-family domains conserved from archae through mammals that facilitate adhesion (96). This domain-family plays a role in the binding and hydrolysis of chitin by the *chiA* chitinase of aquatic bacterial strain *Alteromonas 0-7* (150). FTN_0308 is annotated to encode for a hypothetical protein with unknown function (www.biohealthbase.org). However, the Phyre protein-folding prediction algorithm (98) indicates a structural homology to the *Streptomyces* chitinase C chitin-binding domain and the C-terminus contains homology to F17c-family bacterial adhesins. We are currently determining the specific roles that these two gene products may have in attachment to both abiotic and chitin surfaces.

As discussed above, factors required for attachment during biofilm formation also facilitate association with host tissues. We conclude from our data that *F. novicida* biofilm genes do not function in mammalian infection.

Only four genes (*mglA, pdpA, ostA2* and *sdaC1*) were identified by others in screens for *F. tularensis* virulence factors (182, 208). MglA and PdpA are known virulence factors of *F. tularensis* (21), while SdaC1 annotates as a serine transport protein (66). FTN_0713 (*ostA2*), the putative LPS-modification gene, was identified by Kraemer *et al.* in a negative selection screen for *F. novicida* mutants attenuated for infection via intranasal inoculation of mice, indicating that this mutant may be more sensitive to the innate immune response in the lung, (e.g., antimicrobial peptides) due to an altered LPS (102, 208).

None of the genes we characterize in this chapter have an apparent role in virulence in our hands (Figure 14). Transposon-mutants for *secA* and *secE* were identified by Su *et al.* to be involved in lung colonization, but not *secB1* or *secB2* (182). These attenuated phenotypes for the non-redundant Sec translocon genes imply that Sec secreted proteins other than those characterized here do influence host colonization. The lack of attenuation for the deletion mutants in *secB1* and *secB2* in the virulence assays tested here supports the idea that these two genes encode for redundant function.

While Sec-secreted attachment factors do not impact *F. novicida* virulence, we identify a role for these gene products in adherence to crab shell pieces (Figure 15). This finding suggests that *F. tularensis* species have maintained separate genetic programs for colonizing mammalian and environmental surfaces. Because such division of function is uncommon amongst biofilm forming bacteria, it is feasible that *F. tularensis* originally

evolved to colonize environmental surfaces and later obtained a specific set of genes to successfully infect mammalian hosts. To further dissect the molecular mechanisms of *F. tularensis* chitin colonization, domains within the biofilm attachment genes could be mutated to find key determinants of surface association. Such analysis on putative chitin-binding proteins encoded by FTN_0308 and FTN_0714 may prove particularly fruitful. While our biofilm screen did not identify the annotated chitin-binding protein, *cbpA*, elucidating the role of this gene in chitin colonization may also be informative.

To further tie the Sec-secreted attachment mediators to colonization of non-mammalian environments and disease transmission, we asked if deletion mutants in these genes conferred attenuation in *D. melanogaster,* an established model for mosquito and tick infection (201). All deletion mutants demonstrated an approximate 10-fold reduction in systemic colonization compared to wild-type *F. novicida* (Figure 16). While suggestive that biofilm mediators function in fruit fly colonization, injection is not a natural route of inoculation. *D. melanogaster* are not colonized by *F. novicida* or LVS after oral inoculation (personal communication with Madaleine Moule and (201)). Therefore, an artificial route of inoculation was used to bypass the peritrophic matrix that protects the fly from microbes crossing the gut lining. We, therefore, cannot conclude that *F. novicida* biofilm factors mediate arthropod colonization during a natural infection; however we can suggest that once systemic, this pathogen utilizes Sec-secreted attachment factors to persist and replicate. This assertion is further supported by the large overlap between

genes required for biofilm formation and *D. melanogaster* infection. Madeleine Moule performed a negative selection screen to find *F. novicida* genes that contribute to fruit fly colonization. Twenty-eight of the 89 fly-specific genes identified by this screen were also required for *F. novicida* biofilm formation (unpublished data from Madeleine Moule). The list of overlapping genes included FTN_0308 and FTN_1750 which we test for fitness in fruit flies above. While *ostA2* and FTN_0714 were not attenuated in Madeleine Moule's screen, we show here a competitive index defect for these deletion mutants. Additionally, we plan to follow up on the fact that both chitinases genes described in Chapter 2 were attenuated in the negative selection screen. Therefore, *F. novicida* biofilm genes may play a greater role in *D. melanogaster* colonization than is evident by comparing screen results. To date, the localization of *F. tularensis* strains during transmission by arthropod vectors remains unknown. *F. tularensis* biofilm formation may support persistence both on the external chitin exoskeleton and the chitinous matrix that lines the digestive tract.

While the chitin colonization work was performed with the *F. novicida* strain of *F. tularensis,* we do establish that multiple subspecies can form biofilms in vitro (Figures 8 and 9). In particular, we demonstrate that two Type A strains form biofilms to statistically higher level than the attenuated Type B strain, LVS (Figure 9). This result was not intuitive given the environments where Type A and Type B strains reside. While Type A strains are more associated with arid climates (103), Type B strains have become endemic in

Europe (185) and outbreaks of tularemia on this continent are correlated with the times of heavy rain (156). Testing wild-type Type B strains along with a larger sample of Type A strains would provide additional insight into the relative biofilm capabilities of different *F. tularensis* isolates. By better understanding where biofilm formation may occur, one can target efforts against these populations to the appropriate geographic areas.

From our collective data we propose a model in which the early determinants of biofilm formation identified in this chapter allow for association with chitin surfaces in nature. These surfaces may include fresh water arthropods where this pathogen can persist in a nutrient-poor aquatic environment and arthropod vectors where biofilm formation may facilitate transmission to mammalian hosts. Through the interaction with chitin, *F. tularensis* chitinases have access to this substrate and provide bacteria with GlcNAc, which is utilized for growth in nutrient-limiting environments. Biofilm maturation on chitin would then create a local microenvironment enriched for this carbon source, providing a non-host niche for this zoonotic pathogen.

Chapter 4: Static and nutrient limited growth enhance *Francisella tularensis* subspecies *novicida* biofilm formation.

Jeffrey J. Margolis and Denise M. Monack

4.1 CHAPTER 4 SUMMARY

In Chapter 1, we found carbon limitation promoted increased biofilm formation on chitin surfaces. Various environmental factors are known to regulate the regulatory switch between planktonic and biofilm growth. Results of the forward genetic screen for altered biofilm formation indicated that oligotrophy triggers *F. novicida* biofilm formation. We identified MglA, a known *F. tularensis* virulence factor and stress response regulator, as a potential modulator of *F. novicida* biofilm formation. We demonstrate a role for the known MglA signaling pathway components in biofilm formation, suggesting that this regulatory pathway may function in more than intracellular infection. Additionally, we observed 117 transposon-insertion mutants in our forward genetic screen, representing 105 genes, with a hyper-biofilm phenotype. Amino acid and nucleotide biosynthesis genes as well as metabolite transport genes facilitated this increased biofilm response, implicating starvation as a key signal.

Given the genetic data connecting environmental stress and biofilm formation, we tested the effect of nutrient limitation and static growth on the early stages of *F. novicida* biofilm formation. While growth in minimal medium alone did not effect early biofilm kinetics, static growth which subjects the bacteria to both local nutrient and oxygen deprivation resulted in 5- to 10-fold increase in crystal violet staining up to two hours post-inoculation. Treatment with bacteriostatic antibiotics ablated the static growth effect in rich MH broth, but not in minimal CDM. We hypothesized that key biofilm determinants are

expressed before attachment in the CDM static growth condition. Indeed, microarray analysis revealed a cluster of gene highly expressed during stationary phase of the CDM ST samples. Three genes overlapped with the results of the current biofilm mutant screen. We also identify 26 highly expressed nutrient transporters that may promote growth in oligotrophic conditions during *F. tularensis* biofilm formation. By synergizing our expression and genetic biofilm work we can further understand the regulation and mechanisms of *Francisella* species biofilm formation.

4.2 INTRODUCTION

In Chapter 2 we found that a lack for available carbon promoted biofilm formation on chitin surfaces. Absence of exogenous GlcNAc increased surface colonization by more than 10-fold at 2 d (Figure 5). This result indicated that different environmental stress may promote a switch from planktonic growth to surface association and biofilm formation. Nutrient limitation is one known trigger for biofilm formation in other bacteria (17, 70, 205). Environmental stresses are sensed in a number of ways by bacteria, including nutrient sensing and intercellular communication (64, 111, 112, 128, 158, 168, 213).

The study of stress responses in *F. tularensis* has been limited and focused on the regulation of virulence factors. The MglA signaling pathway is one of the few characterized regulators of *F. tularensis* virulence. MglA, FevR

and SspA are required for expression of the *Francisella* pathogenecity island (FPI), 17 genes that may form a Type-VI secretion system and are essential for intracellular replication (12, 19-21, 27). Brotcke *et al.* demonstrated the MglA signaling pathway regulates 102 genes at the transcriptional level (20, 21). At least the MglA-regulated *ospD3* homolog does not function in mammalian infection (21). We identified mutants in *mglA, ospD3,* and five additional MglA-regulated genes in the biofilm mutant screen, suggesting that this signaling pathway influences more than virulence regulation. In a study of the post-transcriptional effects of MglA, a role in general stress response was further described (79). Deletion of MglA regulated genes attenuated *F. novicida* survival in stationary phase and resistance to reactive oxygen species. Additionally, Guina *et al.* found MglA to post-transcriptional regulate several general response genes including chaperones and general response regulators (79). Both MglA and SspA are homologous to stringent starvation protein A (SspA) from *E. coli* that functions as a general stress response regulator (12, 27).

The orphan response regulators, *pmrA*, was also described to mediate virulence determinant expression in *F. tularensis* (137). A recent publication identified a *qseB/pmrA* homolog as another determinant of *F. novicida* biofilm formation (48). Quorum sensing molecule, autoinducer 2, triggers *E. coli* biofilm via *qseB/pmrA* response regulator homologs (77). PmrA positively regulates 52 genes including *fevR* and the FPI (136).

The stringent response, another bacterial stress response, was recently connected with *F. tularensis* virulence regulation as well (43). Accumulation of the guanosine tetraphosphate (ppGpp) alarmone influences a variety of stress responses. Alarmone synthases, *relA* and *spoT*, are triggered by uncharged t-RNAs which occur during amino acid starvation (209). Other triggers for this response include iron limitation (133) and antibiotic treatment (67). Stringent response induction leads to expression of stress response genes that promote survival during slow growth (67). Pathogens, like *Legionella pneumophila* (171) and *Campylobacter jejuni* (67), require stringent response activation for expression of essential virulence factors. Dean *et al.* recently connected the stringent response to *F. tularensis* biofilms (43). This manuscript reported that a *relA F. novicida* mutant strain formed greater biofilms; potentially due to an inability to successfully enter stationary phase. This result was contradictory to the requirement of the stringent response for biofilm formation reported for other bacteria such as *E. coli* (11), *Myxococcus xanthus* (86), and *Streptococcus mutans* (113).

In this chapter we provide evidence from our biofilm mutant screen that nutrient deprivation and other stress responses regulate *F. novicida* biofilm formation. We show that statically grown *F. novicida* produces biofilms with faster kinetics than aerated cultures. This enhancement was dependent on protein synthesis in rich medium, but not minimal medium. Cell envelope, nutrient transporters, and the FTN_0714 putative adhesin (Chapter 3) are highly expressed in CDM ST conditions providing potential insight into the

mechanisms of *F. novicida* persistence and biofilm formation in nutrient-pour environments.

4.3 RESULTS

4.3.1 The MglA stress response pathway facilitates *F. novicida* biofilm formation

The identification of a biofilm-attenuated *mglA* transposon-insertion mutant (Table 2) was intriguing given the focus on virulence regulation by this protein. This signaling pathway has previously been characterized to regulate virulence factors, including the FPI (21). MglA and RNA polymerase-binding partner, *sspA,* show strong homology to a known general stress response regulator in *E. coli* (21, 27). Identification of *mglA* in our biofilm screen indicated that nutrient and/or environmental stress may trigger the switch from planktonic to biofilm growth in *F. tularensis*.

We postulated MglA may regulate more than virulence factors for *F. tularensis*, as only a subset of MglA-regulated genes have been investigated. Additionally, *pdpA,* a putative effector protein of the FPI (172) was identified by our screen, suggesting the FPI itself may contribute to biofilm formation. To test these possibilities, a well characterized *mglA* point mutant, GB2 (12, 145), and a full deletion of *pdpA* were examined for biofilm formation. While both the *mglA* and *pdpA* transposon-insertion mutants were attenuated in the 8 h crystal violet assay, the GB2 but not the Δ*pdpA* strain exhibited lower crystal violet staining (Figure 17). MglA, therefore, truly does influence *F. novicida* biofilm formation, but in an FPI-independent manner. The attenuation of the

pdpA transposon-insertion mutant may be the result of a secondary mutation in the transposon-insertion mutant strain.

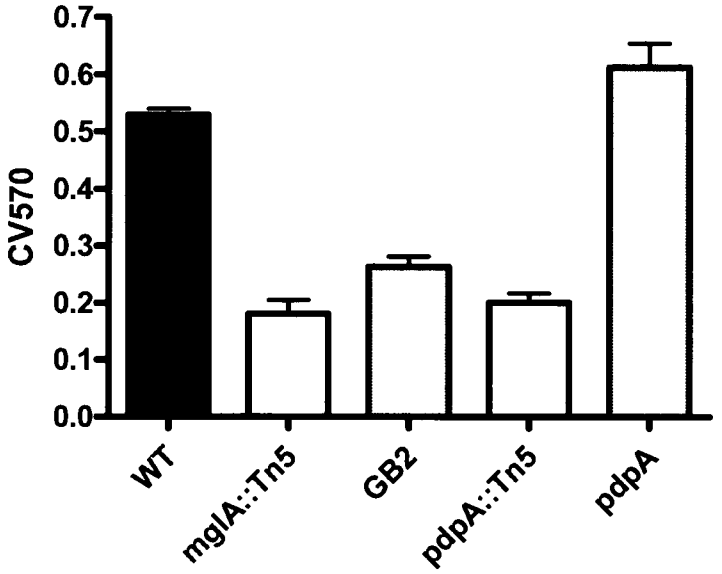

Figure 17– The *mglA* gene product influences *F. novicida* biofilm formation in a FPI-independent manner.

The GB2 *mglA* point mutant and *pdpA* full deletion strains (grey) were tested in comparison to the corresponding transposon-insertion mutant strains (white) for biofilm formation. Both the *mglA* transposon-insertion mutant and characterized point mutant demonstrated statistically lower crystal violet staining than wild-type *F. novicida* (black) at 8 h post-inoculation ($P<0.0001$). While the transposon-insertion mutant identified in the forward genetic screen for *pdpA* was attenuated for 8 h biofilm formation ($P<0.001$), the deletion mutant strain was equivalent to wild-type *F. novicida*.

In addition to the MglA, FevR, SspA complex that binds to RNA polymerase, Brotcke *et al.* identified CphA and CaiC as additional factors in the MglA signaling pathway (20). A transposon-insertion mutant for *sspA* was

not present in the Two Allele library indicating that this gene is essential for *F. novicida* viability. The transposon-insertion mutants for *fevR* were present in the library plate that was unavailable from BEI Resources due to quality control issues. Transposon-insertion mutants were represented, however, for *cphA* and *caiC*. While only *cphA* was biofilm attenuated based on our screen (Table 2), we queried whether additional MglA pathway genes contributed to *F. novicida* biofilm formation. Clean deletions in *fevR, cphA,* and *caiC* along with the GB2 *mglA* point mutant were tested for a biofilm phenotype. After 8 h growth in microtiter wells in MH broth, all MglA pathway mutants demonstrated significantly lower crystal violet staining (Figure 18). Unlike the Sec secreted factors characterized in Chapter 3, mutations in this pathway conferred intermediate biofilm attenuation. Therefore, the MglA signaling pathway aids in, but is not required for, *F. novicida* biofilm gene expression.

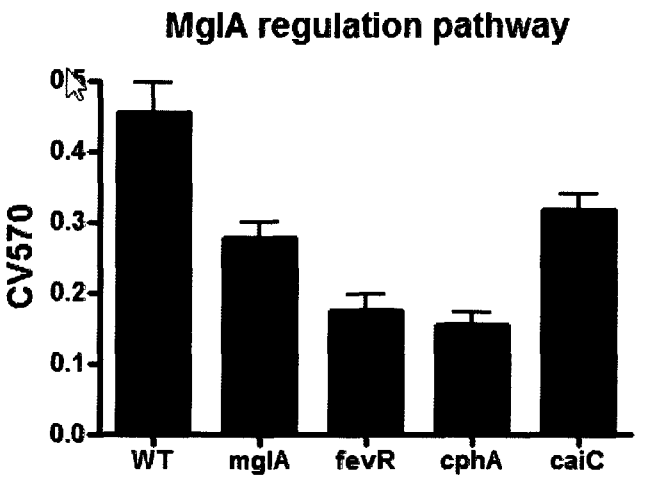

Figure 18 – The MglA signaling pathway contributes to *F. novicida* biofilm formation. The above graph shows the crystal violet staining of a *mglA* point mutant and deletion mutants in other components of the MglA signaling pathway compared to wild-type *F. novicida*. All signaling mutants were found to be statistically defective for static biofilm formation ($P>0.01$).

Of the 102 genes shown to be regulated by the MglA signaling pathway (21), 6 were identified as contributing to biofilm formation (Table 4). While FTN_0431 is annotated as a hypothetical membrane protein, SMART analysis (114, 173) found that this gene product contains a *wzy_C* domain that functions as a glycosylase in other Gram negative bacteria. The FTN_0785 is annotated as an isochorismatase-family hydrolase. The hypothetical gene FTN_1071 contains ankyrin repeat domains that most often bind to eurkaryotic proteins inside of the host cell cytoplasm. A deletion in this gene, a homolog of the *Shigella flexneri ospD3*, was previously shown to have no affect on virulence, however (21). All MglA-regulated transposon-insertion mutants

identified in the screen were confirmed to have a biofilm phenotype upon retesting (Figure 19). Given that the *sspA* homolog in *E. coli* is activated by nutrient and environmental stress and MglA signaling pathway and MglA-regulated genes are attenuated for biofilm formation (Figure 19), we hypothesized that such stresses may trigger *F. novicida* biofilm formation in an MglA-dependent manner.

Table 4 – MglA-regulated biofilm genes

FTN[a]	Well Id[b]	Gene	Gene Product	Biological Process
FTN_0431	26H05		hypothetical membrane protein	hypothetical - novel
FTN_0785	5B06		isochorismitase family protein	putative enzyme
FTN_0910	9H11		sugar:cation symporter family protein	transport - carbohydrates
FTN_1071	26B06		protein of unknown function	unknown - novel
FTN_1112	27B03	cphA	cyanophycin synthetase	metabolism - macromolecule biosynthesis
FTN_1039	5F04	pdpA	protein of unknown function	unknown - novel

(A)

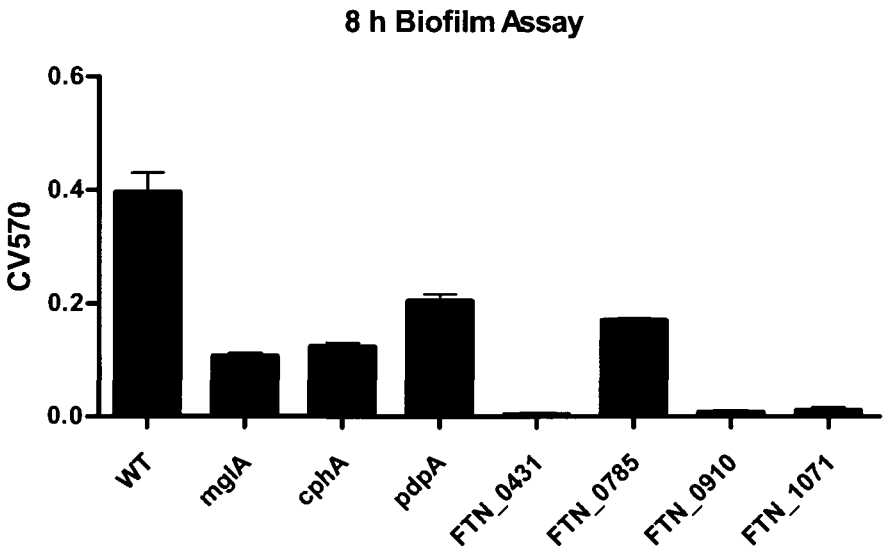

(B)

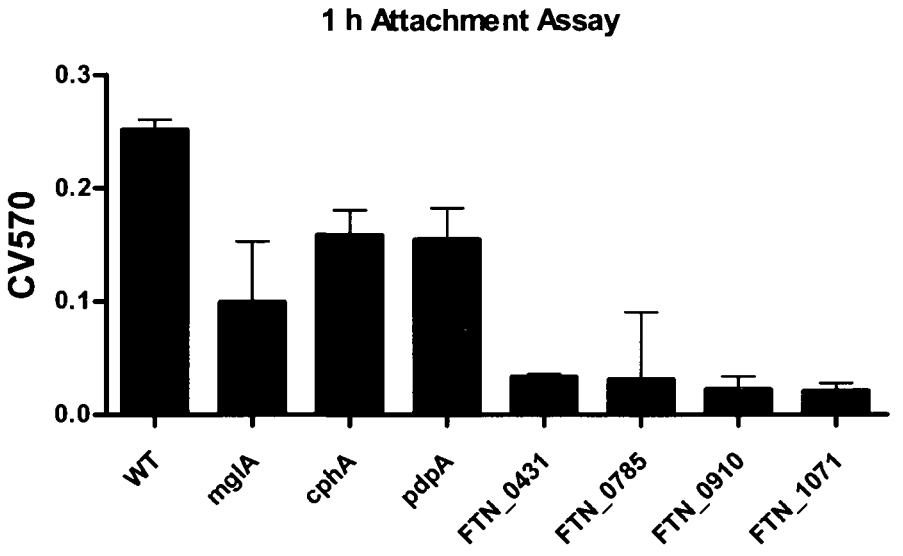

Figure 19 – MglA-regulated genes affect *F. novicida* biofilm formation and attachment to polystyrene.

MglA-regulated transposon-insertion mutant strains identified as biofilm-attenuated were tested for crystal violet staining at 8 h post-inoculation (A) and for 1 h attachment (B). Four replicates were tested per strain.

4.3.2 Metabolism and metabolite transport mutants exhibit a hyper-biofilm phenotype in *F. novicida*.

If nutrient deprivation does trigger *F. novicida* biofilm formation, we hypothesized that mutations in metabolic pathways would increase biofilm formation by effectively starve the bacteria. Indeed, in addition to biofilm-deficient mutants, we also observed transposon-insertion mutants that exhibited a hyper-biofilm phenotype during our screen for *F. novicida* mutants with altered biofilm formation. We identified 117 transposon-insertion mutants, representing 105 genes that demonstrated a hyper-biofilm phenotype (Table 4). As with the biofilm-deficient mutants, a large percentage (19%) was hypothetical or had no known function. Of the annotated biological processes of hyper-biofilm mutants (Figure 20), metabolism, transport, and cell wall/LPS/capsule were represented the most. Being that 31 of 105 genes (30%) function in amino acid or nucleic acid biosynthesis or transport of these molecules into the bacterium, starvation appears to be a key trigger of *F. novicida* biofilm formation. Enhanced biofilm formation was defined as wells with crystal violet staining two standard deviations above the mean of the plate. As before, mutants with significant growth defects were eliminated from further consideration. Hyper-biofilm metabolism mutants were a second indication that nutrient availability may regulate the switch of this bacterium from a planktonic to biofilm phenotype.

Table 5 – Hyper-biofilm transposon-insertion mutants

FTN[a]	Well Id[b]	Gene	Gene Product	Biological Process
FTN_0021	30D08	carA	carbamoyl-phosphate synthase small chain	nucleotides and nucleosides metabolism
FTN_0024	30B09	pyrC	dihydroorotase	nucleotides and nucleosides metabolism
FTN_0036	32G12	pyrD	dihydroorotate oxidase	nucleotides and nucleosides metabolism
FTN_0050	18B08		protein of unknown function	unknown function - novel
FTN_0064	18C08	ppdK	phosphoenolpyruvate synthase/pyruvate phosphate dikinase	energy metabolism
FTN_0080	23D08		SAM-dependent methyltransferase	putative enzymes
FTN_0082	12D08		predicted hydrolase of the HAD superfamily	putative enzymes
FTN_0103	12C08		protein of unknown function	unknown function - novel
FTN_0116	9C06	ipdC	indolepyruvate decarboxylase	amino acid metabolism - degradation, utilization, assimilation
FTN_0123	19C12	recX	inhibitor of RecA	signal transduction and regulation
FTN_0168	9B07	lysU	lysyl-tRNA synthetase	other metabolism - biosynthesis
FTN_0171	6G08	glsA	glutaminase	amino acid metabolism - degradation, utilization, assimilation
FTN_0184	30B10		major facilitator superfamily (MFS) transport	protein transport
FTN_0199	2 E08	cyoE	heme O synthase	cofactors, prosthetic groups, electron carriers metabolism
FTN_0223	23 E05		amino acid-polyamine-organocation (APC) superfamily	protein - amino acid transport

FTN_0271	5G12	ndk	nucleoside diphosphate kinase	nucleotides and nucleosides metabolism
FTN_0271	32F07	ndk	nucleoside diphosphate kinase	nucleotides and nucleosides metabolism
FTN_0298	13D09	gplX	fructose 1,6-bisphosphatase II	energy metabolism
FTN_0317	28F09		amino acid transporter	transport - amino acid
FTN_0368	2 E07		hypothetical protein	hypothetical - novel
FTN_0392	31F05		transcriptional regulator, LysR family	signal transduction and regulation
FTN_0412	32F11	recN	DNA repair protein	DNA replication, recombination, modification and repair - restriction/modification
FTN_0449	11C08		conserved protein of unknown function	unknown function - conserved
FTN_0451	28D09		signal transduction protein with a PAS, a PAC, an EAL and a GGDEF domain	signal transduction and regulation
FTN_0494	29C09		hypothetical membrane protein	hypothetical - novel
FTN_0517	28D06	glgP	glycogen phosphorylasecarbohydrate	metabolism - degradation, utilization, assimilation
FTN_0520	30D09	murE	UDP-N-acetylmuramoylalanyl-D-glutamate--2,6-diaminopimelate ligase	cell wall / LPS / capsule
FTN_0529	29C04	pyrE	orotate phosphoribosyltransferase	nucleotides and nucleosides metabolism
FTN_0530	8C08		UDP-N-acetylmuramate:L-alanyl-gamma-D-glutamyl-meso-diaminopimelate ligase	cell wall / LPS / capsule
FTN_0543	32F09	ftsW	cell division protein FtsW	cell cycle
FTN_0546	16D09		dolichyl-phosphate-mannose-protein mannosyltransferase family protein	cell wall / LPS / capsule

FTN_0558	25C03	ostA1	organic solvent tolerance protein, OstA	cell wall / LPS / capsule
FTN_0569	32F08	recJ	single-stranded-DNA-specific exonuclease	DNA replication, recombination, modification and repair - restriction/modification
FTN_0577	3F03	mutL	DNA mismatch repair enzyme with ATPase activity	DNA replication, recombination, modification and repair - restriction/modification
FTN_0592	9B09		hypothetical membrane protein	hypothetical - novel
FTN_0598	31D09		tRNA-dihydrouridine synthase	translation, ribosomal structure and biogenesis
FTN_0605	7G05	mraW	S-adenosylmethionine-dependent methyltransferase	cell wall / LPS / capsule
FTN_0616	29B12		RNA methyltransferase, trmA family	translation, ribosomal structure and biogenesis
FTN_0636	8B07	glpT	glycerol-3-phosphate transporter	transport
FTN_0687	31F09	galP1	galactose-proton symporter, major facilitator superfamily (MFS) transport protein	transport - carbohydrates (sugars, polysaccharides)
FTN_0688	30C08	galP2	galactose-proton symporter, major facilitator superfamily (MFS) transport protein	transport - carbohydrates (sugars, polysaccharides)
FTN_0692	24H08	nadA	quinolinate sythetase A	cofactors, prosthetic groups, electron carriers metabolism
FTN_0720	20G01	srpS	transcriptional regulator, IclR family	signal transduction and regulation
FTN_0744	21 E05		protein of unknown function	unknown function - novel

FTN_0766	6D06	spoU	rRNA methyltransferase	translation, ribosomal structure and biogenesis
FTN_0768	29D03	tspO	tryptophan-rich sensory protein	signal transduction and regulation
FTN_0772	22C02		conserved protein of unknown function	unknown function - conserved
FTN_0777	24G11		protein of unknown function	unknown function - novel
FTN_0811	28B12		biotin--acetyl-CoA-carboxylase ligase	fatty acids and lipids metabolism
FTN_0814	22F05	bioF	8-amino-7-oxononanoate synthase	cofactors, prosthetic groups, electron carriers metabolism
FTN_0816	26 E06	bioA	adenosylmethionine-8-amino-7-oxononanoate aminotransferase	cofactors, prosthetic groups, electron carriers metabolism
FTN_0818	12C10		lipase/esterase	fatty acids and lipids metabolism
FTN_0875	14C10		metabolite:H+ symporter (MHS) family	transport
FTN_0898	9B05		amino acid permease	transport - amino-acid
FTN_0898	32F10		amino acid permease	transport - amino-acid
FTN_0901	10C08		isomerase	putative enzymes
FTN_0923	28B09		protein of unknown function	unknown function - novel
FTN_0939	32G09		hypothetical protein	hypothetical - novel
FTN_0996	29 E10	hslU	ATP-dependent protease HslVU, ATPase subunit	post-translational modification, protein turnover, chaperones
FTN_0999	19G08	udhA	soluble pyridine nucleotide transhydrogenase	cofactors, prosthetic groups, electron carriers metabolism
FTN_1006	20C08		transporter-associated protein, HlyC/CorC family	transport
FTN_1010	18D08		major facilitator superfamily (MFS) transport protein	transport
FTN_1020	18 E06		conserved protein of unknown function	unknown function - conserved
FTN_1041	13A03	ilvN	acetolactate synthase small subunit	amino acid metabolism - biosynthesis

FTN_1057	23D05	clpP	ATP-dependent Clp protease subunit P	post-translational modification, protein turnover, chaperones - protein degradation
FTN_1138	19D05	pilP	Type IV pili periplasmic component	motility, attachment and secretion structure
FTN_1146	2B07		aspartate aminotransferase	other metabolism - degradation, utilization, assimilation
FTN_1146	23B10		aspartate aminotransferase	other metabolism - degradation, utilization, assimilation
FTN_1151	23 E07		conserved protein of unknown function	unknown function - conserved
FTN_1243	31G12	recO	RecFOR complex, RecO component	DNA replication, recombination, modification and repair - restriction/modification
FTN_1253	10F09	lpcC	glycosyl transferase, group 1	cell wall / LPS / capsule
FTN_1253	25C10	lpcC	glycosyl transferase, group 1	cell wall / LPS / capsule
FTN_1254	32C05		protein of unknown function	unknown function - novel
FTN_1255	5C11		glycosyl transferase, family 8	cell wall / LPS / capsule
FTN_1256	7B06		membrane protein of unknown function	unknown function - novel
FTN_1273	32A07		long chain fatty acid CoA ligase	other metabolism - degradation, utilization, assimilation
FTN_1276	30C03	ermA1	membrane fusion protein	motility, attachment and secretion structure
FTN_1313	9D06	iglF	hypothetical protein	hypothetical - novel
FTN_1328	23D12		trehalase carbohydrate	metabolism - degradation, utilization, assimilation
FTN_1362	21 E08		hypothetical protein	hypothetical - novel
FTN_1372	29 E09		protein of unknown function	unknown function - novel
FTN_1381	29D08		hypothetical protein	hypothetical - novel

FTN_1413	30D10		ATPase, AAA family, related to the helicase subunit of the Holliday junction resolvase	DNA replication, recombination, modification and repair
FTN_1417	16G02	manB	phosphomannomutase	carbohydrate metabolism - biosynthesis
FTN_1417	31F11	manB	phosphomannomutase	carbohydrate metabolism - biosynthesis
FTN_1418	20H09	manC	mannose-1-phosphate guanylyltransferase	cell wall / LPS / capsule
FTN_1418	31D04	manC	mannose-1-phosphate guanylyltransferase	cell wall / LPS / capsule
FTN_1420	30 E07	wzx	O antigen flippase	transport
FTN_1420	26F05	wzx	O antigen flippase	transport
FTN_1421	6C03	wbtH	glutamine amidotransferase/asparagine synthase	amino acid metabolism - biosynthesis
FTN_1421	28H02	wbtH	glutamine amidotransferase/asparagine synthase	amino acid metabolism - biosynthesis
FTN_1422	6D05	wbtN	glycosyl transferase, group 1	cell wall / LPS / capsule
FTN_1422	28B06	wbtN	glycosyl transferase, group 1	cell wall / LPS / capsule
FTN_1423	17F12	wbtG	glycosyl transferase, group 1	cell wall / LPS / capsule
FTN_1425	6 E08	wbtF	NAD dependent epimerase	cell wall / LPS / capsule
FTN_1425	32 E05	wbtF	NAD dependent epimerase	cell wall / LPS / capsule
FTN_1427	24D12	wbtD	glycosyl transferase, group 1cell wall / LPS / capsule	cell wall / LPS / capsule
FTN_1427	1B05	wbtD	glycosyl transferase, group 1	cell wall / LPS / capsule
FTN_1428	3B11	wbtO	transferase	cell wall / LPS / capsule
FTN_1430	24B08	wbtQ	aminotransferase	putative enzymes
FTN_1430	4C01	wbtQ	aminotransferase	putative enzymes
FTN_1431	6G03	wbtA	dTDP-glucose 4,6-dehydratase	cell wall / LPS / capsule
FTN_1431	23B09	wbtA	dTDP-glucose 4,6-dehydratase	cell wall / LPS / capsule
FTN_1433	5F07		protein of unknown function	unknown function - novel
FTN_1448	5 E09		protein of unknown function	unknown function - novel

FTN_1491	30A12		adenine specific DNA methylase	DNA replication, recombination, modification and repair - restriction/modification
FTN_1513	31 E12	xerC	site-specific recombinase	DNA replication, recombination, modification and repair
FTN_1544	29D10	hemK	modification methylase, HemK family	translation, ribosomal structure and biogenesis
FTN_1608	5A10	dsbB	disulfide bond formation protein	putative enzymes
FTN_1681	25F06		ferric uptake regulation protein	signal transduction and regulation
FTN_1686	29 E11		hypothetical membrane protein	hypothetical - novel
FTN_1715	31D11	kdpD	two component regulator, sensor histidine kinase kdpD	signal transduction and regulation
FTN_1732	31C10		Mg-dependent Dnase	DNA replication, recombination, modification and repair - degradation
FTN_1777	30H08	trpG	anthranilate synthase component II	amino acid metabolism - biosynthesis
intergenic	21 E02		intergenic	
intergenic	7C07		intergenic	
intergenic	17D02		intergenic	

[a] Well ID annotation from BEI Resources *F. novicida* Two-Allele Transposon Library

[b] Results of secondary attachment screen. (+) indicates ability and (–) indicates inability of biofilm-mutant to adhere to polystyrene based on 1h attachment assay.

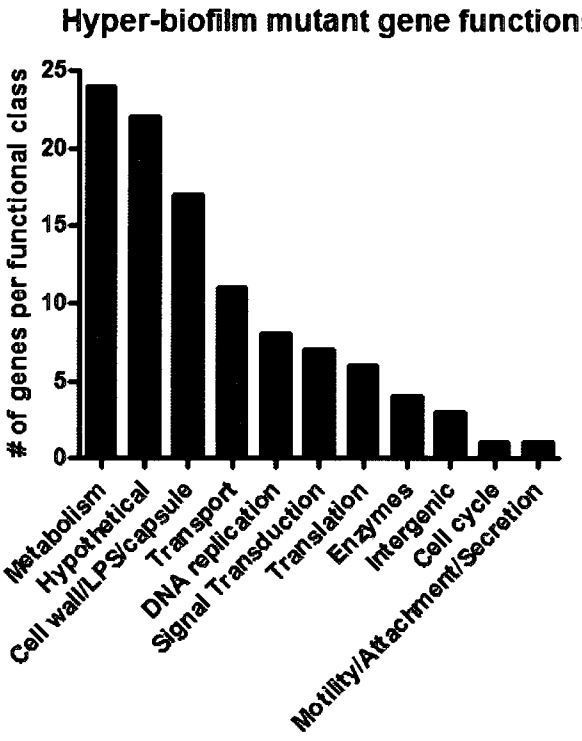

Figure 20 – Biological processes of hyper-biofilm mutants.
Transposon-insertion mutants demonstrating increased biofilm formation were identified during the Two-Allele library crystal violet screen. Hyper-biofilm mutants were defined by wells exhibiting two standard deviations higher crystal violet staining than the mean of the plate. The biological process for each mutant strain was determined and the number of instances is graphed above.

4.3.3 Nutrient limitation and static growth enhances early biofilm events.

To formally address the role of environmental stresses on biofilm formation, *F. novicida* was grown under different growth conditions prior to biofilm inoculation. MH and CDM broth grown bacteria were compared to determine the impact of nutrient limitation on biofilm growth. Additionally, we examined

the role of static growth on *F. novicida* biofilm formation. Growth without aeration subjects bacteria to decreased oxygen tension, as well as local nutrient depletion. We inoculated overnight cultures grown under each growth condition into microtiter wells and biofilm formation was assayed at 30, 75, and 120 min by crystal violet staining. Do to differences in overnight growth, we normalized biofilm formation for each condition to population size as measured by OD_{570} (Normalized OD = CV_{570}/OD_{570}). Surprisingly, growth in CDM did not increase the kinetic or overall amount of crystal violet staining (Figure 21). In fact, decreased normalized crystal violet staining was observed in the CDM samples. Static growth, however, significantly enhanced the early biofilm kinetics of *F. novicida* (Figure 21). In MH and CDM media, both the initial attachment at 30 min and the subsequent early stages of biofilm formation were statistically higher in the static condition (ST) compared to the shaking condition (SH).

The effect of static growth could result from pre-expression and production of adherence and biofilm determinants or quicker sensing of surface attachment and subsequent upregulation of biofilm genes. We pre-treated cultures with bacteriostatic antibiotics (tetracycline or chloramphenicol) to discern which of these possibilities accounts for the increased kinetics of statically pre-grown *F. novicida* biofilms. If statically grown bacteria are primed for biofilm formation we expected the addition of antibiotics to have little effect on the enhanced biofilm phenotype. However, if static growth allows *F. novicida* to respond faster to surface association, then pre-incubating static

cultures with bacteriostatic antibiotics would prevent this rapid response and block increased biofilm formation. For MH grown bacteria (Figure 21A), the addition antibiotics blocked the static growth enhancement of biofilm formation, while the CDM ST samples still exhibited higher crystal violet staining after antibiotic pre-treatment (Figure 21B). These results indicate that biofilm determinants are pre-expressed during static growth in minimal media, but not rich media.

(A)

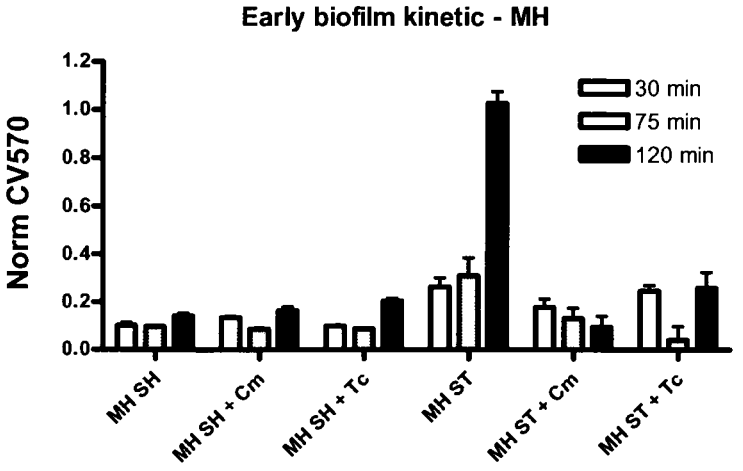

(B)

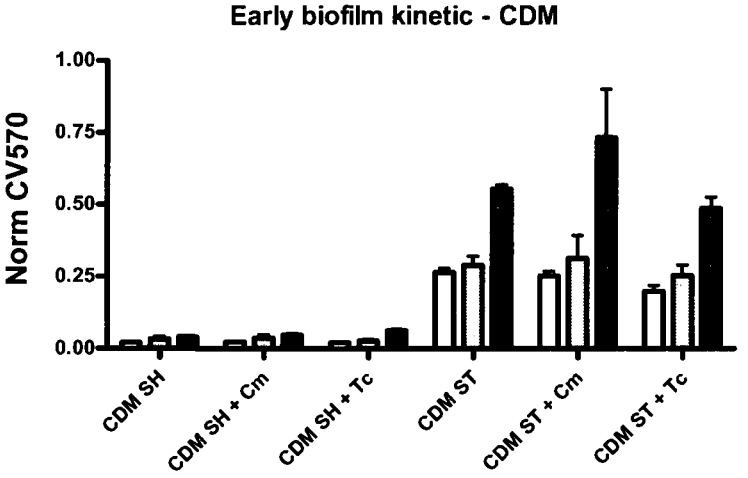

Figure 21 – Static growth enhances early biofilm kinetics.

Early biofilm kinetics were determined for *F. novicida* cultures grown overnight in rich MH broth (A) or minimal CDM media (B), shaking (SH) or standing (ST). For each growth condition, samples were pre-treated for 30 min with 5 µg/ml chloramphenicol (Cm), 10 µg/ml tetracycline (Tc) or no antibiotic. Biofilm formation was tracked over two hours by crystal violet staining. Four replicates were averaged per growth condition.

4.3.4 Static growth in minimal media upregulates *F. novicida* biofilm genes.

The effects of antibiotic pre-treatment on statically grown CDM cultures strongly suggested that key determinants of *F. novicida* biofilm formation were highly expressed under these conditions. We utilized global expression profiling to identify these genes. We performed growth curves on *F. novicida* cultures grown in MH and CDM media and grown statically or with aeration (Figure 22). RNA was recovered from samples taken at equivalent points in the growth curves from each condition and converted to cDNA. Amino-allyl labeled cDNA from each time point was labeled with Cy5 dye. We used Cy3-labeled pool of all samples as the reference sample and labeled with Cy3. 1 µg each of sample and reference were hybridized to a previously described 70-mer oligonucleotide array (21). We then performed hierarchical clustering on all expression array data using the Clustal program (117). Imaging the resulting clustering data in Java TreeView (170) revealed distinct gene expression clusters for each growth condition (Figure 23A). Multiclass significance analysis of microarrays (SAM) with a false discovery rate of 1% identified 235 genes that were differentially expressed in one or more condition, including 74 genes that were specifically upregulated in the CDM ST condition. Visualization of these statistically significant genes showed a distinct pattern of expression under different growth conditions (Figure 23B). Three *F. novicida* biofilm determinants were expressed highly in CDM ST (Chapter 3). The Sec-secreted FTN_0714 gene was expressed over 10-fold

higher in CDM ST than under other growth conditions. The FTN_0100 membrane protein and cytochrome B561 biofilm genes were also highly expressed in these conditions. Key factors in cell well recycling and biosynthesis including *ampD* and *ampG*, were also highly expressed during CDM ST growth. While transposon-insertion mutants for these genes were not present in the Two Allele library, the genes were previously implicated in *F. novicida* biofilm formation during a screen of a mutant library generated by David Weiss, a former postdoctoral fellow in the lab. Our results confirm that potential *F. novicida* biofilm determinants are highly expressed under conditions that promote biofilm formation.

Twenty-six of the 74 genes identified in the multiclass SAM analysis of CDM ST cultures were involved in transport (Table 5). Transported materials included amino acids, fatty acids, and inorganic nutrients. The CDM ST condition also promoted rapid biofilm formation, potentially linking biofilms and nutrient uptake during *F. novicida* persistence in nutrient-limiting conditions. Additionally, stringent response ppGpp synthase *spoT* was also in the highly expressed CDM ST cluster. The other ppGpp synthase, *relA,* was highly expressed during static growth in both media. The upregulation ppGpp synthase genes in biofilm-promoting conditions indicated a potential role for the stringent response in biofilm regulation. Additionally, a *spoT* transposon-insertion mutant was also identified in our previous biofilm screen attempt.

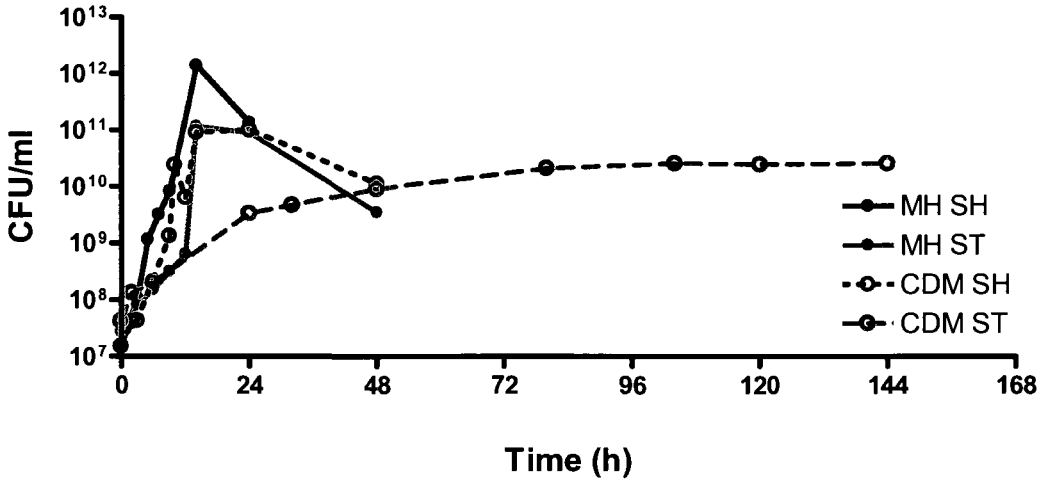

Figure 22 – *F. novicida* growth curves in different growth conditions for microarray analsysis.

Growth curves in MH or CDM broth and shaking (SH) or standing (ST) were performed. Samples were removed from each culture at various timepoints for RNA extraction. MH SH samples were taken at 1, 3, 5, 9 and 24 h and MH ST at 3, 6, 14, 24 and 48 h. The CDM SH culture was sampled at 3, 9, 14, 48 h and the CDM ST culture at 3, 24, 74, and 144 h.

(A)

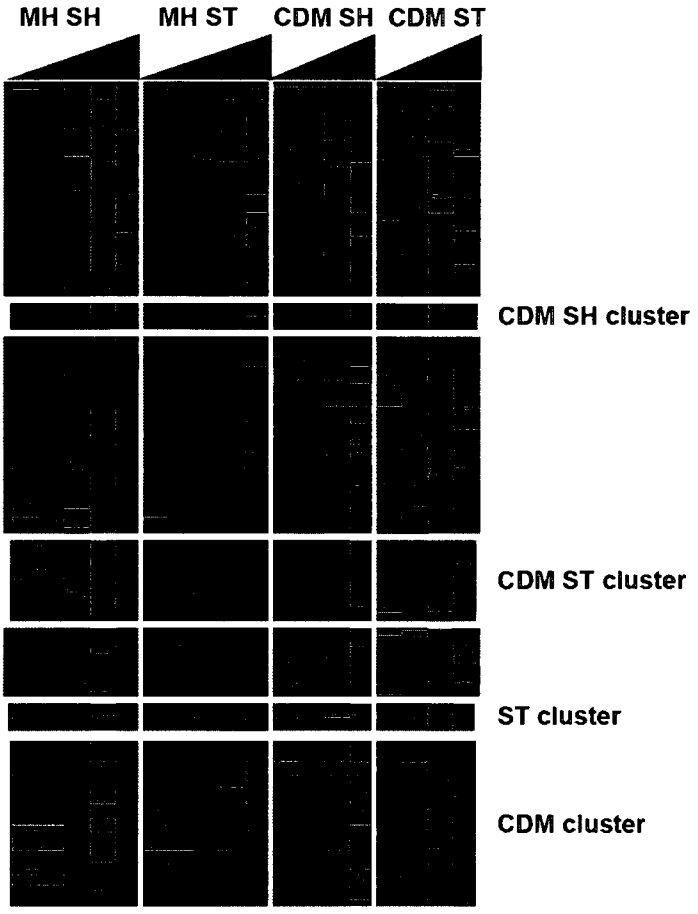
MH SH
MH ST
CDM SH
CDM ST
CDM SH cluster
CDM ST cluster
ST cluster
CDM cluster

(B)

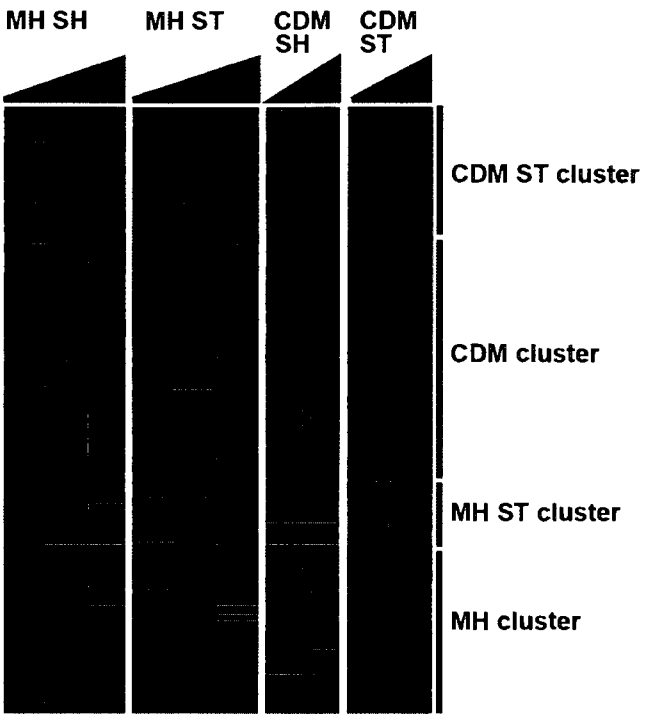

Figure 23 – Distinct gene expression patterns during biofilm-promoting growth.
The microarray data presented shows the expression profile of *F. novicida* grown in different media and aeration conditions. Hierarchical clustering of the timecourse arrays from each condition was visualized using Java Treeview. Global expression profiling (A) and SAM analysis (B) using a 70-mer oligonucleotide array revealed a distinct expression response to CDM ST growth; conditions that promote *F. novicida* biofilm formation. Late-logarithmic and stationary phase culture expression profiles were used to generate the SAM data.

Table 6 - *F. novicida* genes expressed statistically higher in CDM ST

FTN	Gene	Gene Function
FTN_0003		MFS family multidrug efflux protein
FTN_0003		MFS family multidrug efflux protein
FTN_0023	tmpT	SAM-dependent methyltransferases
FTN_0081		hypothetical protein
FTN_0086		MFS family multidrug efflux protein
FTN_0096		putative transmembrane protein
FTN_0100		predicted membrane protein
FTN_0211	pcp	pyrrolidone carboxylylate peptidase
FTN_0223		amino acid permease
FTN_0233	dut	dUTPase
FTN_0269		Short-chain fatty acids transporter
FTN_0281		conserved hypothetical protein
FTN_0296	lysP	lysine-specific permease
FTN_0299	putP	sodium/proline symporter
FTN_0319		amino acid permease
FTN_0361		hypothetical protein
FTN_0498		predicted membrane protein
FTN_0579		MFS family multidrug efflux protein
FTN_0588		asparginase family 2 protein
FTN_0588		plant-type l-asparginase
FTN_0588		capsule biosynthesis protein
FTN_0588		asparginase family 2 protein
FTN_0589		putative peptide transporter
FTN_0589		putative peptide transporter

FTN_0589		proton/peptide symport family protein
FTN_0640	dctA	C4-dicarboxylate transport protein
FTN_0640	dctA	C4-dicarboxylate transport protein
FTN_0656		polysaccharide biosynthesis protein
FTN_0714		hypothetical liprotein
FTN_0687	galP	galactose-proton symport protein
FTN_0731		hypothetical protein
FTN_0741		proton/peptide symport family protein
FTN_0767	betT	choline transporter
FTN_0767	betT	choline transporter
FTN_0848		amino acid antiporter
FTN_0860		amino acid permease
FTN_0875		MFS family multidrug efflux protein
FTN_0886		hypothetical protein
FTN_1011		MFS family multidrug efflux protein
FTN_1021		hypothetical protein
FTN_1121	phrB	deoxyribodipyrimidine photolyase
FTN_1125		dormancy related protein
FTN_1198	spoT	GDP diphosphokinase/guanosine-3',5'-bis(diphosphate) 3'-diphosphatase
FTN_1199		hypothetical transmembrane protein
FTN_1200	capC	capsule biosynthesis protein
FTN_1200	capC	capsule biosynthesis protein
FTN_1251	yjdL	proton-dependent oligopeptide transport (POT) family protein
FTN_1251	yjdL	proton-dependent oligopeptide transport (POT) family protein
FTN_1251	yjdL	proton-dependent oligopeptide transport (POT) family protein
FTN_1268	mce	ABC family transport protein

FTN_1269		hypothetical protein
FTN_1321	iglD	hypothetical protein
FTN_1409		MFS family multidrug efflux protein
FTN_1409		MFS family multidrug efflux protein
FTN_1458		conserved hypothetical protein
FTN_1458		conserved hypothetical protein
FTN_1459		conserved hypothetical protein
FTN_1459		conserved hypothetical protein
FTN_1461	ampG	MFS family multidrug efflux protein - cell wall recylcing
FTN_1525		conserved hypothetical protein
FTN_1536		amino acid transport protein
FTN_1551	ampD	N-acetylmuramoyl-L-alanine amidase
FTN_1592	oppB	oligopeptide ABC transporter
FTN_1593	oppA	oligopeptide ABC transporter
FTN_1593	oppA	oligopeptide ABC transporter
FTN_1654		MFS family multidrug efflux protein
FTN_1654		MFS family multidrug efflux protein
FTN_1715	kdpD	two component sensor kinase
FTN_1733		predicted membrane protein
FTN_1740	trpA	tryptophan synthase alpha chain
FTN_1752		Na+/H+ antiporter protein
FTN_1754		cytochrome B561
FTN_1773		nitrile hydratase
FTN_1773		nitrile hydratase
FTN_1774		rhodanese-related sulfurtransferase

Given the role we establish for the MglA pathway in biofilm formation, we asked how the reported MglA-regulon (21) responds to growth in different conditions. We found nutrient availability to be the key factor in the expression of MglA-regulated genes (Figure 24). The 102 genes were highly expressed in both CDM SH and CDM ST conditions compared to growth in MH with or without aeration (Figure 24A). Multiclass SAM analysis found that the majority of these expression patterns (67 genes) were statistically significant including the six we found to contribute to biofilm formation (Figure 24B). While we explored the MglA regulon for its potential role in environmental persistence, we did note that the entire FPI was highly expressed during CDM growth (Figure 24C). While we have not determined the MglA-regulon under different growth conditions, expression pattern of the published regulon suggests that nutrient limitation and/or microaerophilic growth are triggers for these genes. Therefore, MglA-regulated genes may be necessary but are not sufficient for the CDM ST enhancement of biofilm formation. We do show, however, that nutrient limited growth may increase the virulence of *F. tularensis*. Activation of the MglA pathway during nutrient limited growth may promote survival both in nature and within a mammalian host.

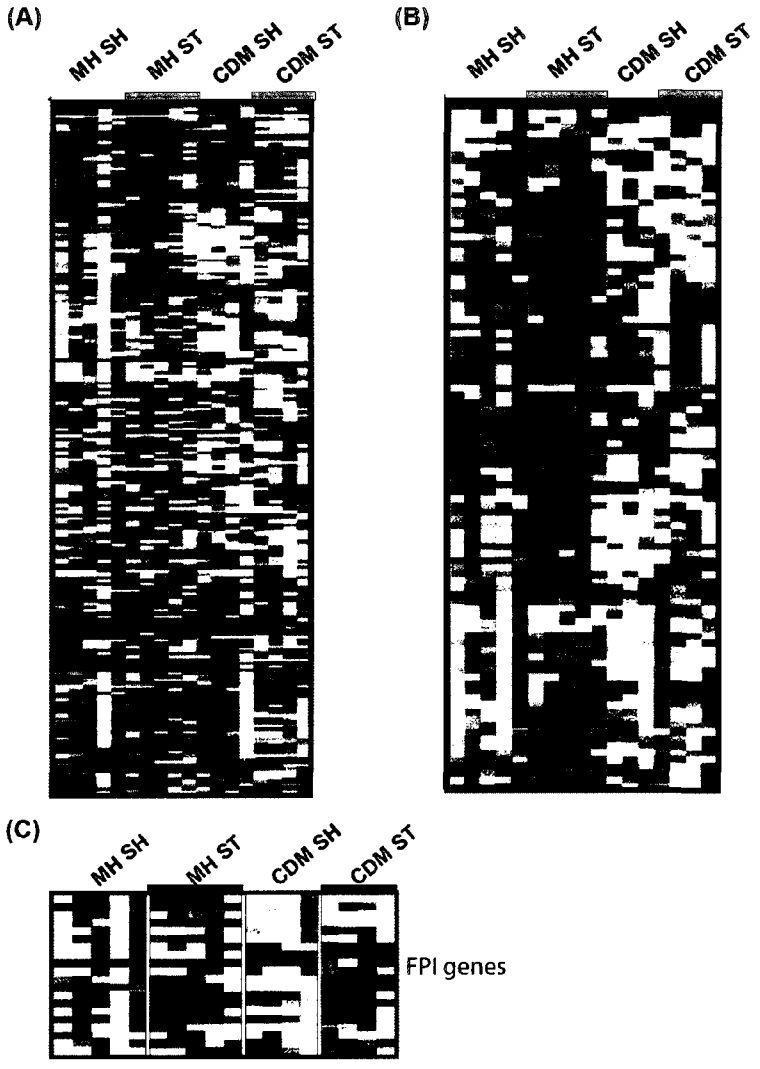

Figure 24 – The MglA-regulon is expressed at statistically higher levels during minimal media growth.

The expression pattern of the MglA-regulon was examined for MH SH, MH ST, CDM SH, and CDM ST growth curves (A). SAM analysis demonstrated that 103 spots had higher signal for *F. novicida* grown in CDM regardless of aeration (B). Of these significant genes, the entire FPI was highly expressed during nutrient limited growth (C). In all cases, timecourse microarray data are displayed left to right.

4.4 DISCUSSION

Investigating the role of nutritional and environmental stresses on *F. novicida* biofilm formation was one step in understanding how this pathogen senses and adapts to the environment. In Chapter 2, we characterize the response of *F. novicida* to carbon limitation and found the pathogen responds enhanced biofilm formation. Here, we identify static growth that limits oxygen and nutrient availability, as a key promoter of biofilm initiation. Environmental and pathogenic bacteria form biofilms to promote survival in non-ideal conditions (129, 142, 163, 186). Biofilm regulation occurs at many levels, integrating multiple environmental and bacterial signals to control the transition from planktonic to surface-associated growth.

The biofilm mutant screen described in the previous chapter provided clues to the influence of nutritional state in *F. novicida* biofilms. We first determined that all known players in the MglA signaling pathway are deficient for biofilm formation (Figure 18). Six MglA-regulated genes were attenuated for both biofilm formation and initial attachment (Figure 19). Importantly, MglA influence on *F. novicida* biofilm formation is not FPI mediated despite the attenuated phenotype of a *pdpA* transposon-insertion mutant (Figure 18). The role of MglA and its regulon in virulence has been well characterized (7, 12, 21, 110). Given the homology of MglA and co-regulator SspA to known general stress response regulators in other Gram negative bacteria (20, 27), the potential role in the MglA pathway in mediating survival outside of a eukaryotic cell is intriguing. In *E. coli*, the *sspA* homolog controls acid

resistance (85), osmotic tolerance (195), and starvation response (212). Of the 102 MglA-regulated genes (21), only small subset have been evaluated for function in any context. Brotcke *et al.* did find that an *ospD3* homolog (FTN_1071) is regulated by MglA and has no role in mammalian infection (21). This gene was among the MglA-regulated biofilm mutants, further suggesting that some regulon genes may function in environmental persistence. We also observed strong expression of the MglA-regulon under biofilm promoting conditions (Figure 24). Given the increased biofilm formation of *F. novicida* grown under these conditions and the requirement of both MglA and FevR for wild-type biofilm formation, we plan to determine the MglA-regulon under the conditions that promote maximum biofilm formation. If the MglA signaling pathway is indeed both a general stress response pathway and a virulence regulation pathway, *F. tularensis* must have a way of integrate multiple signals through this pathway and respond in different manners. Different proteins in the MglA pathway (*e.g.* FevR, CaiC, and CphA) may, therefore, respond to different cues, yielding distinct responses.

The hyper-biofilm phenotype of numerous metabolism and nutrient transport mutant strains also indicated a role for nutrient limitation in biofilm formation. Thirty-one of the 105 hyper-biofilm genes fell into these two biological processes (Table 4). Mutations in these 31 genes should confer an artificial starvation response for the bacteria by inhibiting nutrient important or blockage of various metabolic pathways. We concluded that such physiological stress induces *F. novicida* biofilm formation. We are currently

exploring the role of MglA pathway, the stringent response, and the limited repertoire of two component systems in sensing of nutritient availability is and induction of biofilm formation. Both an orphan response regulator (48) and the stringent response (43) were recently implicated in *F. tularensis* biofilm regulation.

Collectively, the biofilm screen data strongly suggested a role for environmental stresses in *F. novicida* biofilm induction. We measured biofilm levels for bacteria grown under oligotrophic and static conditions to test this hypothesis. Surprisingly, growth in CDM minimal medium alone did not promote greater biofilm formation (Figure 21). CDM media contains glucose, however, explaining why we did not observe the carbon limitation phenotype described in Chapter 2. Static growth however was sufficient to cause higher crystal violet staining. Antibiotic pre-treatment of MH ST cultures blocked the enhanced biofilm kinetic, while treated CDM ST cultures had no effect on biofilm kinetic or magnitude (Figure 21). These results indicated that sensing of oxygen tension and nutrient availability may act synergistically to cue a switch to biofilm formation. Gerstel *et al.* identified nutrient starvation and oxygen tension as the two major signals for *Salmonella typhimurium* biofilm formation (69).

We queried which *F. novicida* gene products were expressed in the CDM ST condition by global expression profiling. Hierarchical clustering of expression microarray data for *F. novicida* grown in each of the four growth conditions demonstrated gene clusters for MH, CDM, ST, and CDM ST

conditions (Figure 23A). Multiclass SAM analysis on pre-stationary phase cultures identified 74 genes expressed highly in CDM ST growth condition that promoted *F. novicida* biofilms (Figure 23B, Table 5). The FTN_0714 lipoprotein was the only biofilm determinant described in Chapter 3 found to be highly expressed in CDM ST. Could this gene product fully explain the increased biofilm formation of CDM ST grown cultures? We previously performed a biofilm mutant screen using a different transposon-insertion mutant library developed by David Weiss (208). While the FTN_0714 was identified numerous times in this earlier screen and confirmed for biofilm formation, technical issues prevented the successful identification of other mutants. Serendipitously, the Weiss library contained transposon-insertion mutants for genes not represented in the Manoil and Gallagher Two Allele library. Several of these, including cell wall synthesis and recycling genes, were confirmed to be biofilm-deficient. The *ampD* and *ampG* genes in this process were also highly expressed in the CDM ST condition. While clean deletions of these genes conferred decreased fitness, the genetic and expression data indicates a role for cell wall expansion and rearrangement in biofilm formation.

The predominance of highly expressed nutrient transporters (26 of 74 genes) strongly indicates a specific starvation response during static growth in minimal media. This growth condition most closely resembles the microenvironment virulent *F. tularensis* strains are likely to encounter in nature. Stressful conditions may, therefore, be sensed by the *qseB/pmrA*

homolog shown to influence *F. novicida* biofilms (48) and stringent response mediators RelA and SpoT that are highly expressed under static conditions. These pathways may integrate environmental signals through the MglA signaling pathway to trigger biofilm formation. Charity *et al.* found in the context of virulence regulation that ppGpp mediates expression of the MglA-regulated virulence factors, including the FPI (personal communication with James Charity). Expression profiling of wild-type and *mglA* mutant bacteria adhered to surfaces such as chitin will elucidate the MglA regulon in an environmentally relevant context and potentially determine how the MglA signaling pathway regulates biofilm formation and environmental persistence mechanisms.

Chapter 5: Identification of a novel *Francisella tularensis* polar appendage

Jeffrey J. Margolis[1], Lydia-Marie Joubert[2], Luis Comolli[3], Nafisa Ghori[1], and Denise M. Monack[1]

[1] Department of Microbiology and Immunology, Stanford University School of Medicine, Stanford, CA 94305.

[2] Cell Sciences Imaging Facility, Stanford University School of Medicine, Stanford, CA 94305.

[3] Life Sciences Division, Lawrence Berkeley National Laboratory, Berkeley, CA 94720.

5.1 CHAPTER 5 SUMMARY

In Chapter 4, we concluded that static growth dramatically increased the kinetics of *F. novicida* biofilm formation. This enhancement suggested that statically grown *F. novicida* may undergo a morphological change that promotes surface association. SEM imaging of biofilms grown under static conditions revealed a novel appendage that closely resembled the structure of the *Caulobacter crescentus* stalk. Stalk formation was conserved in the Type A SchuS4 strain, as well. Further microscopic analysis provided additional structural characterization of the stalk structure and composition.

We previously established that static growth increased the entry of *F. novicida* into host macrophages. We, therefore, visualized the interaction of statically grown bacteria with these immune cells and found that the same stalk appendage interacts with the cell membrane. Additionally, a stalk-like structure was observed on *F. novicida* in the cytoplasm of bone marrow-derived macrophages. The *F. tularensis* stalk may, therefore, also facilitate intracellular infection.

To elucidate the role of *F. novicida* stalk formation, we performed a forward genetic screen to identify stalk-deficient mutants. We developed a fluorescence microscopy technique to assay for stalk formation in a high throughput manner. Twenty-six genes were found to have decreased stalk formation; including LPS and cell wall biosynthesis genes and 7 hypothetical genes. Of note, *F. novicida* stalk formation was independent of Type-IV pili genes and the FPI. The lack of stalk-less mutants suggests that genes

required for stalk biogenesis are essential and furthers the hypothesis that *F. novicida* stalks form through the same machinery that generates the cell envelope. As we further characterize this novel appendage we discovered, we hope to gain insight into the mechanism of *F. novicida* biofilm formation, environmental persistence and potentially intracellular survival.

5.2 INTRODUCTION

Our expression data from Chapter 4 strongly suggested that statically grown *F. novicida* produce factors that enhance surface association and early biofilm formation. We hypothesized that morphological changes in the cell body may explain this result. Bacteria utilize a variety structures to associate with surfaces. Many of these adhesins are proteinaceous, including the various filamentous pili (162). During biofilm formation carbohydrates (24, 211), LPS (10, 42, 63) and DNA (80, 125) can also facilitate non-covalent surface attachment.

A small set of aquatic bacteria produce a large polar appendage that facilitates attachment and synchronizes a complex developmental lifecycle. These prosthecated bacteria belong solely to the α-Proteobacteria and include *C. crescentus* and *Hyphomonas neptunium* (179, 207). This cylindrical structure is a continuation of both bacterial membranes and the peptidoglycan layer in between (160, 181). Stalks have not been described in pathogenic bacteria, nor in non-flagellated organisms. Therefore, the presence of a stalk-

like structure for *F. tularensis* challenges the established roles for this appendage.

The role of the *C. crescentus* stalks in attachment, cell division, secretion and nutrient uptake has been explored both genetically and biochemically. The polar stalk is an essential determinant of asymmetrical cell division of *C. crescentus.* Cell division of dimorphic prosthecate bacteria begins by the biogenesis of a stalk (94). Flagellated bacteria use two phospho-relay systems to transition to a stalked, sessile form (28). A carbohydrate-based adhesin at the tip of the stalk, termed the holdfast, tethers the bacterium to a surface (106, 115). Attachment via the *C. crescentus* holdfast is an essential step in biofilm formation for this aquatic organism (57, 178). The result is asymmetric cell division, leading to a flagellated, swarming daughter cell and a stalked parental cell (94). Asymmetrical division results from the cell polarity established by stalk biogenesis. Key mitotic and septation machinery, including the actin-homolog MreB, are localized by pole-associated PleC and DivJ (9). Because of this highly organized sequence of events, *C. crescentus* is a popular developmental biology model. *F. tularensis* is not reported to divide by asymmetric mechanisms.

The stalk may also function in nutrient acquisition. Ireland *et al.* performed a proteomic analysis of membrane proteins of the *C. crescentus* stalk and discovered an enrichment for amino acid, phosphate, and other nutrient uptake systems (93). Phosphate-limitation in particular was shown to increase the stalk elongation. Growth in the absence of exogenous phosphate

or deletion of a phosphate transporter resulted in a significant increase in stalk length (93, 202, 204). Interestingly, these researchers found that stalk outer membrane proteins represented a selected subset of known cell body outer membrane proteins (93). Limited inner membrane and cytoplasmic proteins were found in the stalk during this study. *C. crescentus* researchers hypothesize that the structure of the stalk with a high surface area to volume ratio optimizes nutrient uptake by this bacterium (202). Additionally, the increased buoyancy of the stalk compared to the cell body may promote maintenance at the oxygen and nutrient enhanced air-liquid interface (165).

Here we describe the identification of a novel *F. tularensis* appendage that morphologically resembles the *C. crescentus* stalk. This polar structure forms during biofilm formation and biogenesis is faster when *F. novicida* is grown statically. Electron microscopy techniques provided a detailed characterization of the *Francisella* stalk structure. To date, we have only inferred the function of the *F. tularensis* stalk. Beyond its potential role in biofilm formation and environmental persistence, this appendage may also facilitate host cell association and intrcellular survival. We observe stalked-bacteria associated with multiple eukaryotic cell types, with the percentage increased for statically grown *F. novicida.* In addition, a high percentage of stalked bacteria are observed in the cytoplasm of bone marrow-derived macrophages. We attempted to identify genes required for stalk biogenesis, but discovered that these genes are likely essential. By further characterizing

this novel structure, we hope to understand unique *F. tularensis* adaptation to environmental stress.

5.3 RESULTS

5.3.1 Identification of a novel *F. novicida* polar appendage

We imaged *F. novicida* attachment and early colonization to determine if morphological alterations explained the enhanced biofilm phenotype of CDM ST grown bacteria. We inoculated aerated, rich medium (MH SH) and static, minimal medium (CDM ST) overnight cultures onto glass coverslips and allowed the bacteria to colonize for 90 min. Samples were then fixed and prepared for SEM visualization. At this timepoint, we observed scattered individual bacteria in the MH SH samples (Figure 26A). Higher numbers of CDM ST grown *F. novicida* adhered at 90 min and more clumps of cells were visible (Figure 26B). At higher magnification, we discovered a polar appendage in the adhered CDM ST population (Figure 26C). This structure closely resembled the appearance of the *C. crescentus* stalk (202). Based on this structurally similarity we termed the novel appendage we observed the *Francisella* stalk. Early stalk biogenesis was captured for some attached bacteria (Figure 26D). A protrusion of the inner membrane appeared to force the outer membrane to stretch outwards, while maintaining a coccobacillus structure.

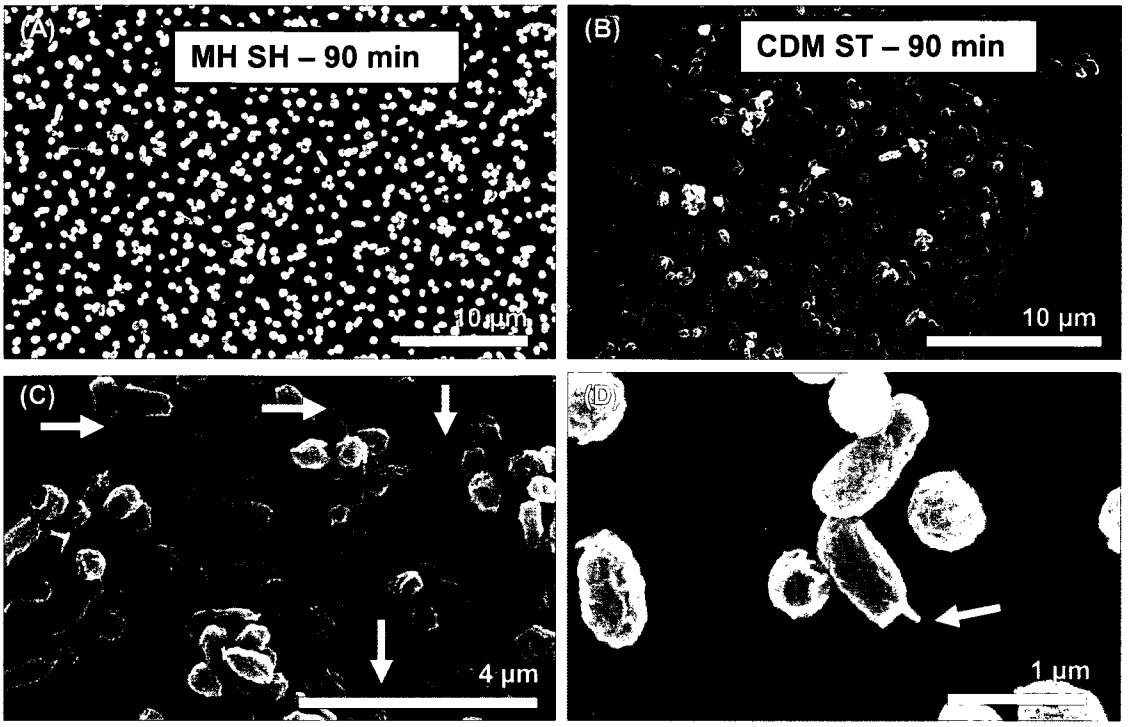

Figure 25 – *F. novicida* biofilms form a novel appendage.
SEM images of 90 min *F. novicida* biofilms from cultures pre-grown in MSH SH (A) and CDM ST (B) conditions are displayed. Greater surface colonization was observed for the CDM ST condition. (C) Higher magnification imaging of the CDM ST adhered population revealed numerous novel polar appendages (white arrows). (D) Appendage biogenesis appeared to initiate by protrusion of the inner membrane (yellow arrow) for the CDM ST biofilm bacteria.

We turned to transmission electron microscopy (TEM) technique to better characterize the structure of the novel *F. novicida* stalk. We found that static growth in 2 ml of tryptic soy broth supplemented with 0.2% cysteine (TSBc) yielded similar stalk structures. Pellicle formation at the air-liquid interface of the statically grown cultures generated *F. novicida* biofilms that were easily recovered for microscopy. After 2 d and 7 d, whole static cultures

were vortexed vigorously for 30 s and pipetted 30 times to generate a single cell suspension of biofilm bacteria. During static incubation, bacterial growth was found predominately at the liquid surface. Therefore, the majority of bacteria imaged were recovered from a biofilm community. Negative staining of the 2 d samples (Figure 27A) demonstrated stalk formation similar to what was observed in the biofilm SEM images (Figure 26). We observed single, polar localization of this appendage at this timepoint. After 7 d of static growth (Figure 27B), we visualized many stalks per field. Interestingly, these structures reached up to several microns in length and were often not associated with the bacterial cell body. Smooth, continuous edges of the cell-free stalks, suggested that these structures are shed by the bacterium rather than sheared off during processing. The role of these removed stalks is unknown.

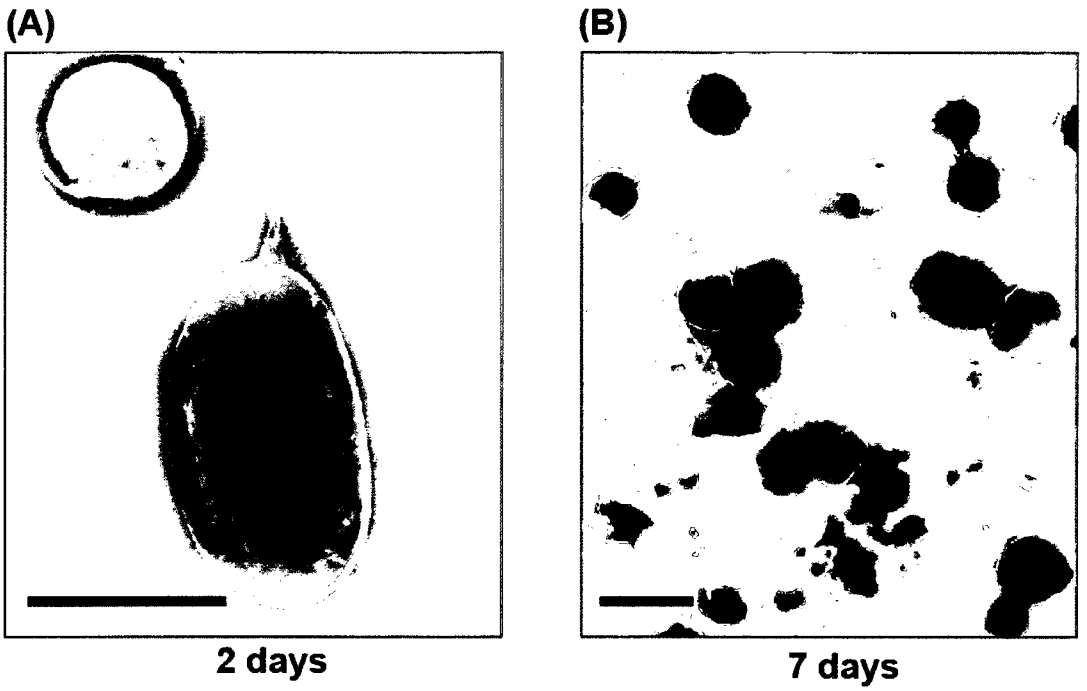

Figure 26 - Formation of *F. novicida* stalk during static broth growth.
Images represent morphologies of *F. novicida* grown statically in TSB broth with 0.2% cysteine. Stalked bacteria were observed after 2 d of static growth (A). At 7 d, stalks were up to 4 μm long and were commonly dissociated from the bacterial cell body. Scale bar equals 1 μm.

SEM and negative staining provided a good characterization of the ultra structure of the *F. novicida* stalk. CryoEM performed in collaboration with Luis Comolli at Lawrence Berkeley National Laboratory investigated how these appendages form and remain associated with the bacterial cell body. Two main stalk compositions were observed in the cryoEM images. The majority of stalked bacteria demonstrated a contiguous continuation of both the inner and outer membranes (Figure 28A) consistent with the *C. crescentus* stalk (202).

For these stalks, we observed electron dense cytoplasm throughout the stalk body. In a minority of cases, only the outer membrane encircled the stalk body (Figure 28B). We visualized only blebs of For these instances blebs of cytoplasm inside the stalk in these instances. TEM of thin sectioned 2 h *F. novicida* biofilms grown on polystyrene support the both stalk compositions (Figure 29). The majority of stalked-bacteria possessed a single, polar appendage. Both inner and outer membranes are visible surrounding the stalk body in most bacteria with the appendage. In other instances, only the outer membrane composes the stalk body.

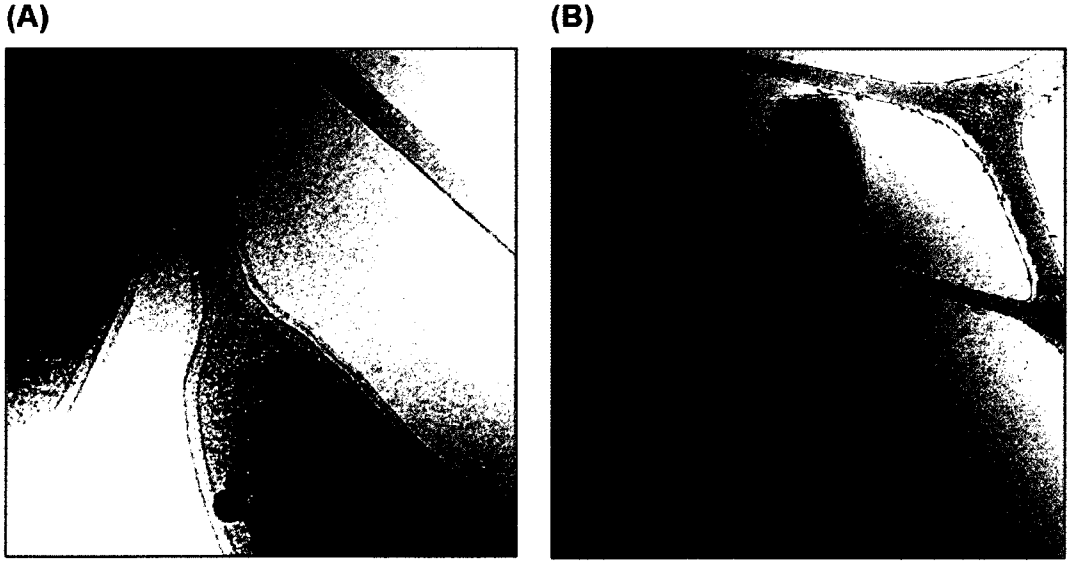

Figure 27 - CryoEM characterization of *F. novicida* stalk.
CryoEM imaging revealed two distinct *F. novicida* stalk morphologies. Bacteria were grown statically for one week before cryoEM processing. The majority of bacteria had a stalk that was contiguous with both the inner and outer membrane of the cell body and contained electron dense cytoplasm (A). *F. novicida* stalks with only blebs of cytoplasm were also observed (B).

Figure 28 - Thin section TEM of *F. novicida* biofilms grown on polystyrene.
Thin sections of 2 h *F. novicida* biofilms were imaged by TEM. Polar stalks were observed on a majority of attached bacteria. Smaller bacterial cells were observed with multiple stalks in the minority of cases. Scale bar equal 1 μm.

While an intriguing morphology for *F. novicida,* we tested a Type A human pathogen strain for stalk production to determine if this appendage may contribute to the fitness of highly virulent *F. tularensis* strains. In Chapter 3, we demonstrate that the *F. tularensis* subsp. *tularensis* strain SchuS4 forms biofilms. If stalk formation facilitates surface colonization or persistence, then we should detect stalk formation on SchuS4 grown in conditions that promote

stalk formation in *F. novicida.* With the help of Jean Celli at Rocky Mountain National Laboratory, 2 d static cultures of this Type A strain were negative stained and imaged by TEM (Figure 30). The structure of the SchuS4 stalk was consistent with what we observed for *F. novicida* (Figure 27).

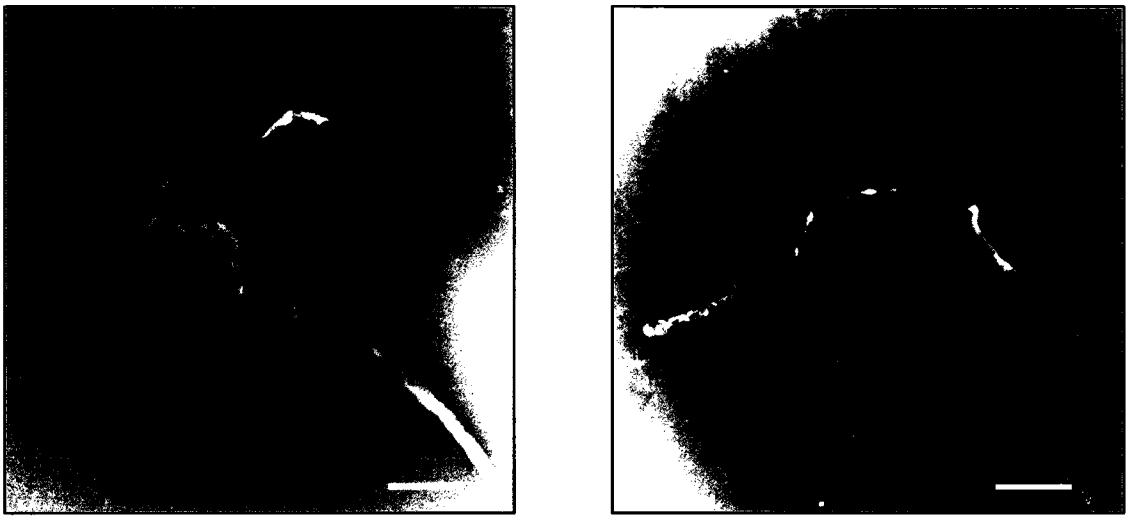

Figure 29 - Virulent Type A strain SchuS4 forms stalk appendages during static growth. Presented images show representative SchuS4 stalk formation during static growth in MH broth for 2 d in polyethylene tubes. Structure and dimensions were consistent with those observed for *F. novicida*. Scale bar equals 500 nm.

5.3.2 *F. novicida* stalks are formed during intracellular infection.

In Chapter 4 we describe the effects of static growth and nutrient limitation on biofilm formation. The enhanced biofilm phenotype with these growth conditions led us to investigate *F. novicida* morphology and led to the discovery of the *Francisella* stalk. We also observed an enhancement for intracellular infection for *F. novicida* growth under these environmental

stresses. Bacteria grown in rich TSBc or minimal CDM with or without aeration were spun unto $2.5x10^5$ cells at a MOI of 100:1. After 1 h at 37° C, free bacteria were washed away and extracellular bacteria were killed with 100 µg/ml gentamicin for 1 h. The infection continued for an additional hour and CFU were recovered 3 h post-infection. Growth in minimal media and lack of aeration had a synergistic effect on the recovery of this organism from RAW264.7 macrophages after 3 h (Figure 31).

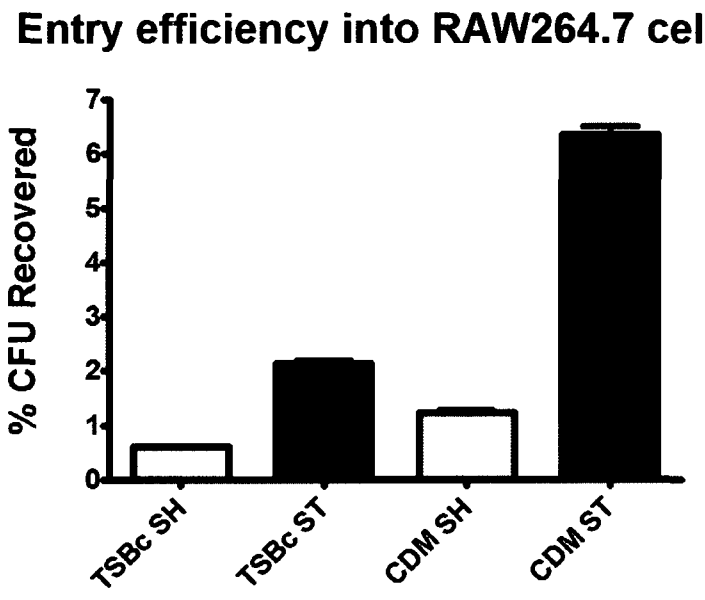

Figure 30 - Enhanced infection after nutrient limitation and static growth.
The graph above shows the infection of RAW264.7 macrophage-like cells with *F. novicida* grown under different conditions prior to inoculation. Efficacy of infection was measured as percent of inocula recovered after 3 h. The average of triplicate samples is displayed. Both growth in minimal medium and static growth promoted increased intracellular CFU recovery ($P<0.01$).

In light of the effect of static growth on *F. novicida* infectivity, we hypothesized that the novel stalk we observed may facilitate intracellular infection. We visualized statically grown *F. novicida* infecting RAW264.7 macrophages to address this question. TEM imaging of a 30 min timepoint demonstrated numerous stalked *F. novicida* attaching to host cells or within a vacuole (Figure 32A). We confirmed that stalked bacteria attach to non-phagocytic cells, as well by testing TIB-73 hepatocytes (Figure 32B) and HeLa epithelial cells (Figure 32C). Additionally, stalked *F. novicida* we found in high numbers inside of infected macrophages (Figure 33). Jonathan Jones, a graduate student in the lab, discovered the presence of these structures during infection using a selective permeabilization technique for labeling cytosolic bacteria. This technique developed by Jean Celli (30) for *F. tularensis* intracellular localization studies utilizes the selective permeabilization of the cholesterol-rich plasma membrane by digitonin to identify cytosolic bacteria. At 6 h post-infection, bone marrow-derived macrophages were treated with this detergent and cytosolic *F. novicida* was labeled in red using a polyclonal *F. novicida* antibody (Aves Labs, Tigard, OR). The cells were next fixed with 4% paraformaldehyde and treated with 1% saponin to permeabilize the entire cell. All bacteria were then labeled in green. The cytosolic structure observed inside of macrophages (Figure 33A,C) closely resembled the appearance of stalks formed on broth grown *F. novicida* (Figure 33D). Interestingly, intracellular stalks were only detected in

the staining for intracellular bacteria. Formation of intracellular stalk was not dependent on the FPI (Figure 33C).

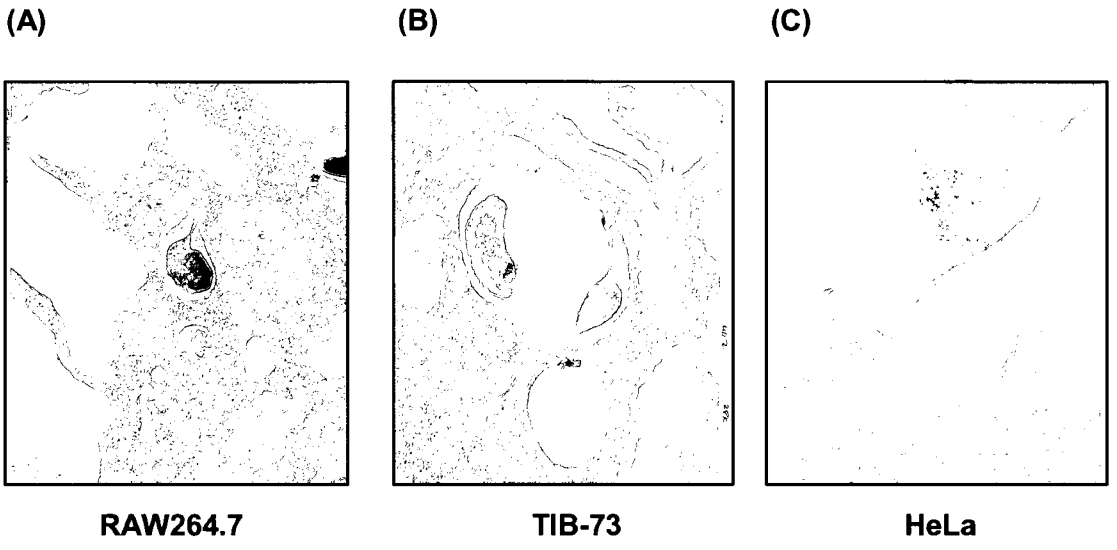

Figure 31 - *F. novicida* stalks associated with eurkaryotic cell membranes during infection.

The provided images show the association of the polar *F. novicida* stalk with the eukaryotic cell membrane during infection 30 min post-infection. This structure was observed in close contact with multiple cell types. Infection of RAW264.7 macrophages (A), TIB-73 hepatocytes (B), and HeLa epithelial cells (C) are shown.

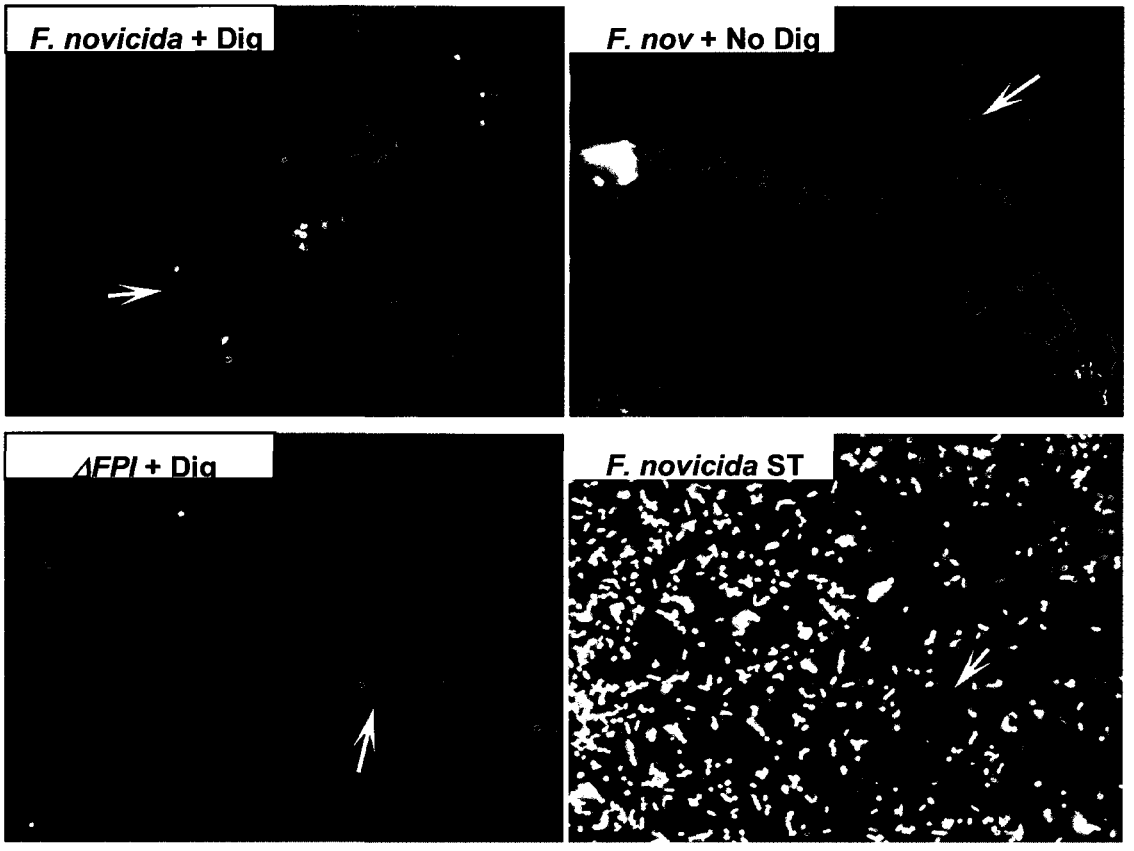

Figure 32 - Stalk-like structures form on intracellular *F. novicida*.

The morphology of stalked *F. novicida* grown in broth and intracellular *F. novicida* were compared. Static culture bacteria (lower right) possessed large numbers of stalk. Inside of bone-marrow derived macrophages, cytoplasmic *F. novicida* were labeled in red by digitonin permeabilization and all bacteria were labeled in green (left panels). The *Francisella* stalk was detected in both wild-type and FPI mutant *F. novicida*, but only in the cytoplasmic staining. Minimal stalked bacteria were observed in infected cells that were permeabilized with 1% saponin (upper right).

5.3.3 *F. novicida* genes required for stalk formation are essential.

The novel stalk appendage we describe for *F. novicida* may play roles in both biofilm formation and host cell infection; potentially by facilitating interaction with these surfaces. We performed a forward genetic screen for genes required for biosynthesis of this structure to address the molecular mechanisms of its formation. By identifying a mutant phenotype for deletion mutants in stalk machinery, we also hoped to cement a role for the *Francisella* stalk in colonization and persistence of this pathogen.

We first established an immunofluorescence imaging protocol to enable high throughput screening. This step was crucial for efficiently screening the Two Allele library. The characterization of stalk morphology described above required electron microscopy imaging; a time and labor intensive process. Given the relatively small size of *F. tularensis* strains (diameter ~1 μm), light microscopy techniques such as phase contrast and DIC did not resolve the stalk structure sufficiently to allow for rapid assessment of stalk biogenesis.

We knew that static growth in TSBc for 5-7 d yielded a pre-dominantly stalked population (Figure 34A). To immobilize these cultures to a surface for imaging, 1:100 dilutions of 10 μl culture spots were dried onto poly-L-lysine coated glass microscope slides. The bacteria were labeled with a polyclonal chicken anti-*F. novicida* primary antibody and stained with a goat anti-chicken 488 nm secondary antibody. Mounted samples could then be visualized by fluorescence microscopy in the green channel. By using fluorescence imaging, we amplified the signal of the stalk structure allowing for visualization

of this appendage in a single focal plane. To scale up this procedure, plates of the Two Allele library were grown statically for one week in TSBc in 96-well plate format. Eighteen samples were then spotted onto a single coated slide and multiple slides were stained by submersion in primary and secondary antibody solutions. All fluorescently-labeled samples were imaged individually by eye for the presence of stalk. Transposon-insertion mutants with qualitatively less stalk formation were retested in triplicate and assessed for wild-type growth in broth. David Halladin, a rotation student in the lab, performed the visual screen of the Two Allele library for stalk-less *F. novicida* mutants.

No transposon-insertion mutants yielded zero stalk production after 7 d of static growth in TSBc. Given the predicted role of cell wall and LPS re-arrangement in *F. novicida* stalk formation we were not surprised that the genes required for stalk formation are essential and not represented in the Two Allele library. We did however find 27 transposon-insertion mutants that conferred reduced stalk formation compared to wild-type *F. novicida* (Table 6). A representative stalk-deficient mutant, *minC::Tn5,* is presented in Figure 34. In many cases, we observed fewer bacteria on the microscope slide than with wild-type *F. novicida* than for transposon-insertion mutants that exhibited decreased stalk formation.

Stalk-deficient mutants fell into three main functional categories. Cell wall/LPS genes were most represented in the screen, with 8 genes contributing to stalk formation. This list included 7 genes whose products

modify LPS and the *minC* septum formation inhibitor. The *ostA2* LPS modification gene characterized in Chapter 3 was among the decreased stalk mutants. An additional 7 genes had no known function and 6 functioned in metabolism. The remaining 5 genes were annotated with various functions including stringent response ppGpp synthase, *relA*, and a drug/metabolite transporter. We concluded from these results that stalk biogenesis requires essential genes for stalk formation. Additional factors including known cell envelope machinery may also contribute to stalk biogenesis.

Table 7 – Transposon-insertion mutants with decreased stalk formation

FTN	Well ID	Gene	Gene Product	Biological Process
FTN_0044	12A07		novel protein of unknown function	unknown function
FTN_0117	6D12		ferredoxin	energy metabolism
FTN_0124	11G07	ssb	single-strand DNA binding protein	DNA replication, recombination, modification, and repair
FTN_0187	29A12	rbn	tRNA rpocessing ribonuclease BN	nucleotide and nucleoside metabolism
FTN_0331	26F09	minC	septum formation inhibitor	LPS/cell wall/capsule
FTN_0332	14C06	rpmG	50S ribosomal protein L33	translation, ribosomal structure and biogenesis
FTN_0337	11D06	fumA	fumarate hydratase	energy metabolism
FTN_0509	20C10		conserved protein of unknown function	unknown function
FTN_0546	26A06		mannosyl transferase family protein	LPS/cell wall/capsule
FTN_0637	9A08	ugpQ	glycerophosphoryl diester phosphodiesterase	LPS/cell wall/capsule
FTN_0713	26E07	ostA2	organic solvent tolerance protein OstA	LPS/cell wall/capsule
FTN_0808	12G02		acetoacetate decarboxylase	other metabolsim - biosynthesis

FTN_0842	32G04	aroG	phospho-2-dehydro-3-deoxyheptonate aldolase	amino acid metabolism - biosynthesis
FTN_0884	9F01		drug/metabolite transporter superfamily protein	transport - drugs / antibacterial compounds
FTN_1028	13E07		conserved protein of unknown function	unknown function
FTN_1038	22H01		conserved hypothetical membrane protein	unknown function
FTN_1091	12A01	aroA	3-phosphoshikimate 1-carboxyvinyltransferase	amino acid metabolism - biosynthesis
FTN_1371	28H07		conserved hypothetical membrane protein	unknown function
FTN_1420	26F05	wzx	O antigen flippase	LPS/cell wall/capsule
FTN_1422	6D05	wbtN	glycosyl transferase, gp1	LPS/cell wall/capsule
FTN_1425	6E08	wbtF	NAD dependent epimerase	LPS/cell wall/capsule
FTN_1429	21B01	wbtP	glactosyl transferase	LPS/cell wall/capsule
FTN_1518	6B02	relA	GDP pyrophosphokinase/GTP pyrophosphokinase	other metabolsim - biosynthesis
FTN_1554	18C04		novel hypothetical membrane protein	unknown function
FTN_1597	29F06	prfC	peptide chain release factor	translation, ribosomal structure and biogenesis
FTN_1741	28H08		novel protein of unknown function	unknown function

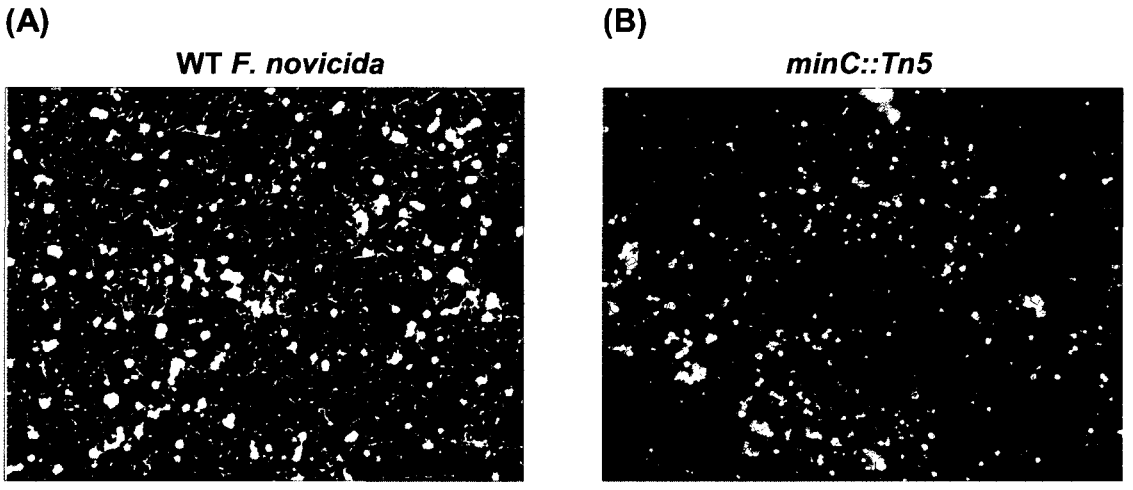

Figure 33 - A transposon-insertion mutant in septum formation gene, *minC*, produces less stalk during static growth.

Stalk formation of a transposon-insertion mutant in the *minC* gene which contributes to bacterial cell division is displayed. This mutant strain was representative of transposon-insertion mutants identified in the stalk screen for decreased stalk biogenesis after 7 d static growth in TSBc at 37° C.

5.4 DISCUSSION

Here we report the initial characterization of a novel polar *F. novicida* structure. We predicted that changes in bacterial morphology may enable increased initial association with a surface. We discovered this appendage that closely resembles the *C. crescentus* stalk in structure when we visualized *F. novicida* grown under conditions that promote biofilm formation. While the

role of *C. crescentus* cytoskeletal proteins in stalk formation (3, 46, 203) and the proteomic contents of this structure (93) have been defined, the mechanism of cell envelope rearrangement to yield this structure remains unknown. For *F. novicida,* stalk morphogenesis appears to begin by a protrusion of the inner membrane and cytoplasmic contents into the outer membrane (Figures 26D, 27-29). By SEM we observed coccobacilli with a nascent stalk formed within the confines of the outer membrane. The mature *F. novicida* stalk has polar localization is approximately 100-200 nm wide by up to several microns in length.

The virulent Type A SchuS4 strain formed the same structure when grown statically (Figure 30). All known prosthecated bacteria live solely in aquatic environments and require the stalk to mediate a complex lifecycle begun by stalk-driven adherence of de-flagellated bacteria (9, 94). Conservation of this structure in virulent *F. tularensis* breaks the existing dogma for prosthecated bacteria and suggests exciting possibilities for the role of this structure in the fitness of this zoonotic pathogen.

While the precise function of this structure currently eludes us, we observed this *Francisella* stalk concurrent with biofilm formation on abiotic surfaces and during infection of host cells including macrophages, the main replicative niche for *F. tularensis* during mammalian infection (32). We hypothesize that the *Francisella* stalk may facilitate interaction with these surfaces. Given the metabolic toll of producing such a structure, this appendage must fulfill some function even if this hypothesis proves incorrect.

Bacteria are known to produce diverse morphologies from the common cocci and bacilli to the more exotic spirochetes and prosthecates (stalked). In most instances, particularly with irregular bacterial shape, structure indicates functions. For instance, spiral-shaped *Helicobacter pylori* utilizes this structure to corkscrew through the mucus that lines the stomach lining (78).

Beyond facilitating attachment, the *Francisella* stalk may also function in nutrient acquisition. Localizing nutrient uptake machinery to this structure may enhance survival during biofilm formation in oligotrophic environments. Ireland *et al.* found an enrichment for nutrient uptake systems in the outer membrane of the *C. crescentus* stalk (93). In Chapter 4, we found that 26 nutrient transport systems are highly expressed in growth conditions we identified to promote both biofilm and stalk formation. We speculate that these transport systems may localize to the *Francisella* stalk and that the increased surface area to volume ratio of this structure increases nutrient uptake. Ireland *et al.* discovered that the proteins localized to the participate mainly in nutrient uptake (93). We attempted to biochemically purify stalk outer membrane proteins with limited success. We had difficulty separating the stalk from the cell body by density gradient centrifugation.

We also provide anecdotal evidence that the *F. tularensis* stalk may participate in biofilm formation. Stalked-bacteria are observed subsequent to surface attachment and presence of these structures occurs earlier in statically grown cultures. *C. crescentus* forms biofilms with a similar matt-structure (57) as we observed for *F. novicida* on both chitin (Figure 2) and glass (Figure 7).

C. crescentus biofilms are enhanced by a stalk structure known as the holdfast (57). The holdfast forms with a polar localization on the tip of the *C. crescentus* stalk and mediates adherence during asymmetric cell division (131). Flagellated daughter cells swim away after cell division, while stalked cells remain attached and form biofilms. Biofilms form predominately at the air-liquid interface and the *C. crescentus* stalk may promote maintenance of surface attached bacteria in this microenvironment due to its increased buoyancy compared to the cell body (165).

Shedding of the *F. tularensis* stalk from the cell body after 3-5 d is atypical of α-Proteobacteria stalks. In *C. crescentus,* while a deletion mutant in the phosphate transport gene, *pstS*, confers stalk shedding (93), extrusion of the stalk from the cell body is not observed in wild-type bacteria. The role of these free stalks is not evident. *F. tularensis* strains are known to enter an avirulent viable-but-non-culturable (VBNC) phase (61). The morphology of this form of *F. tularensis* was not investigated. Shedded stalks may, therefore, serve as a spore-like form of *F. tularensis* that promotes survival in conditions not conducive for growth. We attempted to detect DNA within the shedded stalk body, but did not have sufficient resolution to visualize nucleic acids in either the cell body or stalk. Several bacterial species utilize a VNBC form to persist in the environment (107, 119, 159), but none utilize stalk structure to mediate survival.

The *Francisella* stalk may also facilitate interaction within and survival within host cells. As stalk structures have not been previously described on a

pathogenic bacterium, the further discovery that *F. novicida* forms these structures inside of macrophages (Figure 32) was unexpected. Looking back at the *F. tularensis* literature, Marcus Horwitz's lab observed stalked bacteria when investigating macrophage uptake of *F. tularensis* (33). This observation was dimissed as an artifact of EM processing, however. One predicted role for the *C. crescentus* stalk is localizing protein secretion machinery. The *F. tularensis* FPI is a putative Type-VI secretion system that is required for intracellular replication (144). Could this system be localized to the stalk inside of cells? Stalked *F. novicida* were visualized inside the cytoplasms of macrophages at 6 h post-infection (Figure 33) making this hypothesis feasible. Immunofluorescent detection of FPI structural components during infection could address this possibility. Interestingly, stalks on intracellular bacteria were only stained with the cytoplasmic staining step and not the whole cell stain. Destruction of key epitopes on the *Francisella* stalk by fixation may explain this finding and why the stalk has not been previously identified.

One method of identifying a function for the *Francisella* stalk is to find mutants that do not produce these appendages and then ask if these strains have a phenotype in biofilm or infection assays. Using immunofluorescence imaging we visually screened the Two Allele library for stalk abnormalities. No mutants produced zero stalks. The library represents only non-essential *F. novicida* genes. Therefore, mutants in genes involved in cell wall manipulation would not be present. In Chapter 4, we found that *F. novicida* grown in the CDM ST condition expressed cell wall recycling and biosynthesis genes, such

as *ampD* and *ampG*, to high levels. With the slow growth rate in this condition, it is unlikely that increased cell wall machinery is acting in cell division. Alternatively, these gene products may function in redirecting the cell envelope to form the *Francisella* stalk.

While no stalk-less mutants were found, interruption of 27 genes conferred decreased stalk formation compared to wild-type *F. novicida* (Table 6). This list of genes included 8 cell envelope biosynthesis genes, 7 hypothetical genes, 6 metabolism genes, and 5 genes with other functions. Included in this list is the *ostA2* LPS modification gene, identified in Chapter 3 for its role in attachment to chitin and polystyrene. While these genes are not required for stalk formation, their products may aid in cell envelope rearrangement or provide cues for stalk initiation. We are in the process of confirming the role these genes may play in stalk biogenesis.

Chapter 6: Discussion

The overarching aim of this thesis was to investigate the lifestyle of the highly virulent pathogen, *F.* tularensis, outside of its wide host range. *F. tularensis* is studied for its extremely low infectious dose and the severity of its disease manifestations. As few as 10 organisms can cause lethal disease if inhaled (55). As a result, the CDC classified this pathogen as a Class A bioterrorism agent (44). Since this classification, the number of *F. tularensis* peer-reviewed publications has nearly doubled over the past eight years to almost 2,000 articles (PubMed). This research has focused on a better understanding of *F. tularensis* intracellular replication and the mechanisms of immune clearance with the goal of therapeutic and vaccine development. While many aspects of the intracellular lifecycle of this pathogen have been elucidated in recent years, very little is known about how *F. tularensis* survives outside of mammals to enable disease transmission.

The mechanisms of non-host persistence remain an open question in the *F. tularensis* literature. The high morbidity and mortality of tularemia infections renders *F. tularensis* almost too successful of a pathogen. Mammalian organisms either resolve or succumb to *F. tularensis* infection (146, 153), preventing long term persistence or animal-to-animal transmission. Therefore, an animal reservoir for disease transmission is unknown (146). This may explain why a large number of reported tularemia cases are linked to environmental reservoirs. As such, this organism may persist mainly in the

environment and only intermittently associate with mammals, making the environmental lifestyle of *F. tularensis* an essential step in the emergence of tularemia in Eurasia and parts of North America where disease is now endemic.

The lack of tropism of *F. tularensis* makes this pathogen intriguing from an ecology standpoint, as well. While most pathogens survive in a limited number of environments and hosts, *F. tularensis* inhabits ones of the widest environmental ranges of any studied pathogen (177). For instance, unlike the bacterial pathogen *Y. pestis,* which is transmitted by a single vector type (65), *F. tularensis* is carried by numerous arthropod vectors including several tick species, biting flies, and mosquitoes (138, 146, 164). Additionally, this zoonotic pathogen has been isolated from fresh water, environmental amoeba, and hundreds of mammalian species (5, 146, 153, 154, 177). The disease state in arthropod vectors is unknown, but these organisms are one potential reservoir (164). Environmental amoebae represent an alternative site for *F. tularensis* persistence and replication in nature. Abd *et al.* demonstrated that LVS can infect *Acanthamoeba castellanii* (1). In collaboration with Sahar El-Etr and Amy Rasley at Lawrence Livermore National Laboratory, we recently identified amoeba cysts as a potential long term site of Type A *F. tularensis* persistence (53). Colonization of such diverse environments requires either multiple sets of niche-specific genes or more likely a single set of genes that enables association with multiple environments.

We identify *F. tularensis* biofilm formation on chitin as the first potential non-host niche for this zoonotic pathogen in nature. Our characterization of the *F. tularensis* response to environmental stresses may explain how this pathogen persists in the absence of a host preceding uptake by arthropods and amoeba and subsequent spread to mammals. We hypothesized that the oligotrophic environments *F. tularensis* encounters in nature promote biofilm formation and that production of these communities enables survival by utilizing nutritive surfaces such as chitin for growth. Biofilms play an integral role in bacterial survival in nature (216), disease transmission (95), and infection (6). Slow growing, attached populations resist environmental stresses and permit colonization of environmentally and medically relevant surfaces.

For non-motile bacteria, the first step in environmental persistence likely is association with a nutritive source. Many Gram-negative bacteria utilize filamented proteins, such as pili, to mediate surface colonization. These structures allow attachment to everything from abiotic environmental surfaces to epithelial cells lining mammalian tissues (57, 71, 101, 104, 147, 190). Surprisingly, despite encoding for Type-IV pili, *F. tularensis* has evolved different proteins for surface association. The broad range of permissive environments *F. tularensis* inhabits indicates that this pathogen potentially uses conserved mechanisms to colonize diverse surfaces. The Sec-secreted adherence factors we identified in Chapter 3 which promote attachment to multiple non-mammalian surfaces support this hypothesis. Further, Sec-

secreted FTN_0100 and FTN_0714 gene products were highly expressed in the static, minimal medium conditions that promoted rapid surface colonization. This result indicated that microaerophilic and oligotrophic growth promotes the production of factors that enable association with surfaces such as chitin. Similarly, biofilm formation was 13-fold higher for the carbon-limiting condition in the chitin colonization experiments performed in Chapter 2. These data indicate that nutrient and oxygen stresses upregulate production of *F. tularensis* adhesins which promote surface colonization and biofilm formation. Given the aquatic environments where *F. tularensis* likely survives outside of a host, this regulation furthers our assertion that this pathogen has evolved to colonize environmental surfaces.

Environmental regulation of *F. tularensis* biofilms is consistent with control of biofilm genes in other well-characterized biofilm-forming bacteria. For instance, curli proteins that facilitate initial surface association during biofilm formation by several organisms are triggered by low temperature, microaerophilic conditions, low nitrogen and phosphate, and slow and starved growth (68, 127, 149). Consistent with the curli literature, we demonstrate that static growth and nutrient limitation function as two signals for *F. tularensis* attachment and biofilm formation. We screened the *F. novicida* Two Allele library specifically looking for attachment genes. Bacteria were grown in rich media to minimize growth differences between strains. We, therefore, limited our ability to identify the regulatory machinery that mediates *F. novicida* biofilm formation in response to nutrient limitation. Therefore, regulatory pathways we

identified most likely sense microaerophilic growth. Static growth promotes biofilm formation in *S. typhimurium* and is sensed by the MerR-family regulator *agfD* (69). FevR is a MerR-family regulator in *F. tularensis* species. While this MglA pathway regulator is characterized for its role in virulence regulation (20), we identify in Chapter 4 a role for FevR, and all other known proteins in this signaling pathway, in biofilm regulation, as well. Additionally, *fevR* was highly expressed in the CDM ST condition that enhanced biofilm formation, inferring a possible positive feedback loop. Six genes regulated by MglA/FevR in batch culture also mediated biofilm formation. While this list did not include the Sec-secreted adhesion factors we characterize in Chapter 3, the MglA-regulon during static growth has not been characterized. We also found that both *relA* and *spoT* stringent response pathway genes were highly expressed during static growth, suggesting a role for these genes in biofilm regulation. Additionally, RelA was required for wild-type stalk production in Chapter 5. Charity *et al.* have submitted that stringent response activation is required for MglA/FevR function (personal communication). Little else is known about connections within the stress response regulatory network for *F. tularensis.* Biofilm formation by this organism may provide a model system to dissect the interplay between known components and identify novel players. We plan to determine the potential role of the MglA pathway and other regulatory machinery (*e.g.,* stringent response, PmrA, and QseC) in regulating biofilm mediators (*e.g.,* FTN_0714) and use this information to define interactions between these levels of regulation.

F. tularensis must be able to scavenge metabolites from surfaces after attachment. While almost any surface that bacteria come in contact with can be a substrate for biofilm formation (73), the specific requirement of chitinases for *F. novicida* biofilm formation on chitin suggests that this surface represents an actual niche for this pathogen in nature. Unlike motile *V. cholerae* that can chemotax towards nutrients, *F. tularensis* species are non-flagellated and non-motile under laboratory conditions (39). Therefore, the ability of *Francisella* species to adhere to and colonize chitin may represent a single mechanism for survival in nutrient poor non-host environments. Growth on chitin may trigger a specific biofilm program of genes that promote the retention of scavenged GlcNAc in the local microenvironment for use by *F. tularensis*. We plan to address this hypothesis directly by determining the global expression profile of *F. novicida* attached to chitin and look for overlap with the biofilm determinants we describe in Chapter 3.

The highly expressed nutrient transporters expressed in biofilm promoting conditions may provide the mechanism for the chitin survival strategy. This possibility is consistent with the aquatic persistence for *C. crescentus*. Ireland *et al.* found that numerous nutrient uptake systems localized to the *C. crescentus* stalk (93). This aquatic organism forms stalk in response to nutrient limitation as well; in this case phosphate deprivation (76). Wagner *et al.* demonstrated that inorganic phosphate is imported through a stalk-localized high-affinity phosphate-binding protein (204). *F. tularensis* stalk production during biofilm formation may also facilitate nutrient uptake.

Because general nutrient limitation and static growth promote both *F. tularensis* stalk biogenesis and nutrient transporter expression, this structure may facilitate uptake of amino acids, sugars, and inorganic nutrients. Stalks were difficult to detect during biofilm formation on chitin due to the presence of other extracellular biofilm components (*e.g.,* EPS). In sparser areas, stalked *F. novicida* are observed. Therefore, the stalk may specifically promote GlcNAc uptake allowing hydrolyzed chitin to be utilized for growth, as described in Chapter 2.

The *F. tularensis* stalk may also strengthen attachment and enhance biofilm formation, providing a more intimate association with chitin. Attachment via the stalk is an important step in *C. crescentus* biofilm formation (57). *C. crescentus* stalk-mediated attachment occurs via carbohydrate region at the tip, termed the holdfast (131, 202). While the *F. tularensis* does not encode for homologs of holdfast biosynthetic machinery, we do observe numerous stalked cells associated with surfaces. The Thanassi Lab at Albany Medical College recently also identified the *F. tularensis* stalk and found that the FTN_0714 gene product makes up 17% of the stalk outer membrane protein (personal communication). We establish in Chapter 3 that this protein plays a crucial role in attachment to polystyrene and chitin, and confers the ability to colonize fruit flies to wild-type levels. Initial attachment may, therefore, occur via the FTN_0714 protein spread throughout the bacterial cell body. Subsequent strengthened surface association may occur via localization of the FTN_0714 adhesion to the *F. tularensis* stalk. This model is

further supported by the high expression of FTN_0714 in conditions that promote both biofilm formation and stalk production. We plan to generate a monoclonal antibody to this putative adhesin to establish its localization on the cell body during biofilm formation.

Rearrangement of the cell wall to form stalks may also augment surface association and biofilm formation. We previously identified cell wall alteration genes, including *ampD* and *ampG*, as *F. novicida* biofilm factors, as well (unpublished data). We did not pursue this first screen attempt further due to technical issues in confirming biofilm mutant identity. We did however confirm the mutant phenotype of *ampD* and *ampG*, suggesting that biofilm formation involves cell wall rearrangement. However, clean deletion strains exhibited a significant growth defect during static growth, confounding this result. These genes were also in the highly expressed CDM ST cluster (Table 6). Cell wall rearrangement is known to influence biofilm formation by *Staphylococcus epidermidis* (89), another non-motile bacterium, by directly promoting attachment. For *F. tularensis*, however, we hypothesize that cell wall alteration promotes biofilm formation by generating the stalks described in Chapter 5. Divakaruni *et al.* found this to be the case for *C. crescentus.* Cell shape proteins MreB and FtsZ localized cell wall machinery which mediated stalk elongation (46). *F. tularensis* lacks a *mreB* homolog and *ftsZ* was not represented in the Two Allele library we screened for stalk mutants. While no stalkless mutants existed, the *minC* septation gene and the *ostA2* LPS

modification gene that was required for biofilm formation were among the decreased stalk forming mutants.

In the environment, the stalk may also deliver the chitinase enzymes required to liberate GlcNAc, as well. A third putative *C. crescentus* stalk function is localizing protein secretion machinery. Type-III secretion system machinery localizes to the *C. crescentus* stalk body (93). While *F. novicida* does not encode for this type of secretion system, it does produce a Type-II and a putative Type-VI secretion system. Hager *et al.* showed that the Type-II system secretes proteins important for both survival in nature (chitinases) and inside a mammalian host (PepO) (82).

Combining our data with the published literature, we propose a model where *F. tularensis* persists in nature on chitin surfaces (Figure 34). In this model, *F. tularensis* attaches to chitinous surfaces via adhesins expressed during static, nutrient limited growth. The MglA signaling pathway and PmrA and QseC two component proteins transmit environment cues and regulate biofilm genes. The MglA complex may respond to ppGpp secondary messenger signals, as evidenced by the work of the Dove lab. Integration of this signaling network mediates *F. tularensis* biofilm formation. Formation of biofilm communities allows for the delivery of bacterial chitinase enzymes that hydrolyze chitin into usable breakdown products such as GlcNAc and acetate. The biofilm matrix enables retention of these metabolites for use by the biofilm population. During biofilm maturation, stalk production may enhance surface attachment, increase chitinase secretion and promote uptake of released

GlcNAc, further promoting *F. tularensis* persistence in nature. Survival on environmental chitin surfaces, including copepods, zooplankton, and arthropod vectors, may directly seed typhoidal and inhalational cases of tularemia through ingestion and water aerosolization, respectively.

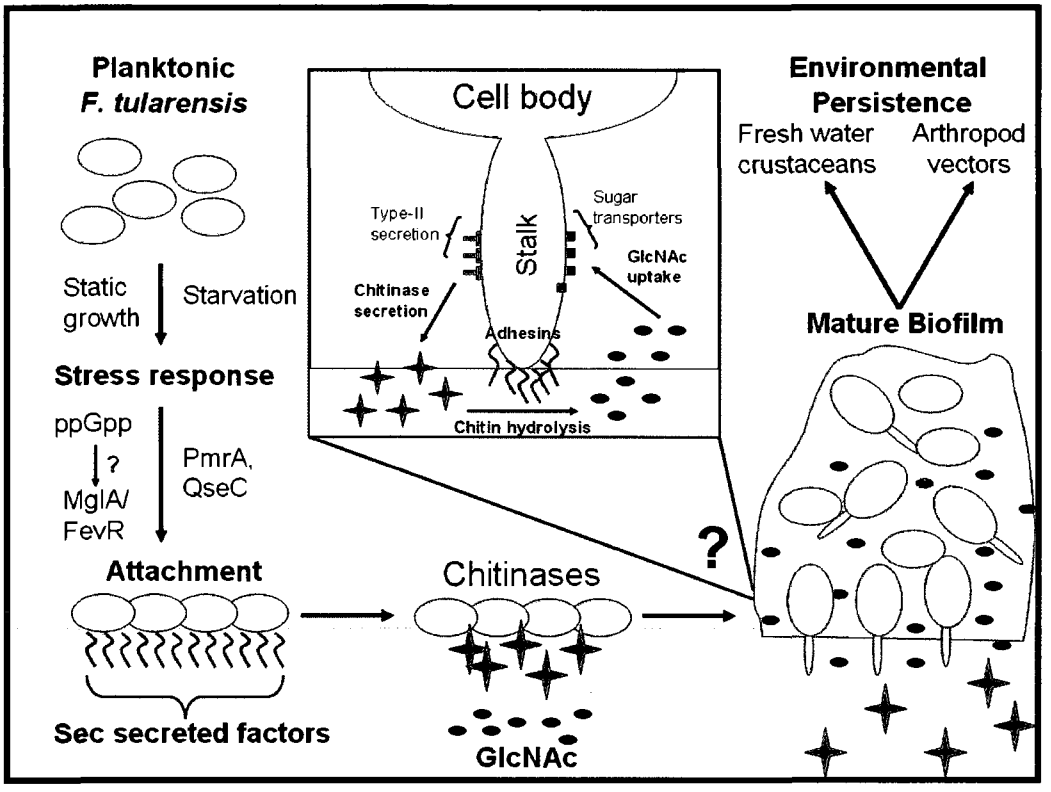

Figure 34 – Model for *F. tularensis* chitin utilization.

Based on our collective data we propose the model diagrammed above for *F. tularensis* persistence on chitin in nature. Static growth in nutrient-limiting conditions triggers a switch from planktonic to sessile growth. The stringent response, the MglA signaling pathway, and the PmrA/QseC two component system respond to these signals. Adherence factors are upregulated by these stress response pathways and mediate attachment to chitin surfaces. Chitinase enzymes are secreted subsequent to attachment and hydrolyze chitin to GlcNAc. This carbon source is retained in the maturing biofilm for catabolic use enabling environmental persistence. Based on stalk function in other organisms, stalk presence in maturing biofilms may 1) enhance surface attachment through increased adhesin interaction with chitin, 2) deliver increased amounts of chitin to further liberate GlcNAc, and 3) localize sugar transporters that import GlcNAc to maximize intracellular carbon availability. This chitin utilization mechanism may permit maintenance in the environment on both arthropods and fresh water crustaceans.

Our discovery that *F. novicida* can endure nutrient limitation by forming biofilms on chitin surfaces provides insight into how this organism can survive outside of a host before being taken up by a vector or amoeba. *F. tularensis* biofilms, therefore, may play a critical step in the ecology of this zoonotic pathogen and provide insight into transmission mechanisms to mammals and other reservoirs for disease. The closely related *Legionella pneumophila* forms biofilms that are grazed on by environmental amoeba (141). This interaction is thought to be critical in the spread of Legionnaire's Disease (109). It will be interesting to test if amoeba can feed on chitin-grown *F. tularensis* biofilms. Through personal communication with Tamara McNealy at Clemson University, we also know that mosquito larvae can feed on LVS biofilms and carry viable bacteria for several days. To date, it is unclear if the larvae survive to adulthood and support *F. tularensis* persistence long enough for disease transmission.

Beyond scavenging carbon in the environment, the secreted chitinases that are vital for biofilm formation on chitin could be important for the establishment of the arthropod infection, similar to the malaria parasite *Plasmodium falciparum*. The *P. falciparum* chitinase allows the parasite to penetrate the chitin-containing peritrophic matrix surrounding the blood meal in the mosquito midgut and establish the infection (200). Efforts to target this chitinase to block transmission of malaria are ongoing (174, 184). Both *F. novicida* chitinase enzymes and chitin-binding protein, *cbpA*, were identified by Madeleine Moule in David Schneider's lab as attenuated for systemic

Drosophila melanogaster colonization (personal communication). We are currently working to discern the role(s) of *F. tularensis* chitinases (and Sec-secreted biofilm determinants) in arthropod vectors in collaboration with the McNeally Lab at Clemson University (mosquito larvae) and Sara Reese and Claudia Schneekloth at the CDC (deer ticks).

Environmental biofilm formation by *F. tularensis* may also provide the bacterium resistance to grazing by fresh water protozoa. For chitin-colonizer *V. cholerae*, biofilm formation was shown to reduce grazing by flagellate organisms compared to planktonic bacteria (126). Thelaus *et al.* found that *F. tularensis* subsp. *holarctica* had increased resistance to both ciliate and flagellate protozoa compared to *E. coli* (187). Although the role of biofilm formation on predation was not addressed, this observation suggests that *F. tularensis* may actively prevent protozoal grazing in nature. Coupled with the ability to survive in nutrient-limited aquatic environments, biofilm-mediated resistance to predation could contribute to *F. tularensis* persistence in the environment and allow for prolonged transmission of this pathogen.

Our findings may help explain how tularemia outbreaks that have been attributed to fresh water crustaceans occur (4, 45). Additionally, chitin utilization may support *F. tularensis* persistence on other arthropods such as zooplankton, copepods, and biting arthropod vectors. A study of *F. tularensis* survival in artificial water found that the presence of chitinous fresh water shrimps, mullosks, diatoms, or zooplankton promoted sustained viability of this pathogen for an additional week to one month in nutrient-poor water (135).

Survival on environmental chitin may, therefore, serve as a reservoir for disease transmission during seasonal tularemia outbreaks. Palo *et al.* identified a strong epidemiological correlation between areas with low water turnover and human cases of tularemia (156). These researchers postulated low water turnover as an environmental cue for a burst of *F. tularensis* replication. Such conditions produce the microaerophilic, nutrient-limited environment that we demonstrate to promote strong biofilm formation. As with cholera outbreaks (58), conditions that promote interaction of *F. tularensis* with chitin surfaces on which the bacteria can replicate may seed infection. Further study of *F. tularensis* biofilm formation and the role of these communities in chitin colonization could clarify the open question of the location of the *F. tularensis* environmental reservoir.

We provide here the first extensive characterization of *F. tularensis* biofilm formation and explore the environmental implications of these communities on environmental persistence and transmission; particularly on chitin surfaces. We found that carbon and other nutrient limitation, coupled with static growth, promotes biofilm formation on multiple surfaces. The *F. novicida* biofilm genes we describe contribute to the ability of this pathogen to colonize a surface it encounters in nature. Chitin interaction may be facilitated by the *F. tularensis* stalk and this structure may promote chitinase secretion and nutrient uptake. Given the potential multiple roles for the novel *F. tularensis* stalk in varying contexts, this appendage may be a unique example of bacterial evolution. Our work provides important first steps to addressing

how and where *F. tularensis* persists in nature, issues that have been largely ignored in the literature. Our findings may focus future efforts to explore the ecology and transmission of this virulent pathogen.

CHAPTER 7: MATERIALS AND METHODS

7.1 Bacterial strains and culture conditions.

Francisella novicida strain U112 and *F. tularensis* subsp. *holarctica* live vaccine strain (LVS), (49, 152) as well as the *F. novicida mglA* point mutant strain (GB2) (12, 21, 110), *F. novicida Francisella* Pathogenecity Island (FPI) and *hspX* deletion mutants (208), have been previously described. *F. tularensis* subsp. *tularensis* strains, SchuS4 and AS2058 (FT.10), were provided by Jean Celli and the New Mexico Department of Health, respectively, and handled under biosafety level-3 (BSL-3) precautions per Centers for Disease Control and Prevention protocol. The *ΔfevR, ΔcphA,* and *ΔcaiC F. novicida* deletion mutants were made by Anna Brotcke (20). Unless otherwise noted, strains were grown in modified Mueller Hinton media (MMH), (Difco, Corpus Christi, TX) supplemented with 0.025% ferric pyrophosphate, 0.02% IsoVitaleX (Becton Dickinson, Franklin Lakes, NJ) as a cysteine source, and 0.1% glucose as a carbon source. For some experiments, *F. tularensis* strains were grown in Chamberlain's Defined Medium (CDM) (124) with or without glucose. For enumeration studies, bacteria were grown on MMH agar plates. *Vibrio cholerae* strain El Tor and the *ΔmshA* isogenic mutant strain were kind gifts of Melanie Blokesch and Gary Schoolnik (129). Strains were grown in Lauria-Bertani (LB) broth or Defined Artifical Salt Water medium (129). *V. cholerae* was plated on LB agar plates for enumeration.

7.2 Imaging *F. novicida* colonization on chitin films and sterile crab shell pieces.

Wild-type *F. novicida* was allowed to attach to either synthetic chitin films (217) or sterile crab shell pieces for 1 h. After 1 h, surfaces were washed 3X with phosphate buffered saline to remove non-adhered bacteria and samples were incubated at 30°C in CDM without glucose. After one hour and one week of incubation, respectively, crab shell and chitin film samples were processed for scanning electron microscopy (SEM) investigation. Substrates with attached cells were fixed for 3 days at 4°C in 4% paraformaldehyde with 2% glutaraldehyde in 0.1M NaCacodylate Buffer (pH 6.3) (EM grade, EMS, Hatfield, PA). After primary fixation, samples were rinsed in the same buffer, post-fixed in 1% aqueous OsO_4 for 1 h, and dehydrated in an ascending ethanol series (30, 50, 70, 80, 90, 100%; for 20min each), followed by critical point drying with liquid CO_2 using a Tousimis SAMDRI-VT-3B apparatus (Tousimis, Rockville, MD). Samples were mounted on adhesive carbon film on 15mm aluminum stubs, and sputter-coated with 100Å gold/palladium using a Denton Desk 11 TSC Sputter Coater. Visualization was carried out with a Hitachi S-3400N VP SEM (Hitachi Ltd, Pleasanton, CA) operated at 10-15kV, working distance 8-10mm, and secondary electron detector. Images were capture in TIF format.

7.3 Growth in CDM broth.

F. novicida was grown overnight in CDM at 37° with aeration. The culture was then diluted to Optical density 600_{nm} (OD_{600}) using an Ultropec 2100 Pro spectrophotomer (Amersham Biosciences, Pittsburgh, PA) 0.05 in either CDM with no sugar, CDM with 10mM glucose or 10mM GlcNAc. Optical density and colony forming units (CFU) were monitored over time for each media condition. The doubling time for each culture was calculated.

7.4 Imaging of flow cell grown biofilms.

Flow cells were assembled as previously described (31, 190). The flow system apparatus was sterilized and pre-conditioned with MMH plus 5µg/mL tetracycline (Tet^5) overnight at ambient temperature (20-22°C). *F. novicida* harboring the pKK219-GFP plasmid (74, 105) was grown overnight at 26° C in MMH Tet^5 with aeration. Overnight-grown bacteria were diluted 1:50 in fresh media and grown to optical density 600 (OD_{600}) 1.0. The culture was then diluted to OD_{600} 0.1. Flow was stopped on the flow system and 1ml of culture was inoculated into each channel of the flow cell. Flow cells were inverted for 1 h to allow the bacteria to adhere. Flow cells were then uprighted and flow was initiated at 0.1 ml/minute. Biofilm progression at ambient temperature was imaged by confocal microscopy (Bio-Rad, Hercules, CA) every 24h over the course of 5 days. Z-sections were taken with 0.1 µm steps and 3-D renderings of the z-stacks were generated using Volocity imaging software (Improvision, Lexington, MA).

7.5 Crystal violet assaying for biofilm formation.

Crystal violet assaying for biofilm formation was performed as previously described (148). Briefly, *Francisella* strains were grown overnight at the appropriate temperature. Cultures were diluted into fresh media to OD_{600} 0.05 and 200µl aliquoted per well in a 96-well polystyrene plate in at least triplicate. The bacteria were allowed to grow statically and sampled at various time points. The OD_{570} was read in a 96-well microplate reader (BioTek, Winooski, VT). At each time point non-adhered bacteria were removed from the well and 30µl of 0.1% crystal violet was added to each well for 15 minutes. Wells were washed three times with distilled water and the remaining biomass-absorbed crystal violet was solubilized with 95% ethanol. Staining was then quantified at OD_{570} in a 96-well microplate reader (labeled CV_{570}). All OD readings for the assay comparing relative crystal violet staining between lab strains of *Francisella* and Type A *Francisella* were obtained at 600nm (CV_{600}) using a NanoDrop spectrophotometer (Thermo Fisher Scientific, Waltham, MA).

7.6 Transposon library screen for biofilm-deficient mutants.

A sequenced two-allele transposon mutant library was used to test for *F. novicida* transposon mutants that were deficient in biofilm formation (the following reagent was obtained through the NIH Biodefense and Emerging Infections Research Resources Repository, NIAID, NIH: *F. tularensis* subsp. *novicida*, "Two-Allele" Transposon Mutant Library Plates 1-14, 16-32). The

library represents two or more transposon insertions in all non-essential genes. At the time of screening, Plate 15 of the library was unavailable due to quality control issues, resulting in a library size of 2,954 mutants. The two-allele library was received frozen in 96-well format. MMH media was inoculated in 96-well plates with the library and mutants grown overnight to stationary phase at 37°C shaking at 200 rpm. Overnight cultures were diluted 1:50 in 200µl of fresh MMH in 96-well plates. Plates were grown statically for 10h in a 37°C incubator and the ability of each transposon-mutant to form a biofilm was assessed as described above. Mutants exhibiting lower potential for biofilm formation were classified by crystal violet staining more than two standard deviations lower than the plate average. Wild-type *F. novicida* was included on each plate as a positive control and a well of MMH only was used as a blank. To account for small differences in culture growth, crystal violet staining was normalized to each mutant culture at OD_{570}. Wells where significant growth defects were observed were excluded. Biofilm-deficient transposon-mutants were retested in triplicate.

7.7 Secondary screening for attachment.

Overnight cultures of biofilm mutants identified in our screen were grown in triplicate with shaking (200 rpm) at 37°C. Stationary phase cultures (200µl) were transferred to new 96-well plates and allowed to adhere statically for 1 h at 37°C. Crystal violet staining was assayed as before. Attachment-

deficiency was defined as crystal violet staining two standard deviations below that of wild-type.

7.8 Bacterial Mutagenesis.

Targeted deletions were generated in the U112 strain as previously described (20) using the primers in Table A1. Briefly, the regions of the chromosome 5' and 3' to the gene of interest were amplified by PCR. Using splicing by overlap extension (SOE) PCR (121), a kanamycin resistance cassette expressed by the *groEL* promoter was introduced between these regions of homology. Briefly, ~500bp sequences flanking the targeted gene were amplified and spliced to either end of the *gro* promoter-resistance cassette construct. The resulting PCR product was transformed into *F. novicida* strain U112 by chemical transformation and transformants were selected on MMH agar with 30µg/ml kanamycin. Gene deletions were confirmed by sequencing. Δ*secB1,* Δ*FTN_1750,* and *chiA* targeted deletion strains were subsequently complemented in cis by re-introducing the wild-type gene into the chromosome at the original locus, along with the CAT cassette chloramphenicol resistance marker, again by SOE and homologous recombination of a spliced PCR construct. Δ*secB2,* Δ*ostA2*, Δ*FTN_0308,* and *chiB* deletion mutants were complemented in trans by introducing the wild-type gene, as well as the CAT cassette, into *gro-gfp* pFNLTP6 (123). ~500bp regions flanking the *gfp* gene of pFNTLTP were amplified and spliced to the wild-type copy of the gene for complementation with the CAT resistance

cassette on the 3' end. SOE PCR complementation constructs were introduced by homologous recombination with the pFNLTP6 at the NdeI and BamHI sites, removing the *gfp* gene. The resulting plasmid expressed the complementing gene under the regulation of the constitutive *groEL* promoter. Complemented strains were selected for growth on 3µg/ml chloramphenicol and also confirmed by sequencing. Complementation plasmids were then chemically transformed into deletion strains. All complementation primers are listed in Table A1. The Δ*chiA*Δ*chiB* double mutant was constructed using the same method as the single deletion strains, except the *chiB* gene was replaced with the CAT cassette instead of the kanamycin resistance cassette.

7.9 RAW264.7 macrophage infections.

RAW264.7 macrophages were seeded at $2.5x10^5$ cells per well in 24-well tissue culture plates (Becton Dickinson, Franklin Lakes, NJ) and incubated overnight at 37°C incubation with 5% CO_2. Wild-type and mutant U112 strains were grown overnight to stationary phase at 37°C with aeration and diluted to $5x10^6$ colony forming units (CFU) per ml in Dulbecco's Modified Eagle Medium (Gibco, Carlsbad, CA) with 10% fetal bovine serum. For each strain, 1ml inocula were added to triplicate wells and centrifuged at 730 x *g* for 15 min to mediate attachment. Infected plates were incubated at 37°C with 5% CO_2 (time zero) for 0.5h and washed three times with warm media. Three wells per strain were harvested at this time using 0.1% saponin to lyse the cells. CFU were enumerated by serial dilution and percent recovered was calculated by

normalizing to the inocula. Fresh warm media was added to the remaining wells and wells were harvested in triplicate, as above, at 8h and 24h post-infection.

7.10 Mouse infections.

Competitive index (CI) mouse infections were performed as previously described (208) in 6-8 week old female C57BL/6J mice (Jackson Laboratories, Bar Harbor, ME). Mice were infected intradermally or intraperitoneally with equal amounts ($5x10^3$ CFU) of wild type and mutant *F. novicida* in 0.05 ml. Mice were monitored for morbidity and mortality during the course of infection. Mice were sacrificed 2 d post-infection and the spleens were removed and homogenized for CFU enumeration. Competitive indices were calculated as the ratio of mutant to wild type of the output, normalized for the input, and significance was calculated by comparing the CI to 1 (CI of gene with no role in virulence) using one sample *t*-tests. All animal infection experiments were approved by the Institutional Animal Care and Use Committee and the Institutional Biosafety Committee of Stanford University. Deletion mutants for the entire *Francisella* Pathogenecity Island (FPI) and negative control, *hspX* chaperone gene were described previously (208).

7.11 Crab shell attachment.

Overnight cultures were grown at 30°C in MMH medium. Approximately $1cm^2$ pieces of sterile crab shell were inoculated with 2ml of stationary phase

cultures in 12-well plates. After 1 h at 30°C, the shells were washed to remove unattached bacteria. Attached bacteria were recovered by vortexing and enumerated for colony forming units (CFUs). All strains were tested in triplicate. Unpaired t-tests were used to determine statistical differences between wild type and mutant counts.

7.12 *Drosophila melanogaster* infections.

Oregon Red (OR) *Drosophila melanogaster* were maintained on dextrose medium at 25° C and 65% humidity. All experiments were performed on 5-7 day old age-matched male flies with the assistance of Madeleine Moule. Wild-type and mutant *F. novicida* were grown overnight in TSBc at 37° C. $5x10^3$ CFU each of wild-type and mutant bacteria were injected into OR *D. melanogaster* in 50 nl using a glass needle and a Picospritzer III injector system (Parker Hannifin, Cleveland, OH) on the ventrolateral surface of the fly abdomen. Infected flies ($\geq$5 flies/mutant group) were maintained at 29° C for 2 d and then *F. novicida* were recovered for enumeration by homogenization. CI values for each mutant tested were determined as described above.

7.13 Statistical analysis.

Statistical analysis was performed using Prism4 software (GraphPad, La Jolla, CA). Unless otherwise stated, unpaired Student's *t* tests were applied, and two-tailed *P*-values are shown. For mouse CI data, one-sample *t*-test was used to compare mutant:wild-type bacteria ratio to an expected value of 1.

7.14 Microarray analysis of broth grown *F. novicida* expression profiles.

F. novicida was grown overnight in either MH or CDM medium. Cultures were then diluted to OD_{600} 0.01 in the appropriate medium. Aerated cultures were grown in 500 ml total volume, while static cultures were grown in several 50 ml aliquots. Bacteria were grown at 37° C and sampled over time for both CFU and OD enumeration. Approximately $1x10^8$ CFU were harvested at each timepoint for RNA preparation as previously described (188). Bacteria were collected on 0.22 micron filters (Whatman, Kent, ME) and flash frozen in liquid nitrogen and stored at -80° C. RNA from each samples was recovered by Trizol reagent (Invitrogen, Carlsbad, CA) followed by chloroform extraction. RNA preparations were cleaned up and concentrated using the RNeasy Mini kit (Qiagen, Valencia, CA). *F. tularensis* microarrays and hybridization protocol were previously characterized by Anna Brotcke (20, 21). For each microarray, 1 µg of RNA from a single sample was reverse transcribed using 5 µg of random hexamers (Amersham Biosciences, Piscataway, NJ) and Superscript III (Invitrogen, Carlsbad, CA). This reaction incorporated amino allyl dUTP (2.5 mM) into nascent cDNA. We purified cDNA using Zymo DNA purification columns per manufacturer's instructions (Zymo Research Corporation, Orange, CA). Samples were then labeled with Cy5. A pooled reference was also generated by combining equal amounts of each sample. Reference samples were labed with Cy3. Unincorporated dye was quenched using 5 µl 4M hydroxylamine and removed using Zymo DNA purification

columns. 2 µl 20mg/ml yeast tRNA (Invitrogen, Carlsbad, CA), 4.25 µl 20X SSC, and 0.75 10% SDS were added to combined cDNA sample and reference (in 19 µl TE). Probes were boiled at 99° C for 2 min to denature cDNA strands. Probes were then hybridized to the 70-mer oligonucleotide microarray developed by the Monack lab for 14 h at 99° C (21). Two minute stringency washes were performed as described by Eisen *et al.* (51): 1) 2X SSC, 0.3% SDS; 2) 2X SSC; 3) 1X SSC; 4) 0.2X SSC. Microarrays were scanned and analyzed using a GenePix 4000A scanner and GENEPIX5.1 software (Axon Instruments, Redwood City, CA). TIFF files of microarray scan were uploaded to the Stanford Microarray Database (176) and normalized data were retrieved. Problematic spots were excluded based on irregular spot appearance, a regression correlation of <0.6 or a Cy3 net mean intensity <100. Only spots with good data for ≥70% of the microarrays were subjected to further data analysis. Hierarchical clustering of the $\log_2$(red/green) values using Cluster (52) was visualized in Java TreeView (170). Expression profiles of each growth condition were compared using Significance Analysis for Microarrays v.1.21 (197). Two-class and Multiclass analyses were used in this software implementing a false discovery rate of 1%.

7.15 TEM characterization of *F. tularensis* stalk formation.

F. novicida and *F. tularensis* subsp. *tularensis* strain SchuS4 were grown statistically in TSBc for 5-7 d. Pellicle bacteria were recovered by scraping and processed for negative stain or thin section TEM.

Negative staining: Cultures were washed 3X in PBS and 20 µl of 1:5 dilutions were spotted onto carbon coated grids and allowed to adhere for 2 min. Grids were washed 2X with distilled water and stained for 2 min with 1% uranyl acetate. Stained samples were washed 2X with distilled water and dried with filter paper.

Thin sectioning of bacteria and infected eukaryotic cells: Biofilms grown on polystyrene and eukaryotic cells infected as described above were thin sectioning. Cells were fixed with 2% gluteraldehyde in phosphate buffer for 30 min at 4° C. Samples were washed 2X phosphate buffer and stained with 1% OsO_4 for 1 h at room temperature. Excess stain was washed away with distilled water (2X) for 10 min each and samples were incubated overnight in 0.5% uranyl acetate. Samples were then dehydrated with increasing ethanol concentrations (25%, 50%, 75%, 95%, and 100%) for 5 min each. Polybed was used to prepare samples for infiltration and samples were embedded in gelatin capsules at 60° C overnight. Embedded cells were section using a 60nm Leica Microtome (Leica Microsystems, Bannockburn, IL) on 200 mesh grid and stained with uranyl acetate and lead citrate.

7.16 Intracellular localization assay.

Localization of intracellular bacteria was determined by selective membrane permeabilization using a procedure developed by Jean Celli (30). Briefly, infected BMDMs were washed three times with KHM buffer (110 mM potassium acetate, 20 mM HEPES, 2 mM $MgCl_2$, pH 6.3) and the plasma

membrane selectively permeabilized by incubation with 50 µg/ml digitonin (Sigma) in KHM buffer for 1 min at room temperature. Cells were then washed immediately with KHM buffer and rabbit polyclonal anti-calnexin (specific to the cytoplasm-facing C-terminal tail; Stressgen Biotechnologies, Ann Arbor, MI), and Chicken polyclonal anti-*F. tularensis* antibodies (Aves Labs, Tigard, OR) were delivered to the macrophage cytosol for 12 min at 37°C to label the endoplasmic reticulum of permeabilized cells and accessible intracellular bacteria, respectively. BMMs were then washed with PBS, fixed with 3% paraformaldehyde, pH 6.4, at 37°C for 10 min, washed three times with PBS, and then incubated for 10 min in 50 mM NH_4Cl in PBS in order to quench free aldehyde groups. Goat anti-chicken 594 secondary antibodies were used to label cytoplasmic *F. novicida* red. All host cell membranes were then permeabilized in 10% horse serum-0.1% saponin in PBS for 30 min at room temperature. Bound anti-calnexin antibodies were detected using cyanin 5-conjugated donkey anti-rabbit antibodies (Jackson ImmunoResearch Laboratories), and all intracellular bacteria were labeled using the same anti-*F.novicida* antibodies. All intracellular bacteria were then labeled green with goat anti-chicken 488 secondary antibodies. This technique resulted in a differential staining of cytoplasmic bacteria (Alexa Fluor 488/594 dual fluorescence) and those enclosed within an intact phagosome (488 single fluorescence). Infected cells were imaged by CLSM (Bio-Rad, Hercules, CA).

7.17 Screen for *F. novicida* stalk mutants.

The Two Allele *F. novicida* library described above was grown for 7 d statically in TSBc in 96-well plates at 37° C. Cultures were diluted 1:100 in PBS and 18 10-µl were spotted per glass microscope slide and allow to dry for 30 min. Multiple slides were placed in a holder and stained in 400 ml solutions by submersion. Samples were labeled with a chicken anti-*F. novicida* polyclonal antibody and stained with a goat anti-chicken 488 secondary antibody. Stalk formation was determined by epifluorescence microscopy (Zeiss, Thornwood, NY). Stalk-deficient mutants were confirmed in triplicate.

Table 8 – Primers for *F. novicida* cloning and mutagenesis

Primers	Sequence
Cm F	ggttgtcactcatcgtattt
Cm R	ttacgccccgccctgccact
Kan F	atctctttgggttgtcactc
Kan R	tacaaccaattaaccaattctg
pFNLTP6 F1	taatgtgagttagctcactc
pFNLTP6 R1	atggtacctgcacgacgaac
pFNLTP6 F2	ggatccactagctcgtttca
pFNLTP6 R2	tacttcctgttctcaatctc
chiA F	ttgctataactctctcactc
chiA inv1	aaatacgatgagtgacaacctgtaagcacaatgcttacac
chiA inv2	agtggcagggcggggcgtaaactcaaggagatattccttc
chiA R	actctctcatcaagcttatc
chiB F	aagatgctgtaatggaaatgg
chiB inv1	gagtgacaacccaaagagatttctccagttaatatctctag
chiB inv2	cagaattggttaattggttgtaatagatgctgttgactttgg
chiB R	acaggcttaatcacaaatgg
secB1 F	tttacctgctgaaatgagtc
secB1 inv1	gagtgacaacccaaagagattgctgatccatactatgatc
secB1 inv2	cagaattggttaattggttgtaagatagcaagcaacactaag
secB1 R	aacataaccccgatcttc
secB2 F	ttctcaataatgctagtgcc
secB2 inv1	gagtgacaacccaaagagatttggatttcattattttgcatg
secB2 inv2	cagaattggttaattggttgtaaaagaaatcttcgccaaagc
secB2 R	tattcttaagcacttggtgc

ostA2 F	aagcttcaacaattacggtc
ostA2 inv1	gagtgacaacccaaagagataaataatcccaacttcctcg
ostA2 inv2	cagaattggttaattggttgtaaaaccaattagcagcttctg
ostA2 R	attggtaagcaactggattc
FTN_0308 F	tcaagtcatttcccacaatc
FTN_0308 inv1	gcttatcgataccgtcgacctcactctacgaaacctatatac
FTN_0308 inv2	gatatcgatcctgcagctatgcttcagccatatcttaatatgg
FTN_0308 R	attacctgtcatagcatcag
FTN_0714 F	tatatatccttgtttccggc
FTN_0714 inv1	gagtgacaacccaaagagatatcctcataatactccgtac
FTN_0714 inv2	cagaattggttaattggttgtaaataacggtaaggacatacg
FTN_0714 R	tgatatatgaacacgttgcc
FTN_1750 F	tttcattcgcataacaggtc
FTN_1750 inv1	gagtgacaacccaaagagatatctgtttacctcttttaacc
FTN_1750 inv2	cagaattggttaattggttgtaaaaccaaatctttcggtggc
FTN_1750 R	agaagctgttcatcatcatg
chiAcomp chrom F	ttgctataactctctcactc
chiAcomp chrom inv1	gagtgacaacccaaagagatttattgtttttcccaaacattac
chiAcomp chrom inv2	cagaattggttaattggttgtataaagtcttatatataatctaattc
chiAcomp chrom R	actctctcatcaagcttatc
chiBcomp pFNLTP6 F	gttcgtcgtgcaggtaccatatgaaatacaaaaagttattattaa
chiBcomp pFNLTP6 R	aaatacgatgagtgacaaccttatttatcatttataggataaaac
secB1comp chrom F	tttacctgctgaaatgagtc
secB1comp chrom inv1	aaatacgatgagtgacaaccttagtgttgcttgctatctg
secB1comp chrom inv2	agtggcagggcggggcgtaagaaactaataggagtcagtt
secB1comp chrom R	aacataaccccgatcttc
secB2comp pFNLTP6 F	gagtattagttcgtcgtgcaggtaccatatgcaaaataatgaaatccaacc
secB2comp pFNLTP6 R	aaatacgatgagtgacaaccttaatgctcacgctttggcg
ostA2comp pFNLTP6 F	gttcgtcgtgcaggtaccatatgttgaaattaaattatcagaa
ostA2comp pFNLTP6 R	aaatacgatgagtgacaaccttaattctgcccccattgac
FTN_0308comp pFNLTP6 F	gttcgtcgtgcaggtaccatatggtagcaaaaaatagagga
FTN_0308comp pFNLTP6 R	aaatacgatgagtgacaaccctaatactcaaaacctttataaa
FTN_1750comp chrom F	tttcattcgcataacaggtc
FTN_1750comp chrom inv1	aaatacgatgagtgacaaccttagccaccgaaagatttgg
FTN_1750comp chrom inv2	agtggcagggcggggcgtaaatttcttatttgatacaaaattc
FTN_1750comp chrom R	agaagctgttcatcatcatg

REFERENCES

1. **Abd, H., T. Johansson, I. Golovliov, G. Sandstrom, and M. Forsman.** 2003. Survival and growth of Francisella tularensis in Acanthamoeba castellanii. Appl Environ Microbiol **69:**600-6.
2. **Adams, J. L., and R. J. C. McLean.** 1999. Impact of rpoS Deletion on Escherichia coli Biofilms. Appl. Environ. Microbiol. **65:**4285-4287.
3. **Alyahya, S. A., R. Alexander, T. Costa, A. O. Henriques, T. Emonet, and C. Jacobs-Wagner.** 2009. RodZ, a component of the bacterial core morphogenic apparatus. Proc Natl Acad Sci U S A **106:**1239-44.
4. **Anda P., J. S. d. P., J. M. Díaz García, R. Escudero, F. J. García Peña, M. C. López Velasco, R. E. Sellek, M. R. Jiménez Chillarón, L. P. Sánchez Serrano, and J. F. Martínez Navarro.** 2001. Waterborne Outbreak of Tularemia Associated with Crayfish Fishing. Emerging Infectious Diseases **7:**575-582.
5. **Anders, S.** 2007. Tularemia: History, Epidemiology, Pathogen Physiology, and Clinical Manifestations. Annals of the New York Academy of Sciences **1105:**1-29.
6. **Anderson, G. G., J. J. Palermo, J. D. Schilling, R. Roth, J. Heuser, and S. J. Hultgren.** 2003. Intracellular bacterial biofilm-like pods in urinary tract infections. Science **301:**105-7.
7. **Anthony, L. D., R. D. Burke, and F. E. Nano.** 1991. Growth of Francisella spp. in rodent macrophages. Infect Immun **59:**3291 - 3296.
8. **Aono, R., T. Negishi, and H. Nakajima.** 1994. Cloning of organic solvent tolerance gene ostA that determines n-hexane tolerance level in Escherichia coli. Appl. Environ. Microbiol. **60:**4624-4626.
9. **Ausmees, N., and C. Jacobs-Wagner.** 2003. Spatial and temporal control of differentiation and cell cycle progression in Caulobacter crescentus. Annu Rev Microbiol **57:**225-47.
10. **Balestrino, D., J. M. Ghigo, N. Charbonnel, J. A. Haagensen, and C. Forestier.** 2008. The characterization of functions involved in the establishment and maturation of Klebsiella pneumoniae in vitro biofilm reveals dual roles for surface exopolysaccharides. Environ Microbiol **10:**685-701.
11. **Balzer, G. J., and R. J. McLean.** 2002. The stringent response genes relA and spoT are important for Escherichia coil biofilms under slow-growth conditions. Can J Microbiol **48:**675-80.
12. **Baron, G. S., and F. E. Nano.** 1998. MglA and MglB are required for the intramacrophage growth of Francisella novicida. Mol Microbiol **29:**247-59.
13. **Bartnicki-Garcia, S.** 1968. Cell wall chemistry, morphogenesis, and taxonomy of fungi. Annu Rev Microbiol **22:**87-108.
14. **Bassler, B. L., C. Yu, Y. C. Lee, and S. Roseman.** 1991. Chitin utilization by marine bacteria. Degradation and catabolism of chitin oligosaccharides by Vibrio furnissii. J. Biol. Chem. **266:**24276-24286.
15. **Bendtsen, J. D., H. Nielsen, G. von Heijne, and S. Brunak.** 2004. Improved prediction of signal peptides: SignalP 3.0. J Mol Biol **340:**783-95.

16. **Boddicker, J. D., R. A. Anderson, J. Jagnow, and S. Clegg.** 2006. Signature-Tagged Mutagenesis of Klebsiella pneumoniae To Identify Genes That Influence Biofilm Formation on Extracellular Matrix Material. Infect. Immun. **74:**4590-4597.
17. **Bowden, G. H., and Y. H. Li.** 1997. Nutritional influences on biofilm development. Adv Dent Res **11:**81-99.
18. **Braun, M., and T. J. Silhavy.** 2002. Imp/OstA is required for cell envelope biogenesis in Escherichia coli. Mol Microbiol **45:**1289-302.
19. **Broms, J. E., M. Lavander, and A. Sjostedt.** 2009. A conserved alpha-helix essential for a type VI secretion-like system of Francisella tularensis. J Bacteriol **191:**2431-46.
20. **Brotcke, A., and D. M. Monack.** 2008. Identification of fevR, a novel regulator of virulence gene expression in Francisella novicida. Infect Immun **76:**3473-80.
21. **Brotcke, A., D. S. Weiss, C. C. Kim, P. Chain, S. Malfatti, E. Garcia, and D. M. Monack.** 2006. Identification of MglA-regulated genes reveals novel virulence factors in Francisella tularensis. Infect Immun **74:**6642-55.
22. **Brundage, L., J. P. Hendrick, E. Schiebel, A. J. Driessen, and W. Wickner.** 1990. The purified E. coli integral membrane protein SecY/E is sufficient for reconstitution of SecA-dependent precursor protein translocation. Cell **62:**649-57.
23. **Buchan, B. W., M. K. McLendon, and B. D. Jones.** 2008. Identification of Differentially Regulated Francisella tularensis Genes by Use of a Newly Developed Tn5-Based Transposon Delivery System. Appl. Environ. Microbiol. **74:**2637-2645.
24. **Byrd, M. S., I. Sadovskaya, E. Vinogradov, H. Lu, A. B. Sprinkle, S. H. Richardson, L. Ma, B. Ralston, M. R. Parsek, E. M. Anderson, J. S. Lam, and D. J. Wozniak.** 2009. Genetic and biochemical analyses of the Pseudomonas aeruginosa Psl exopolysaccharide reveal overlapping roles for polysaccharide synthesis enzymes in Psl and LPS production. Mol Microbiol **73:**622-38.
25. **Celebi, S., M. Hacimustafaoglu, and S. Gedikoglu.** 2008. Tularemia in children. Indian Journal of Pediatrics **75:**1129-1132.
26. **Chakraborty, S., M. Monfett, T. M. Maier, J. L. Benach, D. W. Frank, and D. G. Thanassi.** 2008. Type IV pili in Francisella tularensis: roles of pilF and pilT in fiber assembly, host cell adherence, and virulence. Infect Immun **76:**2852-61.
27. **Charity, J. C., M. M. Costante-Hamm, E. L. Balon, D. H. Boyd, E. J. Rubin, and S. L. Dove.** 2007. Twin RNA Polymerase-Associated Proteins Control Virulence Gene Expression in Francisella tularensis. PLoS Pathog **3:**e84.
28. **Chen, Y. E., C. G. Tsokos, E. G. Biondi, B. S. Perchuk, and M. T. Laub.** 2009. Dynamics of two phosphorelays controlling cell cycle progression in Caulobacter crescentus. J Bacteriol.

29. **Chitadze, N., T. Kuchuloria, D. V. Clark, E. Tsertsvadze, M. Chokheli, N. Tsertsvadze, N. Trapaidze, A. Lane, L. Bakanidze, S. Tsanava, M. J. Hepburn, and P. Imnadze.** 2009. Water-Borne Outbreak of Oropharyngeal and Glandular Tularemia in Georgia: Investigation and Follow-up. Infection.
30. **Chong, A., T. D. Wehrly, V. Nair, E. R. Fischer, J. R. Barker, K. E. Klose, and J. Celli.** 2008. The early phagosomal stage of Francisella tularensis determines optimal phagosomal escape and Francisella pathogenicity island protein expression. Infect Immun **76:**5488-99.
31. **Christensen, B. B., C. Sternberg, J. B. Andersen, R. J. Palmer, A. Toftgaard Nielsen, M. Givskov, S. Molin, and J. D. Ron.** 1999. [2] Molecular tools for study of biofilm physiology, p. 20-42, Methods in Enzymology, vol. Volume 310. Academic Press.
32. **Clemens, D. L., and M. A. Horwitz.** 2007. Uptake and intracellular fate of Francisella tularensis in human macrophages. Ann N Y Acad Sci **1105:**160-86.
33. **Clemens, D. L., B. Y. Lee, and M. A. Horwitz.** 2005. Francisella tularensis enters macrophages via a novel process involving pseudopod loops. Infect Immun **73:**5892-902.
34. **Colson, S., G. P. van Wezel, M. Craig, E. E. Noens, H. Nothaft, A. M. Mommaas, F. Titgemeyer, B. Joris, and S. Rigali.** 2008. The chitobiose-binding protein, DasA, acts as a link between chitin utilization and morphogenesis in Streptomyces coelicolor. Microbiology **154:**373-82.
35. **Costerton, J. W.** 2001. Cystic fibrosis pathogenesis and the role of biofilms in persistent infection. Trends in Microbiology **9:**50-52.
36. **Costerton, J. W., K. J. Cheng, G. G. Geesey, T. I. Ladd, J. C. Nickel, M. Dasgupta, and T. J. Marrie.** 1987. Bacterial biofilms in nature and disease. Annu Rev Microbiol **41:**435-64.
37. **Costerton, J. W., P. S. Stewart, and E. P. Greenberg.** 1999. Bacterial Biofilms: A Common Cause of Persistent Infections. Science **284:**1318-1322.
38. **Cotter, P. A., and S. Stibitz.** 2007. c-di-GMP-mediated regulation of virulence and biofilm formation. Curr Opin Microbiol **10:**17-23.
39. **Cowan S.T., G. I. B., Kenneth John Steel, R. K. A. Feltham.** 2004. Cowan and Steel's manual for the identification of medical bacteria, 3rd ed. Cambridge Press.
40. **Darby, C., J. W. Hsu, N. Ghori, and S. Falkow.** 2002. Caenorhabditis elegans: Plague bacteria biofilm blocks food intake. Nature **417:**243-244.
41. **Davey, M. E., and A. O'Toole G.** 2000. Microbial biofilms: from ecology to molecular genetics. Microbiol Mol Biol Rev **64:**847-67.
42. **de Lima Pimenta, A., P. Di Martino, E. Le Bouder, C. Hulen, and M. A. Blight.** 2003. In vitro identification of two adherence factors required for in vivo virulence of Pseudomonas fluorescens. Microbes Infect **5:**1177-87.
43. **Dean, R. E., P. M. Ireland, J. E. Jordan, R. W. Titball, and P. C. Oyston.** 2009. RelA regulates virulence and intracellular survival of Francisella novicida. Microbiology.
44. **Dennis, D. T., T. V. Inglesby, D. A. Henderson, J. G. Bartlett, M. S. Ascher, E. Eitzen, A. D. Fine, A. M. Friedlander, J. Hauer, M. Layton, S.**

R. Lillibridge, J. E. McDade, M. T. Osterholm, T. O'Toole, G. Parker, T. M. Perl, P. K. Russell, and K. Tonat. 2001. Tularemia as a biological weapon: medical and public health management. JAMA **285:**2763-73.

45. **Díaz de Tuesta A.M., C.-Q., M.P. Geijo Martínez, J. Dimas Núñez a, F.J. Díaz de Tuesta, C.R. Herranz, E. Val Pérez** 2001. Tularemia outbreak in the province of Cuenca associated with crab handling. Rev Clin Esp **201:**385-9.
46. **Divakaruni, A. V., C. Baida, C. L. White, and J. W. Gober.** 2007. The cell shape proteins MreB and MreC control cell morphogenesis by positioning cell wall synthetic complexes. Mol Microbiol **66:**174-88.
47. **Driscoll, M. E., M. F. Romine, F. S. Juhn, M. H. Serres, L. A. McCue, A. S. Beliaev, J. K. Fredrickson, and T. S. Gardner.** 2007. Identification of diverse carbon utilization pathways in Shewanella oneidensis MR-1 via expression profiling. Genome Inform **18:**287-98.
48. **Durham-Colleran, M. W., A. B. Verhoeven, and M. L. van Hoek.** 2009. Francisella novicida Forms In Vitro Biofilms Mediated by an Orphan Response Regulator. Microb Ecol.
49. **Eigelsbach, H. T., and C. M. Downs.** 1961. Prophylactic effectiveness of live and killed tularemia vaccines. I. Production of vaccine and evaluation in the white mouse and guinea pig. J Immunol **87:**415-25.
50. **Einbu, A., and K. M. Varum.** 2008. Characterization of chitin and its hydrolysis to GlcNAc and GlcN. Biomacromolecules **9:**1870-5.
51. **Eisen, M. B., and P. O. Brown.** 1999. DNA arrays for analysis of gene expression. Methods Enzymol **303:**179-205.
52. **Eisen, M. B., P. T. Spellman, P. O. Brown, and D. Botstein.** 1998. Cluster analysis and display of genome-wide expression patterns. Proc Natl Acad Sci U S A **95:**14863-8.
53. **El-Etr, S. J. J. M., D.M. Monack, R. Robison, M. Cohen, E. Moore, and A. Rasley.** 2009. Francisella tularensis type A Strains Cause the Rapid Encystment of Acanthamoeba castellanii and Survive in Amoebal Cysts for Three Weeks post Infection. Appl Environ Microbiol **E-publication.**
54. **Eliasson, H., and E. Back.** 2007. Tularaemia in an emergent area in Sweden: an analysis of 234 cases in five years. Scand J Infect Dis **39:**880-9.
55. **Ellis, J., P. C. Oyston, M. Green, and R. W. Titball.** 2002. Tularemia. Clin Microbiol Rev **15:**631 - 646.
56. **Enos-Berlage, J. L., Z.T. Guvener, C.E. Keenan, and L.L. McCarter** 2004. Genetic determinants of biofilm development of opaque and translucent Vibrio parahaemolyticus. 55 **4.**
57. **Entcheva-Dimitrov, P., and A. M. Spormann.** 2004. Dynamics and Control of Biofilms of the Oligotrophic Bacterium Caulobacter crescentus. J. Bacteriol. **186:**8254-8266.
58. **Epstein, P. R.** 1993. Algal blooms in the spread and persistence of cholera. Biosystems **31:**209-21.
59. **Farlow, J., D. M. Wagner, M. Dukerich, M. Stanley, M. Chu, K. Kubota, J. Petersen, and P. Keim.** 2005. Francisella tularensis in the United States. Emerging Infectious Diseases **11:**1835-1841.

60. **Faruque, S. M., M. J. Albert, and J. J. Mekalanos.** 1998. Epidemiology, genetics, and ecology of toxigenic Vibrio cholerae. Microbiol Mol Biol Rev **62:**1301-14.
61. **Forsman, M., E. W. Henningson, E. Larsson, T. Johansson, and G. Sandstrom.** 2000. Francisella tularensis does not manifest virulence in viable but non-culturable state. FEMS Microbiol Ecol **31:**217-224.
62. **Friedman, N., S. Vardi, M. Ronen, U. Alon, and J. Stavans.** 2005. Precise temporal modulation in the response of the SOS DNA repair network in individual bacteria. PLoS Biol **3:**e238.
63. **Fujise, O., Y. Wang, W. Chen, and C. Chen.** 2008. Adherence of Aggregatibacter actinomycetemcomitans via serotype-specific polysaccharide antigens in lipopolysaccharides. Oral Microbiol Immunol **23:**226-33.
64. **Gaddy, J. A., and L. A. Actis.** 2009. Regulation of Acinetobacter baumannii biofilm formation. Future Microbiol **4:**273-8.
65. **Gage, K. L., and M. Y. Kosoy.** 2005. Natural history of plague: perspectives from more than a century of research. Annu Rev Entomol **50:**505-28.
66. **Gallagher, L. A., E. Ramage, M. A. Jacobs, R. Kaul, M. Brittnacher, and C. Manoil.** 2007. A comprehensive transposon mutant library of Francisella novicida, a bioweapon surrogate. Proceedings of the National Academy of Sciences **104:**1009-1014.
67. **Gaynor, E. C., D. H. Wells, J. K. MacKichan, and S. Falkow.** 2005. The Campylobacter jejuni stringent response controls specific stress survival and virulence-associated phenotypes. Mol Microbiol **56:**8-27.
68. **Gerstel, U., C. Park, and U. Romling.** 2003. Complex regulation of csgD promoter activity by global regulatory proteins. Mol Microbiol **49:**639-54.
69. **Gerstel, U., and U. Romling.** 2001. Oxygen tension and nutrient starvation are major signals that regulate agfD promoter activity and expression of the multicellular morphotype in Salmonella typhimurium. Environ Microbiol **3:**638-48.
70. **Gilbert, P., T. Maira-Litran, A. J. McBain, A. H. Rickard, and F. W. Whyte.** 2002. The physiology and collective recalcitrance of microbial biofilm communities. Adv Microb Physiol **46:**202-56.
71. **Giltner, C. L., E. J. van Schaik, G. F. Audette, D. Kao, R. S. Hodges, D. J. Hassett, and R. T. Irvin.** 2006. The Pseudomonas aeruginosa type IV pilin receptor binding domain functions as an adhesin for both biotic and abiotic surfaces. Mol Microbiol **59:**1083-96.
72. **Gold, V. A. M., F. Duong, and I. Collinson.** 2007. Structure and function of the bacterial Sec translocon (Review). Molecular Membrane Biology **24:**387-394.
73. **Goller, C. a. T. R.** 2008. Environmental Influences on Biofilm Development. Current Topics in Microbiology and Immunology **Bacterial Biofilms** 37-66.
74. **Golovliov, I., V. Baranov, Z. Krocova, H. Kovarova, and A. Sjostedt.** 2003. An attenuated strain of the facultative intracellular bacterium Francisella tularensis can escape the phagosome of monocytic cells. Infect Immun **71:**5940 - 5950.

75. **Golovliov, I., M. Ericsson, G. Sandstrom, A. Tarnvik, and A. Sjostedt.** 1997. Identification of proteins of Francisella tularensis induced during growth in macrophages and cloning of the gene encoding a prominently induced 23-kilodalton protein. Infect. Immun. **65:**2183-2189.
76. **Gonin, M., E. M. Quardokus, D. O'Donnol, J. Maddock, and Y. V. Brun.** 2000. Regulation of stalk elongation by phosphate in Caulobacter crescentus. J Bacteriol **182:**337-47.
77. **Gonzalez Barrios, A. F., R. Zuo, Y. Hashimoto, L. Yang, W. E. Bentley, and T. K. Wood.** 2006. Autoinducer 2 controls biofilm formation in Escherichia coli through a novel motility quorum-sensing regulator (MqsR, B3022). J Bacteriol **188:**305-16.
78. **Goodwin, C. S.** 1994. How Helicobacter pylori acquired its name, and how it overcomes gastric defence mechanisms. J Gastroenterol Hepatol **9 Suppl 1:**S1-3.
79. **Guina, T., D. Radulovic, A. J. Bahrami, D. L. Bolton, L. Rohmer, K. A. Jones-Isaac, J. Chen, L. A. Gallagher, B. Gallis, S. Ryu, G. K. Taylor, M. J. Brittnacher, C. Manoil, and D. R. Goodlett.** 2007. MglA Regulates Francisella tularensis subsp. novicida (Francisella novicida) Response to Starvation and Oxidative Stress. J. Bacteriol. **189:**6580-6586.
80. **Guiton, P. S., C. S. Hung, K. A. Kline, R. Roth, A. L. Kau, E. Hayes, J. Heuser, K. W. Dodson, M. G. Caparon, and S. J. Hultgren.** 2009. Contribution of autolysin and Sortase a during Enterococcus faecalis DNA-dependent biofilm development. Infect Immun **77:**3626-38.
81. **Gunn, J. S., and R. K. Ernst.** 2007. The structure and function of Francisella lipopolysaccharide. Ann N Y Acad Sci **1105:**202-18.
82. **Hager, A. J., D. L. Bolton, M. R. Pelletier, M. J. Brittnacher, L. A. Gallagher, R. Kaul, S. J. Skerrett, S. I. Miller, and T. Guina.** 2006. Type IV pili-mediated secretion modulates Francisella virulence. Mol Microbiol **62:**227-37.
83. **Hall-Stoodley, L., and P. Stoodley.** 2005. Biofilm formation and dispersal and the transmission of human pathogens. Trends in Microbiology **13:**7-10.
84. **Hammer, B. K., and B. L. Bassler.** 2009. Distinct Sensory Pathways in Vibrio cholerae El Tor and Classical Biotypes Modulate Cyclic Dimeric GMP Levels To Control Biofilm Formation. J. Bacteriol. **191:**169-177.
85. **Hansen, A. M., Y. Qiu, N. Yeh, F. R. Blattner, T. Durfee, and D. J. Jin.** 2005. SspA is required for acid resistance in stationary phase by downregulation of H-NS in Escherichia coli. Mol Microbiol **56:**719-34.
86. **Harris, B. Z., D. Kaiser, and M. Singer.** 1998. The guanosine nucleotide (p)ppGpp initiates development and A-factor production in myxococcus xanthus. Genes Dev **12:**1022-35.
87. **Hassett, D. J., P. A. Limbach, R. F. Hennigan, K. E. Klose, R. E. W. Hancock, M. D. Platt, and D. F. Hunt.** 2003. Bacterial biofilms of importance to medicine and bioterrorism: proteomic techniques to identify novel vaccine components and drug targets. Expert Opinion on Biological Therapy **3:**1201-1207.

88. **Hazlett, K. R. O., S. D. Caldon, D. G. McArthur, K. A. Cirillo, G. S. Kirimanjeswara, M. L. Magguilli, M. Malik, A. Shah, S. Broderick, I. Golovliov, D. W. Metzger, K. Rajan, T. J. Sellati, and D. J. Loegering.** 2008. Adaptation of Francisella tularensis to the Mammalian Environment Is Governed by Cues Which Can Be Mimicked In Vitro. Infect. Immun. **76:**4479-4488.
89. **Heilmann, C., G. Thumm, G. S. Chhatwal, J. Hartleib, A. Uekotter, and G. Peters.** 2003. Identification and characterization of a novel autolysin (Aae) with adhesive properties from Staphylococcus epidermidis. Microbiology **149:**2769-78.
90. **Hopla, C.** 1974. The ecology of tularemia. Adv Vet Sci Comp Med **18:**25-53.
91. **Horzempa, J., P. Carlson, D. O'Dee, R. Shanks, and G. Nau.** 2008. Global transcriptional response to mammalian temperature provides new insight into Francisella tularensis pathogenesis. BMC Microbiology **8:**172.
92. **Hunt, D. E., D. Gevers, N. M. Vahora, and M. F. Polz.** 2008. Conservation of the chitin utilization pathway in the Vibrionaceae. Appl Environ Microbiol **74:**44-51.
93. **Ireland, M. M., J. A. Karty, E. M. Quardokus, J. P. Reilly, and Y. V. Brun.** 2002. Proteomic analysis of the Caulobacter crescentus stalk indicates competence for nutrient uptake. Mol Microbiol **45:**1029-41.
94. **Jacobs, C., and L. Shapiro.** 1998. Microbial asymmetric cell division: localization of cell fate determinants. Curr Opin Genet Dev **8:**386-91.
95. **Jarrett, ClaytonÂ O., E. Deak, KarenÂ E. Isherwood, PetraÂ C. Oyston, ElizabethÂ R. Fischer, AdelineÂ R. Whitney, ScottÂ D. Kobayashi, FrankÂ R. DeLeo, and B. Â J. Hinnebusch.** 2004. Transmission of Yersinia pestis from an Infectious Biofilm in the Flea Vector. The Journal of Infectious Diseases **190:**783-792.
96. **Jing, H., J. Takagi, J.-h. Liu, S. Lindgren, R.-g. Zhang, A. Joachimiak, J.-h. Wang, and T. A. Springer.** 2002. Archaeal Surface Layer Proteins Contain [beta] Propeller, PKD, and [beta] Helix Domains and Are Related to Metazoan Cell Surface Proteins. Structure **10:**1453-1464.
97. **Kanehisa, M., M. Araki, S. Goto, M. Hattori, M. Hirakawa, M. Itoh, T. Katayama, S. Kawashima, S. Okuda, T. Tokimatsu, and Y. Yamanishi.** 2008. KEGG for linking genomes to life and the environment. Nucleic Acids Res **36:**D480-4.
98. **Kelley, L. A., and M. J. Sternberg.** 2009. Protein structure prediction on the Web: a case study using the Phyre server. Nat Protoc **4:**363-71.
99. **Keyhani, N. O., and S. Roseman.** 1999. Physiological aspects of chitin catabolism in marine bacteria. Biochimica et Biophysica Acta (BBA) - General Subjects **1473:**108-122.
100. **Kirisits, M. J., and M. R. Parsek.** 2006. Does Pseudomonas aeruginosa use intercellular signalling to build biofilm communities? Cell Microbiol **8:**1841-9.
101. **Klausen, M., A. Heydorn, P. Ragas, L. Lambertsen, A. Aaes-Jorgensen, S. Molin, and T. Tolker-Nielsen.** 2003. Biofilm formation by Pseudomonas

aeruginosa wild type, flagella and type IV pili mutants. Mol Microbiol **48:**1511-24.

102. **Kraemer, P. S., A. Mitchell, M. R. Pelletier, L. A. Gallagher, M. Wasnick, L. Rohmer, M. J. Brittnacher, C. Manoil, S. J. Skerett, and N. R. Salama.** 2009. Genome-Wide Screen in Francisella novicida for Genes Required for Pulmonary and Systemic Infection in Mice. Infect. Immun. **77:**232-244.
103. **Kugeler, K. J., P. S. Mead, A. M. Janusz, J. E. Staples, K. A. Kubota, L. G. Chalcraft, and J. M. Petersen.** 2009. Molecular Epidemiology of Francisella tularensis in the United States. Clin Infect Dis **48:**863-70.
104. **Kulkarni, R., B. K. Dhakal, E. S. Slechta, Z. Kurtz, M. A. Mulvey, and D. G. Thanassi.** 2009. Roles of putative type II secretion and type IV pilus systems in the virulence of uropathogenic Escherichia coli. PLoS One **4:**e4752.
105. **Kuoppa, K., Å. Forsberg, and A. Norqvist.** 2001. Construction of a reporter plasmid for screening in vivo promoter activity in Francisella tularensis. FEMS Microbiology Letters **205:**77-81.
106. **Kurtz, H. D., Jr., and J. Smit.** 1994. The Caulobacter crescentus holdfast: identification of holdfast attachment complex genes. FEMS Microbiol Lett **116:**175-82.
107. **Lai, C. J., S. Y. Chen, I. H. Lin, C. H. Chang, and H. C. Wong.** 2009. Change of protein profiles in the induction of the viable but nonculturable state of Vibrio parahaemolyticus. Int J Food Microbiol **135:**118-24.
108. **Larsson, P., P. C. Oyston, P. Chain, M. C. Chu, M. Duffield, H. H. Fuxelius, E. Garcia, G. Halltorp, D. Johansson, K. E. Isherwood, P. D. Karp, E. Larsson, Y. Liu, S. Michell, J. Prior, R. Prior, S. Malfatti, A. Sjostedt, K. Svensson, N. Thompson, L. Vergez, J. K. Wagg, B. W. Wren, L. E. Lindler, S. G. Andersson, M. Forsman, and R. W. Titball.** 2005. The complete genome sequence of Francisella tularensis, the causative agent of tularemia. Nat Genet **37:**153-9.
109. **Lau, H. Y., and N. J. Ashbolt.** 2009. The role of biofilms and protozoa in Legionella pathogenesis: implications for drinking water. J Appl Microbiol **107:**368-78.
110. **Lauriano, C. M., J. R. Barker, S. S. Yoon, F. E. Nano, B. P. Arulanandam, D. J. Hassett, and K. E. Klose.** 2004. MglA regulates transcription of virulence factors necessary for Francisella tularensis intraamoebae and intramacrophage survival. Proc Natl Acad Sci U S A **101:**4246 - 4249.
111. **Lebeer, S., S. C. De Keersmaecker, T. L. Verhoeven, A. A. Fadda, K. Marchal, and J. Vanderleyden.** 2007. Functional analysis of luxS in the probiotic strain Lactobacillus rhamnosus GG reveals a central metabolic role important for growth and biofilm formation. J Bacteriol **189:**860-71.
112. **Lee, J. H., J. E. Rhee, U. Park, H. M. Ju, B. C. Lee, T. S. Kim, H. S. Jeong, and S. H. Choi.** 2007. Identification and functional analysis of vibrio vulnificus SmcR, a novel global regulator. J Microbiol Biotechnol **17:**325-34.
113. **Lemos, J. A., T. A. Brown, Jr., and R. A. Burne.** 2004. Effects of RelA on key virulence properties of planktonic and biofilm populations of Streptococcus mutans. Infect Immun **72:**1431-40.

114. **Letunic, I., T. Doerks, and P. Bork.** 2009. SMART 6: recent updates and new developments. Nucl. Acids Res. **37:**D229-232.
115. **Levi, A., and U. Jenal.** 2006. Holdfast formation in motile swarmer cells optimizes surface attachment during Caulobacter crescentus development. J Bacteriol **188:**5315-8.
116. **Levin, M. A., J. S. Trupin, and V. J. Cabelli.** 1962. Clear media for the recovery of Pasteurella tularensis. Appl Microbiol **10:**407-12.
117. **Li, K. B.** 2003. ClustalW-MPI: ClustalW analysis using distributed and parallel computing. Bioinformatics **19:**1585-6.
118. **Lill R., K. C., L.A. Brundage, K. Ito, D. Oliver, and W. Wickner.** 1989. SecA protein hydrolyzes ATP and is an essential component of the protein translocation ATPase of Escherichia coli. EMBO J **8:**961–966.
119. **Lindback, T., M. E. Rottenberg, S. M. Roche, and L. Marit Rorvik.** 2009. The ability to enter into an avirulent Viable But Non-Culturable (VBNC) form is widespread among Listeria monocytogenes isolates from salmon, patients and environment. Vet Res **41:**8.
120. **Lisa Friedman, R. K.** 2004. Genes involved in matrix formation in Pseudomonas aeruginosa PA14 biofilms. Molecular Microbiology **51:**675-690.
121. **Liu, J., X. Zogaj, J. R. Barker, and K. E. Klose.** 2007. Construction of targeted insertion mutations in Francisella tularensis subsp. novicida. Biotechniques **43:**487-90, 492.
122. **Loo, C. Y., D. A. Corliss, and N. Ganeshkumar.** 2000. Streptococcus gordonii Biofilm Formation: Identification of Genes that Code for Biofilm Phenotypes. J. Bacteriol. **182:**1374-1382.
123. **Maier, T. M., A. Havig, M. Casey, F. E. Nano, D. W. Frank, and T. C. Zahrt.** 2004. Construction and Characterization of a Highly Efficient Francisella Shuttle Plasmid. Appl. Environ. Microbiol. **70:**7511-7519.
124. **Maier, T. M., R. Pechous, M. Casey, T. C. Zahrt, and D. W. Frank.** 2006. In vivo Himar1-based transposon mutagenesis of Francisella tularensis. Appl Environ Microbiol **72:**1878-85.
125. **Mann, E. E., K. C. Rice, B. R. Boles, J. L. Endres, D. Ranjit, L. Chandramohan, L. H. Tsang, M. S. Smeltzer, A. R. Horswill, and K. W. Bayles.** 2009. Modulation of eDNA release and degradation affects Staphylococcus aureus biofilm maturation. PLoS One **4:**e5822.
126. **Matz, C., D. McDougald, A. M. Moreno, P. Y. Yung, F. H. Yildiz, and S. Kjelleberg.** 2005. Biofilm formation and phenotypic variation enhance predation-driven persistence of Vibrio cholerae. Proc Natl Acad Sci U S A **102:**16819-24.
127. **Maurer, J. J., T. P. Brown, W. L. Steffens, and S. G. Thayer.** 1998. The occurrence of ambient temperature-regulated adhesins, curli, and the temperature-sensitive hemagglutinin tsh among avian Escherichia coli. Avian Dis **42:**106-18.
128. **McDougald, D., W. H. Lin, S. A. Rice, and S. Kjelleberg.** 2006. The role of quorum sensing and the effect of environmental conditions on biofilm formation by strains of Vibrio vulnificus. Biofouling **22:**133-44.

129. **Meibom, K. L., X. B. Li, A. T. Nielsen, C.-Y. Wu, S. Roseman, and G. K. Schoolnik.** 2004. The Vibrio cholerae chitin utilization program. Proc Natl Acad Sci U S A **101:**2524-2529.
130. **Melillo, A., D. D. Sledjeski, S. Lipski, R. M. Wooten, V. Basrur, and E. R. Lafontaine.** 2006. Identification of a Francisella tularensis LVS outer membrane protein that confers adherence to A549 human lung cells. FEMS Microbiol Lett **263:**102-8.
131. **Merker, R. I., and J. Smit.** 1988. Characterization of the Adhesive Holdfast of Marine and Freshwater Caulobacters. Appl Environ Microbiol **54:**2078-2085.
132. **Merzendorfer, H., and L. Zimoch.** 2003. Chitin metabolism in insects: structure, function and regulation of chitin synthases and chitinases. J Exp Biol **206:**4393-412.
133. **Miethke, M., H. Westers, E. J. Blom, O. P. Kuipers, and M. A. Marahiel.** 2006. Iron starvation triggers the stringent response and induces amino acid biosynthesis for bacillibactin production in Bacillus subtilis. J Bacteriol **188:**8655-7.
134. **Mikalsen, J., A. B. Olsen, H. Rudra, T. Moldal, H. Lund, B. Djonne, O. Bergh, and D. J. Colquhoun.** 2009. Virulence and pathogenicity of Francisella philomiragia subsp. noatunensis for Atlantic cod, Gadus morhua L., and laboratory mice. J Fish Dis **32:**377-81.
135. **Mironchuk I.V., A. V. M.** 2002. Viability and virulence of Francisella tularensis subsp. Holarctica in water ecosystems (experimental study). Zh Mikrobiol Epidemiol Immunobiol **March-April:**9-13.
136. **Mohapatra, N. P., S. Soni, B. L. Bell, R. Warren, R. K. Ernst, A. Muszynski, R. W. Carlson, and J. S. Gunn.** 2007. Identification of an orphan response regulator required for the virulence of Francisella spp. and transcription of pathogenicity island genes. Infect Immun **75:**3305-14.
137. **Mohapatra, N. P., S. Soni, B. L. Bell, R. Warren, R. K. Ernst, A. Muszynski, R. W. Carlson, and J. S. Gunn.** 2007. Identification of an Orphan Response Regulator Required for the Virulence of Francisella spp. and Transcription of Pathogenicity Island Genes. Infect. Immun. **75:**3305-3314.
138. **Morner, T.** 1992. The ecology of tularaemia. Rev Sci Tech **11:**1123-30.
139. **Mueller, R. S., D. McDougald, D. Cusumano, N. Sodhi, S. Kjelleberg, F. Azam, and D. H. Bartlett.** 2007. Vibrio cholerae Strains Possess Multiple Strategies for Abiotic and Biotic Surface Colonization. J. Bacteriol. **189:**5348-5360.
140. **Munoz-Elias, E. J., J. Marcano, and A. Camilli.** 2008. Isolation of Streptococcus pneumoniae biofilm mutants and their characterization during nasopharyngeal colonization. Infect Immun **76:**5049-61.
141. **Murga, R., T. S. Forster, E. Brown, J. M. Pruckler, B. S. Fields, and R. M. Donlan.** 2001. Role of biofilms in the survival of Legionella pneumophila in a model potable-water system. Microbiology **147:**3121-6.

142. **Murphy, C., C. Carroll, and K. N. Jordan.** 2006. Environmental survival mechanisms of the foodborne pathogen Campylobacter jejuni. J Appl Microbiol **100:**623-32.
143. **Naczk, M., J. Williams, K. Brennan, C. Liyanapathirana, and F. Shahidi.** 2004. Compositional characteristics of green crab (Carcinus maenas). Food Chemistry **88:**429-434.
144. **Nano, F. E., and C. Schmerk.** 2007. The Francisella pathogenicity island. Ann N Y Acad Sci **1105:**122 - 137.
145. **Nano, F. E., N. Zhang, S. C. Cowley, K. E. Klose, K. K. Cheung, M. J. Roberts, J. S. Ludu, G. W. Letendre, A. I. Meierovics, G. Stephens, and K. L. Elkins.** 2004. A Francisella tularensis pathogenicity island required for intramacrophage growth. J Bacteriol **186:**6430 - 6436.
146. **Nigrovic, L. E., and S. L. Wingerter.** 2008. Tularemia. Infectious Disease Clinics of North America **22:**489-504.
147. **O'Toole, G. A., and R. Kolter.** 1998. Flagellar and twitching motility are necessary for Pseudomonas aeruginosa biofilm development. Mol Microbiol **30:**295-304.
148. **O'Toole, G. A., and R. Kolter.** 1998. Initiation of biofilm formation in Pseudomonas fluorescens WCS365 proceeds via multiple, convergent signalling pathways: a genetic analysis. Mol Microbiol **28:**449-61.
149. **Olsen, A., A. Arnqvist, M. Hammar, and S. Normark.** 1993. Environmental regulation of curli production in Escherichia coli. Infect Agents Dis **2:**272-4.
150. **Orikoshi, H., S. Nakayama, C. Hanato, K. Miyamoto, and H. Tsujibo.** 2005. Role of the N-terminal polycystic kidney disease domain in chitin degradation by chitinase A from a marine bacterium, Alteromonas sp. strain O-7. J Appl Microbiol **99:**551-7.
151. **Otto, M.** 2008. Staphylococcal biofilms. Curr Top Microbiol Immunol **322:**207-28.
152. **Owen, C. R., E. O. Buker, W. L. Jellison, D. B. Lackman, and J. F. Bell.** 1964. COMPARATIVE STUDIES OF FRANCISELLA TULARENSIS AND FRANCISELLA NOVICIDA. J. Bacteriol. **87:**676-683.
153. **Oyston, P. C., A. Sjostedt, and R. W. Titball.** 2004. Tularaemia: bioterrorism defence renews interest in Francisella tularensis. Nat Rev Microbiol **2:**967 - 978.
154. **Oyston, P. C. F.** 2008. Francisella tularensis: unravelling the secrets of an intracellular pathogen. J Med Microbiol **57:**921-930.
155. **Palmer, J. R. J., and D. C. White.** 1997. Developmental biology of biofilms: implications for treatment and control. Trends in Microbiology **5:**435-440.
156. **Palo, R., C. Ahlm, and A. Tärnvik.** 2005. Climate variability reveals complex events for tularemia dynamics in man and mammals. Ecology and Society **10:**22.
157. **Paranjpye, R. N., and M. S. Strom.** 2005. A Vibrio vulnificus Type IV Pilin Contributes to Biofilm Formation, Adherence to Epithelial Cells, and Virulence. Infect. Immun. **73:**1411-1422.

158. **Parsek, M. R., and E. P. Greenberg.** 2000. Acyl-homoserine lactone quorum sensing in Gram-negative bacteria: A signaling mechanism involved in associations with higher organisms. Proc Natl Acad Sci U S A **97:**8789-8793.
159. **Passerat, J., P. Got, S. Dukan, and P. Monfort.** 2009. Respective roles of culturable and viable-but-nonculturable cells in the heterogeneity of Salmonella enterica serovar typhimurium invasiveness. Appl Environ Microbiol **75:**5179-85.
160. **Pate, J. L., and E. J. Ordal.** 1965. The fine structure of two unusual stalked bacteria. J Cell Biol **27:**133-50.
161. **Pedersen, K.** 1982. Method for Studying Microbial Biofilms in Flowing-Water Systems. Appl Environ Microbiol **43:**6-13.
162. **Pelicic, V.** 2008. Type IV pili: e pluribus unum? Mol Microbiol **68:**827-37.
163. **Percival, S. L., and J. G. Thomas.** 2009. Transmission of Helicobacter pylori and the role of water and biofilms. J Water Health **7:**469-77.
164. **Petersen, J. M., P. S. Mead, and M. E. Schriefer.** 2009. Francisella tularensis: an arthropod-borne pathogen. Vet Res **40:**7.
165. **Poindexter, J. S.** 1978. Selection for nonbuoyant morphological mutants of Caulobacter crescentus. J Bacteriol **135:**1141-5.
166. **Potrykus, K., and M. Cashel.** 2008. (p)ppGpp: Still Magical?*. Annual Review of Microbiology **62:**35-51.
167. **Pruzzo, C., L. Vezzulli, and R. R. Colwell.** 2008. Global impact of Vibrio cholerae interactions with chitin. Environ Microbiol **10:**1400-10.
168. **Reeser, R. J., R. T. Medler, S. J. Billington, B. H. Jost, and L. A. Joens.** 2007. Characterization of Campylobacter jejuni biofilms under defined growth conditions. Appl Environ Microbiol **73:**1908-13.
169. **Rosen, D. A., J. S. Pinkner, J. M. Jones, J. N. Walker, S. Clegg, and S. J. Hultgren.** 2008. Utilization of an Intracellular Bacterial Community Pathway in Klebsiella pneumoniae Urinary Tract Infection and the Effects of FimK on Type 1 Pilus Expression. Infect. Immun. **76:**3337-3345.
170. **Saldanha, A. J.** 2004. Java Treeview--extensible visualization of microarray data. Bioinformatics **20:**3246-8.
171. **Sauer, J. D., M. A. Bachman, and M. S. Swanson.** 2005. The phagosomal transporter A couples threonine acquisition to differentiation and replication of Legionella pneumophila in macrophages. Proc Natl Acad Sci U S A **102:**9924-9.
172. **Schmerk, C. L., B. N. Duplantis, P. L. Howard, and F. E. Nano.** 2009. A Francisella novicida pdpA mutant exhibits limited intracellular replication and remains associated with the lysosomal marker LAMP-1. Microbiology **155:**1498-504.
173. **Schultz, J. r., F. Milpetz, P. Bork, and C. P. Ponting.** 1998. SMART, a simple modular architecture research tool: Identification of signaling domains. Proceedings of the National Academy of Sciences of the United States of America **95:**5857-5864.
174. **Shahabuddin, M., and J. M. Vinetz.** 1999. Chitinases of human parasites and their implications as antiparasitic targets. EXS **87:**223-34.

175. **Shanks, R. M. Q., N. A. Stella, E. J. Kalivoda, M. R. Doe, D. M. O'Dee, K. L. Lathrop, F. L. Guo, and G. J. Nau.** 2007. A Serratia marcescens OxyR Homolog Mediates Surface Attachment and Biofilm Formation. J. Bacteriol. **189:**7262-7272.
176. **Sherlock, G., T. Hernandez-Boussard, A. Kasarskis, G. Binkley, J. C. Matese, S. S. Dwight, M. Kaloper, S. Weng, H. Jin, C. A. Ball, M. B. Eisen, P. T. Spellman, P. O. Brown, D. Botstein, and J. M. Cherry.** 2001. The Stanford Microarray Database. Nucleic Acids Res **29:**152-5.
177. **Sjostedt, A.** 2007. Tularemia: history, epidemiology, pathogen physiology, and clinical manifestations. Ann N Y Acad Sci **1105:**1-29.
178. **Smit, J., C. S. Sherwood, and R. F. Turner.** 2000. Characterization of high density monolayers of the biofilm bacterium Caulobacter crescentus: evaluating prospects for developing immobilized cell bioreactors. Can J Microbiol **46:**339-49.
179. **Stahl, D. A., R. Key, B. Flesher, and J. Smit.** 1992. The phylogeny of marine and freshwater caulobacters reflects their habitat. J Bacteriol **174:**2193-8.
180. **Stickler, D. J., N. S. Morris, R. J. C. McLean, and C. Fuqua.** 1998. Biofilms on Indwelling Urethral Catheters Produce Quorum-Sensing Signal Molecules In Situ and In Vitro. Appl. Environ. Microbiol. **64:**3486-3490.
181. **Stovepoindexter, J. L., and G. Cohen-Bazire.** 1964. The Fine Structure of Stalked Bacteria Belonging to the Family Caulobacteraceae. J Cell Biol **23:**587-607.
182. **Su, J., J. Yang, D. Zhao, T. H. Kawula, J. A. Banas, and J.-R. Zhang.** 2007. Genome-Wide Identification of Francisella tularensis Virulence Determinants. Infect. Immun. **75:**3089-3101.
183. **Svensson, K., P. Larsson, D. Johansson, M. Bystrom, M. Forsman, and A. Johansson.** 2005. Evolution of Subspecies of Francisella tularensis. J. Bacteriol. **187:**3903-3908.
184. **Takeo, S., D. Hisamori, S. Matsuda, J. Vinetz, J. Sattabongkot, and T. Tsuboi.** 2009. Enzymatic characterization of the Plasmodium vivax chitinase, a potential malaria transmission-blocking target. Parasitol Int **58:**243-8.
185. **Tarnvik, A., H.-S. Priebe, and R. Grunow.** 2004. Tularaemia in Europe: An Epidemiological Overview 1 1 This overview is based on data presented within a Fogarty workshop "Epidemiology and Ecology of Q fever, tularaemia and plague" at the National Institutes of Health, Bethesda, MD, February 12-13, 2003. Scandinavian Journal of Infectious Diseases **36:**350-355.
186. **Taylor, M., K. Ross, and R. Bentham.** 2009. Legionella, protozoa, and biofilms: interactions within complex microbial systems. Microb Ecol **58:**538-47.
187. **Thelaus, J., A. Andersson, P. Mathisen, A. L. Forslund, L. Noppa, and M. Forsman.** 2009. Influence of nutrient status and grazing pressure on the fate of Francisella tularensis in lake water. FEMS Microbiol Ecol **67:**69-80.
188. **Thompson, L. J., D. S. Merrell, B. A. Neilan, H. Mitchell, A. Lee, and S. Falkow.** 2003. Gene expression profiling of Helicobacter pylori reveals a

growth-phase-dependent switch in virulence gene expression. Infect Immun **71:**2643-55.

189. **Thormann, K. M., S. Duttler, R. M. Saville, M. Hyodo, S. Shukla, Y. Hayakawa, and A. M. Spormann.** 2006. Control of formation and cellular detachment from Shewanella oneidensis MR-1 biofilms by cyclic di-GMP. J Bacteriol **188:**2681-91.
190. **Thormann, K. M., R. M. Saville, S. Shukla, D. A. Pelletier, and A. M. Spormann.** 2004. Initial Phases of Biofilm Formation in Shewanella oneidensis MR-1. J. Bacteriol. **186:**8096-8104.
191. **Thormann, K. M., R. M. Saville, S. Shukla, and A. M. Spormann.** 2005. Induction of rapid detachment in Shewanella oneidensis MR-1 biofilms. J Bacteriol **187:**1014-21.
192. **Titball, R. W., and J. F. Petrosino.** 2007. Francisella tularensis genomics and proteomics. Ann N Y Acad Sci **1105:**98 - 121.
193. **Tolker-Nielsen, T., and S. Molin.** 2000. Spatial Organization of Microbial Biofilm Communities. Microbial Ecology **40:**75-84.
194. **Toratani, T., T. Shoji, T. Ikehara, K. Suzuki, and T. Watanabe.** 2008. The importance of chitobiase and N-acetylglucosamine (GlcNAc) uptake in N,N'-diacetylchitobiose [(GlcNAc)2] utilization by Serratia marcescens 2,170. Microbiology **154:**1326-32.
195. **Tsuzuki, M., X. Y. Xu, K. Sato, M. Abo, M. Arioka, H. Nakajima, K. Kitamoto, and A. Okubo.** 2005. SspA, an outer membrane protein, is highly induced under salt-stressed conditions and is essential for growth under salt-stressed aerobic conditions in Rhodobacter sphaeroides f. sp. denitrificans. Appl Microbiol Biotechnol **68:**242-50.
196. **Tu Quoc, P. H., P. Genevaux, M. Pajunen, H. Savilahti, C. Georgopoulos, J. Schrenzel, and W. L. Kelley.** 2007. Isolation and Characterization of Biofilm Formation-Defective Mutants of Staphylococcus aureus. Infect. Immun. **75:**1079-1088.
197. **Tusher, V. G., R. Tibshirani, and G. Chu.** 2001. Significance analysis of microarrays applied to the ionizing radiation response. Proc Natl Acad Sci U S A **98:**5116-21.
198. **Valent, Q. A., P.A. Scotti, S. High, J.W. de Gier, G. von Heijne, G. Lentzen, W. Wintermeyer, B. Oudega, and J. Luirink.** 1998. The Escherichia coli SRP and SecB targeting pathways converge at the translocon. EMBO J **19:**2504–2512.
199. **Vilain, S., J. M. Pretorius, J. Theron, and V. S. Brozel.** 2009. DNA as an adhesin: Bacillus cereus requires extracellular DNA to form biofilm. Appl. Environ. Microbiol.:AEM.01317-08.
200. **Vinetz, J. M., S. K. Dave, C. A. Specht, K. A. Brameld, B. Xu, R. Hayward, and D. A. Fidock.** 1999. The chitinase PfCHT1 from the human malaria parasite Plasmodium falciparum lacks proenzyme and chitin-binding domains and displays unique substrate preferences. Proc Natl Acad Sci U S A **96:**14061-6.

201. **Vonkavaara, M., M. V. Telepnev, P. Ryden, A. Sjostedt, and S. Stoven.** 2008. Drosophila melanogaster as a model for elucidating the pathogenicity of Francisella tularensis. Cell Microbiol **10:**1327-38.
202. **Wagner, J. K., and Y. V. Brun.** 2007. Out on a limb: how the Caulobacter stalk can boost the study of bacterial cell shape. Mol Microbiol **64:**28-33.
203. **Wagner, J. K., C. D. Galvani, and Y. V. Brun.** 2005. Caulobacter crescentus requires RodA and MreB for stalk synthesis and prevention of ectopic pole formation. J Bacteriol **187:**544-53.
204. **Wagner, J. K., S. Setayeshgar, L. A. Sharon, J. P. Reilly, and Y. V. Brun.** 2006. A nutrient uptake role for bacterial cell envelope extensions. Proc Natl Acad Sci U S A **103:**11772-7.
205. **Wai, S. N., Y. Mizunoe, and S. Yoshida.** 1999. How Vibrio cholerae survive during starvation. FEMS Microbiol Lett **180:**123-31.
206. **Wall, D., and D. Kaiser.** 1999. Type IV pili and cell motility. Molecular Microbiology **32:**1.
207. **Weiner, R. M., M. Melick, K. O'Neill, and E. Quintero.** 2000. Hyphomonas adhaerens sp. nov., Hyphomonas johnsonii sp. nov. and Hyphomonas rosenbergii sp. nov., marine budding and prosthecate bacteria. Int J Syst Evol Microbiol **50 Pt 2:**459-69.
208. **Weiss, D. S., A. Brotcke, T. Henry, J. J. Margolis, K. Chan, and D. M. Monack.** 2007. In vivo negative selection screen identifies genes required for Francisella virulence. Proc Natl Acad Sci U S A **104:**6037-42.
209. **Wendrich, T. M., G. Blaha, D. N. Wilson, M. A. Marahiel, and K. H. Nierhaus.** 2002. Dissection of the mechanism for the stringent factor RelA. Mol Cell **10:**779-88.
210. **Whitchurch, C., SA Beatson , JC Comolli, T Jakobsen, JL Sargent, JJ Bertrand, J West, M Klausen, LLWaite, PJ Kang, T Tolker-Nielsen , JS Mattick and JN Engel.** 2005. Pseudomonas aeruginosa fimL regulates multiple virulence functions by intersecting with Vfr-modulated pathways. Mol Microbiol **55:**1357 - 1378.
211. **Williams, A., A. Wilkinson, M. Krehenbrink, D. M. Russo, A. Zorreguieta, and J. A. Downie.** 2008. Glucomannan-mediated attachment of Rhizobium leguminosarum to pea root hairs is required for competitive nodule infection. J Bacteriol **190:**4706-15.
212. **Williams, M. D., T. X. Ouyang, and M. C. Flickinger.** 1994. Starvation-induced expression of SspA and SspB: the effects of a null mutation in sspA on Escherichia coli protein synthesis and survival during growth and prolonged starvation. Mol Microbiol **11:**1029-43.
213. **Williams, P.** 2007. Quorum sensing, communication and cross-kingdom signalling in the bacterial world. Microbiology **153:**3923-38.
214. **Willke, A., M. Meric, R. Grunow, M. Sayan, E. J. Finke, W. Splettstosser, E. Seibold, S. Erdogan, O. Ergonul, Z. Yumuk, and S. Gedikoglu.** 2009. An outbreak of oropharyngeal tularaemia linked to natural spring water. J Med Microbiol **58:**112-116.

215. **Yan, W., T. Qu, H. Zhao, L. Su, Q. Yu, J. Gao, and B. Wu.** The effect of c-di-GMP (3'-5'-cyclic diguanylic acid) on the biofilm formation and adherence of Streptococcus mutans. Microbiological Research **In Press, Corrected Proof**.
216. **Yildiz, F. H., and K. L. Visick.** Vibrio biofilms: so much the same yet so different. Trends in Microbiology **In Press, Corrected Proof**.
217. **Yusof, N. L., L. Y. Lim, and E. Khor.** 2004. Flexible chitin films: structural studies. Carbohydr Res **339:**2701-11.